THE NATURE OF HYDROGEN
IN
RANEY NICKEL CATALYSTS

THE NATURE OF HYDROGEN IN RANEY NICKEL CATALYSTS

By

IOAN NICOLAU, Dipl. Chem.

A Thesis

Submitted to the Faculty of Graduate Studies

in Partial Fulfilment of the Requirements

for the Degree

Doctor of Philosophy

McMaster University

SEPTEMBER 1975

TO

MY PARENTS

and

to my wife

LIANA

DOCTOR OF PHILOSOPHY
(Chemistry)

McMASTER UNIVERSITY
Hamilton, Ontario

TITLE: The Nature of Hydrogen in Raney Nickel Catalysts

AUTHOR: Ioan Nicolau, Dipl. Chem. (Bucharest University, Romania)

SUPERVISOR: Dr. R. B. Anderson

NUMBER OF PAGES: xiv, 219

ABSTRACT

The amount and nature of hydrogen in Raney nickel catalysts were determined by various methods: thermal desorption in a volumetric apparatus, temperature-programmed desorption using argon as a carrier gas and techniques similar to those of Amenomiya and Cvetanovic, hydrogen-deuterium exchange, dissolution in acids and other methods. Most of the hydrogen removed in thermal desorption can not be readsorbed. Desorption was generally exothermic and each type of sample had a characteristic TPD spectrum. Water vapor, introduced over the catalyst, increased the hydrogen evolution sizeably and this process was also exothermic. Under these conditions water will not oxidize bulk nickel. Present results suggest that the reaction of residual aluminum and water is an important source of hydrogen evolved on heating Raney nickel, but part of the hydrogen is held interstitially.

ACKNOWLEDGEMENTS

The author would like to acknowledge his gratitude to those people who have rendered their assistance to this work.

I am deeply indebted to my research director, Professor R. B. Anderson, for his guidance, helpful suggestions and patience.

I would like to thank Drs. O.E. Hileman, Jr. and P.T. Dawson, as members of my supervisory committee, and Dr. C.Calvo, for their helpful discussions during the course of this work.

I wish to thank the Department of Chemistry for the use of their mass spectrometer and X-ray diffractometer.

I would like to thank my wife, Liana, for her moral support, patience and constant encouragement.

I am especially grateful to my parents, since without their support and encouragement my graduate studies would not have been possible.

Financial Acknowledgement:

The author is pleased to acknowledge scholarship funds from the Department of Chemistry, McMaster University and the National Research Council of Canada.

I. Nicolau
Hamilton, September 1975

T. Nicolau

TABLE OF CONTENTS

LIST OF TABLES

LIST OF FIGURES

CHAPTER 1

INTRODUCTION

1.1 GENERAL

A method of preparing metal catalysts is to eliminate one of the constituents of a binary or ternary alloy by an alkaline or acidic attack. This method was applied by Murray Raney[1] in 1925. Treating a powdered nickel-silicon alloy with alkali, he obtained a brown residue of pyrophoric nickel with catalytic properties. Later, Raney found that a nickel-aluminum alloy attacked with aqueous sodium hydroxide gives a porous material with very useful catalytic properties[2]. This method of preparing a catalyst was patented in different countries[3,4,5,6] and since then has undergone different modifications. Raney extends his method to prepare Raney iron, cobalt and copper[7] but finds that Raney nickel (RNi) is a better catalyst. Today, Raney nickel is known as a catalyst obtained by leaching a nickel-aluminum alloy with aqueous alkali.

1.2 PREPARATION OF RANEY NICKEL

1.2.1 Structure of Raney Nickel Alloy

Raney nickel catalysts are used extensively for the hydrogenation of organic compounds, usually in liquid phase. They are also used in desulfurizations, dehalogenations,

dehydrogenations, decarboxylations, etc.[8].

The preparation of the nickel-aluminum alloy is made by the thermite reaction between nickel oxide and aluminum or by the dissolution of nickel in melted aluminum. This process is exothermic and provides enough heat so that it is not necessary to use a special high temperature furnace. The starting Raney alloys normally contain 40 to 50 wt % nickel. Alloys of higher nickel content usually contain significant amounts of the compound NiAl, which does not react with alkali[9], while alloys containing less nickel yield correspondingly less catalyst.

Possible phases for nickel-aluminum alloys containing 40-50 wt % nickel, taken from the phase diagram of Alexander and Vaughan[10a] are the following:

1. Phase α: solid solutions of Ni in Al containing not more than 0.05 wt % Ni
2. Eutectic: α + $NiAl_3$, containing about 5 wt % Ni
3. Phase β: $NiAl_3$, containing 42 wt % Ni
4. Phase γ: Ni_2Al_3, containing 56-60% wt % Ni
5. Phase δ: NiAl, containing 80-83 wt % Ni.

The alloy also contains other elements such as C, Fe, Si, and traces of S. The intermetallic phases have a different reactivity toward alkali. Freel, Pieters and Anderson[10], using the techniques of optical metallography and an electron probe microanalyzer to examine the microstructure of commercial Raney alloys and their reaction with NaOH found that the eutectic and

and β phase reacted more rapidly than γ phase. Mason[11] found equal reactivities for γ and β-phases of Raney alloys to aqueous alkali, but he used substantially less than the stoichiometric amount of NaOH required in the leaching process. This result was confirmed by Freel, et.al.[10].

1.2.2 Activation of Raney Nickel

The activation of a Raney nickel alloy is obtained by leaching the alloy with aqueous alkali, a highly exothermic process. The reaction which takes place during this process can be described by the following equation:

$$2Al + 2NaOH + 2H_2O \rightarrow 2NaAlO_2 + 3H_2 \qquad (1)$$

In dilute aqueous solutions the sodium aluminate formed in the reaction (1) is hydrolized:

$$2NaAlO_2 + 4H_2O \rightarrow Al_2O_3 \cdot 3H_2O + 2NaOH \qquad (2)$$

and NaOH is regenerated in reaction (2). This seems to result in essentially complete conversion of all the aluminum in the alloy if sufficient reaction time is provided. However, it has been shown experimentally that even after prolonged boiling with alkali, it is difficult to obtain an aluminum-free catalyst. Dirksen and Linden suggested another contributory reaction in addition to Eq (1) and (2):

$$2Al + 6H_2O \rightarrow Al_2O_3 \cdot 3H_2O + 3H_2 \; . \qquad (3)$$

During the leaching process several parameters can be varied in order to obtain a catalyst with a desired composition, cataly-

tic properties and hydrogen content: the temperature of the alkali, the composition of the initial alloy and phases present, the concentration of the aqueous solution of the alkali, the duration of the extraction, the order of introducing the reagents, the final washing and storage.

One way of preparing an active Raney nickel was described by Adkins and Billica[12]: they used 25 wt % NaOH at 50°C for 25-30 minutes and the final washing of the nickel catalyst with water is done under 1.5 atmospheres of hydrogen. This preparation was termed W6 Raney nickel. W5 RNi is prepared in the same way but is washed in the presence of air. To dissolve as much aluminum as possible, hot solutions of concentrated alkali are used (40%) and hydrolysis of sodium aluminate is prevented by washing the final catalyst with boiling alkali, preferably of lower concentrations[13]. The pore structure of the Raney nickel is a function of the temperature of extraction: preparations made at the boiling point of the alkali (107°C) had a smaller surface area and higher pore volume than those prepared at 50°C[14]. After the preparation Raney nickel is stored under water or ethanol to minimize oxidation by air and loss of catalytic activity. Relatively new hydrogenating catalysts were prepared in 1951 by Y. Urushibara[44] and denoted as: U-Ni, U-Co, U-Cu, U-Fe. The method of preparation is simple: fine metal particles are precipitated from solutions of their respective metal salts by more electropositive metals and are digested with alkali or acids. These catalysts exhibit high

activities, comparable to those of Raney catalysts. For example, a Urushibara nickel catalyst, U-Ni, can be obtained by adding zinc powder to a solution of nickel chloride. A precipitated nickel powder is obtained which is capable of reducing an alkaline solution of estrone to estradiol in the presence of aluminum grains.

1.3 COMPOSITION AND STRUCTURE OF RANEY NICKEL

The constituents of the activated Raney alloy are the following:

- Nickel, essentially as metallic nickel. Part of it could be present as an alloy with aluminum, especially in the partly activated catalysts. Nickel oxide could be present in very small amounts, due to oxidation by air.
- Aluminum, as residual aluminum in combination with nickel, due to an insufficient attack of the alkali.
- Alumina trihydrate ($Al_2O_3 \cdot 3H_2O$) as gibbsite or bayerite, resulting from the hydrolysis of $NaAlO_2$ and from Al_2O_3 due to the oxidation of the alloy.
- Sodium, as $NaAlO_2$ and NaOH, present to about 0.2 mg Na/g Ni.
- Traces of nickel aluminate, $Ni(AlO_2)_2$, nickel oxide NiO, C, Si, Fe.
- Important amounts of hydrogen, between 12 and 380 cc (STP)/g.

X-ray diffraction studies showed that Ni, NiAl alloys and β-$Al_2O_3 \cdot 3H_2O$ are present in a crystalline form in the activated alloys. Nickel was found to crystallize in the f.c.c. system,

the mean crystallite size varying between 40-60 Å, and usually smaller than 100 Å, depending on the evacuation temperature and temperature of extraction[15]. A hexagonal nickel, which is a nonmagnetic form, can be obtained if special precautions are taken to prevent oxidation[16]. Robertson and Anderson[15] found a linear relationship between the surface area and the inverse of the mean crystallite size of Ni. X-ray diffraction patterns for alumina trihydrates had sharp peaks suggestive of large crystallites. Under aqueous alkali, increased reaction times, higher temperatures, and larger alkali concentrations give, in general, Raney nickels with decreased surface area, increased pore volume and mean pore diameter. It seems that the alumina imparts thermal stability to the catalyst, reducing the sintering effect due to treatment at higher temperatures.

1.4 LITERATURE REVIEW

1.4.1 Methods of Determination of the Hydrogen Content and its Nature in Raney Nickel Catalysts

The origin and the role of the hydrogen content of Raney nickel has caused much controversy and, despite numerous investigations, this problem has not been resolved satisfactorily. To determine the hydrogen content of the catalysts, several methods were designed, using different principles and conditions. Physical methods consist mainly of hydrogen desorption during heating of catalyst sample. For static measurements, the amount of hydrogen liberated is usually determined volumetrically; for dynamic systems determination is made in flow of an inert carrier

gas by means of a thermal conductivity cell. Chemical methods involve hydrogenation of unsaturated compounds in the absence of gaseous hydrogen, the use of different oxidants, amalgamation and electrochemical methods. The amount of hydrogen determined by chemical or electrochemical methods depends on the choice of environment (electrolyte) and this is usually different from the environment where hydrogenation is carried out. Because chemical and electrochemical methods of determining the hydrogen content are based on the oxidation of the hydrogen in the aqueous medium, there is a risk of oxidizing the nickel powder as well as the hydrogen[17] so the values for the hydrogen content may not correspond to the true amount of sorbed hydrogen:

$$Ni + 2H_2O \rightleftharpoons Ni(OH)_2 + 2H_2 \qquad (4)$$

$$Ni + 2OH^- \rightleftharpoons Ni(OH)_2 + 2e^- \qquad (5)$$

Any reactant SH is capable of producing a similar reaction:

$$Ni + 2SH \rightleftharpoons NiS_2 + H_2 \qquad (6)$$

The residual aluminum may also react:

$$2Al + 6H_2O \rightleftharpoons Al(OH)_3 + 3H_2 \qquad (7)$$

so the amount of calculated hydrogen is in excess of the true quantity of sorbed hydrogen.

In the thermal desorption of hydrogen special precautions should be taken to eliminate every trace of the storage liquid,

otherwise nickel and especially aluminum could react with the catalyst impregnating liquid and evolve hydrogen, sometimes accompanied by violent and explosive reactions.

The Table 1-1 gives the principal methods of determining the hydrogen content of the Raney nickel catalysts and interpretations of the results concerning the nature of hydrogen.

From all these methods of determining the hydrogen content, the chemical and electrochemical ones, as it was mentioned earlier, are subject to a considerable error. This was demonstrated by Coenen's findings[38]. He treated a Ni/SiO_2 catalyst with quinone in dioxane solution at 60°C to determine the amount of hydrogen present in, or on, the catalyst and found 107 cc H_2(STP) /g Ni. High vacuum pumping and readsorption of hydrogen gave a value of 23 cc H_2(STP)/g Ni, which was obtained using another method, dissolution by acid and heating in vacuum followed by dissolution in acid. The extra hydrogen found by the chemical method was attributed to the oxidation of metallic nickel by water present on the catalyst carrier. NiO was detected by X-ray diffraction.

Based on measurements of surface area, differential thermal analysis, X-ray diffraction and magnetic and density determinations, Kokes and Emmett[25] give an answer to the following questions:

a) How is the hydrogen held by the nickel?

b) What influence does the hydrogen have on the magnetic properties of the catalyst?

Table 1.1

Summary of the Methods Used for Determination of Hydrogen Content and the Interpretations of the Results

Author	Method of Determination	Postulated Composition	cc H_2/g catalyst	Ref.
Raney	Weighing of the catalyst before and after heating at high temperature	Nickel hydride NiH_2	380	18
Bougault Cattelain Chabrier	Hydrogenation of organic compounds in the absence of gaseous hydrogen	Nickel hydride or Ni containing Ni hydride	140	19
Freidlin Ziminova	Same as above	Nickel with adsorbed and dissolved hydrogen	22(ads) 73(diss)	20
Sokolskii Bezverkhova	Hydrogenation of organic compounds in the absence of gaseous hydrogen, measuring the change in hydrogen concentration potentiometrically	Nickel with adsorbed and absorbed hydrogen	23(ads) 67(abs)	21
Csuros Dusza Petro	Hydrogenation of organic compounds in the absence of gaseous hydrogen	No opinion	130-220 depending on preparation	22

(continued next page)

Table 1.1 (continued)

Author	Method of Determination	Postulated Composition	cc H_2/g Catalyst	Ref.
Mozingo	Volumetric determination by heating a butylphtalate slurry to 250°C	No opinion	43-115 depending on preparation	23
Smith Chadwell Kirslis	Volumetric determination of the amount of evolved hydrogen by heating to high temperature	No indications of presence of NiH_2. Catalyst surface promoted with adsorbed hydrogen which is attached in metastable state	92-157 depending on preparation	24
Kokes Emmett	Same as above	Hydrogen bond with the d-band of Ni. Hydrogen is taken up in the Ni lattice by replacement of Ni atoms. A slight amount of adsorbed and dissolved hydrogen	40-100 depending on preparation	25
Vandael	Oxidation of Raney nickel by $KMnO_4$	Nickel hydride	380	26
Moreau	Selective oxidation of hydrogen by a mixture of O_2-N_2	Hydrogen adsorbed at the surface of the crystallites and easily displaced hydrogen in the interior of crystallites	85(chem) 55(inter)	27
Kagan	Anodic Oxidation	Nonstoichiometric hydride with a partial ionic character, formed at the surface of Ni and protected by other ionic and molecular layers of hydrogen.	120	28

(continued next page)

Table 1.1 (continued)

Author	Method of Determination	Postulated Composition	cc H_2/g Catalyst	Ref.
Mars Scholten Zwietering	Volumetric determination of hydrogen by heating at high temperatures and other methods	H_2 resulting from the reaction of Al and H_2O bound to alumina or adherent water. A relatively small amount of hydrogen is chemisorbed.	19-224 depending on the rate of heating	29
Tarama Kubomatsu Kishida		Same as above		30
Vidal Lefebvre Coussemant	Mild chemical oxidation		100	31
Menard Trambouze Prettre	Desorption by anodic oxidation of hydrogen bound to nickel	Solid solution of inserted hydrogen in a form (H^+-Ni^-) where the atoms play the same role as the atoms eliminated by leaching with alkali. H is an electron donor to the d-band of Ni and is present as H^+ inactive in hydrogenation	120	32
Bezaudun Dalmai Imelik Prettre	Raney nickel used as a negative electrode in a fuel cell. $Ni(OH)_2$ is formed	Reversible chemisorbed hydrogen and structural hydrogen	120(rev) 60(struc)	33

(continued next page)

Table 1 (continued)

Author	Method of Determination	Postulated Composition	cc H_2/g Catalyst	Ref.
Lenfant	Thermodesorption of nickel-boron catalyst with a surface of 25 m^2/g	Hydrogen weakly chemisorbed and hydrogen strongly chemisorbed	3.8 4.0	34
Jamey	Controlled anodic oxidation of Raney nickel	Hydrogen weakly bound to nickel and hydrogen strongly chemisorbed on the surface	22 22	35
Macnab Anderson	Thermodesorption and magnetization experiments	Interstitial hydrogen and/or oxidation of metallic Al by water	23-78 depending on preparation	36
Zapletal Soukup Ruzicka Kolomaznik	Chemical methods, anodic polarization and heat desorption (temperature programmed desorption)	Bonded hydrogen (weakly and strongly)	87-320 depending on preparation and method of determination	37
Fouilloux et al.	Thermodesorption	Chemisorbed hydrogen as H atoms	29.5-50	17,115

c) What influence does the hydrogen have on the catalytic activity?

They conclude that the hydrogen is held in the nickel in the form of substitutional replacement of nickel atoms in the lattice. The magnetic data showed clearly that the magnetization increases more or less linearly with the amount of hydrogen removed until about 90% is removed. If one assumes that each hydrogen atom contributes one electron and each aluminum atom can contribute 3 electrons to the d-band of the nickel atoms, the magnetic data seems to be explainable. In the case of W-6 Raney nickel, on the basis of chemical analysis and hydrogen content, the average number of additional electrons is 1.8 per nickel atom. It decreases to 0.76 when all the hydrogen is removed. If the magnetism depends on the number of additional electrons, the value of specific magnetization, σ, would be expected to increase from 14 to 35 erg/gauss/g as the hydrogen is removed and the slope would be 0.27 units per cc of hydrogen removed. If one assumes[41] that the magnetism disappears when the added electrons amount to 0.6 per atom, then the decrease of the number of additional electrons, due only to hydrogen, from 0.45 to 0.22 per nickel atom as the hydrogen is desorbed, would correspond to a change in σ from 14 to 35 units with a slope of 0.24 units per cc of hydrogen removed. The observed values show an increase from 19.5 to 35 units of specific magnetization and the slope has a value of 0.27 units/cc of hydrogen. These calculations are in satis-

factory agreement with the observed values and suggest that on an average each hydrogen contributes an electron to the nickel.

The same phenomenon is observed by Macnab and Anderson[36] who found that the saturation magnetization at 0 K increases linearly with the amount of hydrogen evolved from two different types of Raney nickels, with different hydrogen contents. As hydrogen was removed from Raney nickel by heating, the magnetization increased about 0.63 μ_B per hydrogen atom (μ_B = Bohr magneton) which may be compared to 0.55-0.60 from other work on Raney nickel[25,17] and to 0.71 obtained for the chemisorption of hydrogen on supported nickel[39,40]. A possible interpretation is the presence of a nickel-aluminum-hydrogen alloy in the activated catalyst.

A completely different view from that of Kokes and Emmett on the nature of hydrogen in Raney nickel was presented by Mars, Scholten and Zwietering[29] at the 2nd International Congress on Catalysis held in 1960 in Paris. They presented evidence that part of hydrogen (ca 23 cc/g Ni), in Raney nickel was formed by the reaction of residual aluminum (present as AlNi or Al_3Ni_2) and water bound to alumina present in the catalyst, when the catalyst was heated. About 27 cc H_2/g Ni was present as chemisorbed hydrogen and a varying amount of hydrogen, depending on the experimental conditions was formed by the reaction of adherent water with aluminum (bound in AlNi or Al_3Ni_2). It was ascertained that only aluminum was oxidized during hydrogen formation, not nickel; NiO was not detected after heating the sample to 250°C. Mars, et.

al., did not find a linear relation between the change in magnetization and the amount of hydrogen removed. However, it supported the conclusion that only part of the total amount of hydrogen evolved was bound directly to the nickel lattice.

The French and Russian schools of thought[32,42] regard Raney nickel as an insertion solid solution where the hydrogen is involved in the following equilibria:

$$H_2(g) \rightleftharpoons 2H(ads) \rightleftharpoons 2H^+(ads) + 2e^- \rightleftharpoons (H^+\text{-}Ni^-) \quad (8)$$

$$\downarrow + \text{acetone} \qquad \downarrow + 2OH^-$$

$$\text{isopropanol} \qquad 2H_2O$$

In addition to this hydrogen there is the catalytically active hydrogen, chemisorbed on the surface of Ni atoms in a ratio 1H/1Ni. Magnetic data[35] seem to support this view on the nature of hydrogen in Raney nickel.

1.4.2 The Hydrogen Content and the Catalytic Activity

The relationship between the catalytic activity and the hydrogen content of Raney nickel has been the subject of a considerable amount of research. A direct correlation between the hydrogen content of the catalyst and its catalytic activity was noted by Freidlin and Ziminova[20]. They found that the Raney nickel used in the hydrogenation of organic compounds lost its activity when all the hydrogen was removed from the catalyst. Smith, et.al.,[24] showed that the activity of these catalysts in the hydrogenation of benzene at 80°C is a function of hydrogen content. Kokes and Emmett[25] found that the activity of Raney

nickel for ethylene hydrogenation and para-hydrogen conversion at first decreases and then increases when the hydrogen contained in these catalysts is removed. At the beginning they attributed this phenomenon to the removal of traces of oxygen poison from the surface of nickel, which increased the activity of the catalyst. Later, they explained that the hydrogen is influencing the activity of the nickel because of electronic factors. The authors attributed to the alumina, contained in the catalyst, the role of promoter.

Sassoulas[13] showed that the differences in the catalytic activity of Raney nickels prepared from alloys with different compositions weredue to a different attack of the surface of the alloy by the alkali so the final catalysts had surfaces of a different nature. The state of the surface was defined by the sites occupied by hydrogen atoms, water and by the free sites.

Menard, et.al.,[32] noticed an increase in the activity of Raney nickel when a fraction of the hydrogen adsorbed on the surface is removed by anodic oxidation: this was the strongly chemisorbed hydrogen which poisoned the catalyst. Csuros and Petro[43] found a maximum in the activity when a certain amount of hydrogen (140 cc/g) is contained in the catalyst.

Mars, et.al., based on activity measurements of Raney nickels in gas and liquid phase for reactions like hydrogen-deuterium exchange, and the hydrogenations of cyclohexene, ethylene, and phenol, demonstrated that the intrinsic activity of Raney Nickel, Ni/ZnO, Urushibara catalyst (Ni/Al_2O_3), and Ni from NiO

is about the same. The authors suggest that any difference in catalytic activity between Raney nickel and other nickel catalysts may arise from secondary effects, like differences in pore structure and hence in diffusion and differences in poisoning and surface area.

CHAPTER 2

PREPARATION OF RANEY NICKEL

2.1 GENERAL

The preparation of Raney nickel consists of two phases:

1) preparation of the Ni-Al alloy.

2) the activation of the alloy.

The alloy A, mostly used in this work, contained nominally 50 wt % nickel and was supplied by W. R. Grace Co. The alloy was crushed, sieved and the 100-200 mesh fraction used throughout. The composition of the alloy was determined by wet chemical methods and atomic absorption spectroscopy: Ni 49.92 wt %, Al 48.67 wt % and Fe_2O_3 0.97 wt %. The alloy B, nominally 42 wt % nickel was used to prepare samples (by S. D. Robertson) only for thermodesorption experiments. The phase content was investigated by optical microscopy and electron probe microanalyzer by Freel et al [14]. Concentrations of the three phases present in each alloy were estimated by standard metallographic procedures and are given in the Table 2.1 [14].

2.2 ACTIVATION OF THE ALLOY. EXPERIMENTAL AND DISCUSSION

The activation of the alloy with aqueous sodium hydroxide was done in a 1-liter round-bottomed 4-neck flask immersed in a thermostatted water bath. Under the water bath a magnetic base

Table 2.1

Chemical and Phase Composition of Starting Alloys

Alloy Designation	Nominal comp. (wt % Ni)	Ni analysis (wt. % Ni)	Metallographic Analysis[a] Ni_2Al_3 (av.vol %)	$NiAl_3$ (av. vol %)	Eutectic (av.vol. %)
A	50	50.1	59	40	~ 1
B	42	40.5	45	32	23

a: A description of the intermetallic phases present in the Raney nickel alloy is given in the Introduction.

was placed to stir the solution in the flask. Aqueous sodium hydroxide was supplied through one of the 4 necks of the flask from a 50 ml graduated burette. A thermometer measured the temperature of the solution during extraction. A rubber tubing was connected to a wet test meter, which was used to measure the hydrogen evolved. All the 4 necks of the flask contained gas tight seals lubricated with temperature resistant silicone grease. The contents of the flask were stirred vigorously during the extraction and washing procedures.

Method II[14] of preparing the catalyst involved the stepwise addition of 40% aqueous sodium hydroxide to a suspension of about 35 g of alloy A in 250 ml distilled water. The Raney nickel alloy was admitted to the reaction flask and 250 ml distilled water added. The suspension was allowed to warm to 50°C and NaOH was added from the burette. The reaction was initiated

by 10 ml of NaOH and similar volumes were added every 10 minutes for the first 1/2 hour. Larger additions were made at 5-minute intervals until 200 ml of NaOH was added. The procedure resulted in fairly constant solution temperature; in the first 10 minutes of alkali addition, the highest recorded temperature was 62°C, the reaction being highly exothermic. After 1/2 hour the temperature was about 54°C. Most of the hydrogen evolution occured in the first 1/2 hour in dilute alkali, the final part in concentrated NaOH. After the hydrogen evolution ceased, the sodium hydroxide solution was decanted off and the catalyst washed several times with distilled water in situ and then stirred and washed in an Erlenmeyer flask, with three separate washings . Finally it was washed and stirred 3 times with absolute ethanol and stored in a plastic jar under absolute ethanol at 0°C. The ethanol was replaced after one night. During washings hydrogen bubbles were evolved from the catalyst.

The catalysts prepared from the alloy A using the method II were termed IIA. The duration of extraction was approximately 1 hour. When the extraction was extended to 4.5 hrs, it led to catalysts with lower alumina content.

To obtain a catalyst with a high alumina content (method IV) less alkali than that required to convert the aluminum content of the alloy to sodium aluminate is used (Dirksen and Linden , ref. 75). In the present work to obtain a high-alumina-content Raney nickel, 34 g of alloy A in 270 ml distilled water was treated

with 250 ml of 22% NaOH for 3.5 hours at 50°C. The IVA Raney nickel obtained had about 49% $Al_2O_3 \cdot 3H_2O$. For this case the more dilute aqueous solution of sodium hydroxide favored the hydrolysis of the sodium aluminate formed:

$$2NaAlO_2 + 4H_2O = Al_2O_3 \cdot 3H_2O + 2NaOH. \qquad (1)$$

A summary of the extraction conditions and chemical composition data for different types of Raney nickel is given in the Table 2.2. The percent hydrogen evolved was calculated from the ratio of the total volume of hydrogen produced in the reaction and measured with the wet test meter and the volume of hydrogen which should have been evolved if all the aluminum in the alloy reacted with alkali. This ratio can be taken only as an approximate degree of activation of the alloy. Evolution of H_2 gives an indication of the end of the reaction between Al and NaOH. It also can be used in preparing a partly activated catalyst, when the reaction is "quenched" by flushing the catalyst with large quantities of ice cold water. Because the hydrolysis of $NaAlO_2$ regenerates NaOH for additional attack upon the alloy, the aluminum oxidation cannot be predicted from the amount of alkali used. The only accurate method for determining the fraction of Al oxidized is from the chemical composition of the catalyst. The following relationship gives the percent oxidation:

$$\text{wt\% Al oxidized} = 100((Al/Ni)_{alloy} - (Al/Ni)_{catal.})/(Al/Ni)_{alloy} \qquad (2)$$

where $(Al/Ni)_{alloy}$ and $(Al/Ni)_{catal}$ are the ratios of the Al and Ni content in the alloy and in the catalyst. Comparing columns

Table 2.2

Summary of Extraction Conditions and Chemical Composition Data for Various Raney Nickels

Sample Notation	Extraction Conditions: Time (min)	Temp (°C)	Conc. of alkali (wt %)	NaOH(g)/Alloy (g)	Final Dilution[a] (ml)	% Hydrogen Evolved	% Al Oxidized	Chemical Analysis: Ni (wt %)	Al_{tot} (wt %)	Al_{Met} (wt %)	$Al_2O_3 \cdot 3H_2O$ (wt. %)	Fe_2O_3 (wt %)
II A-1	290	51.7±4.2	40	2.31	400	80.7	94.0	76.79	10.49	4.52	17.26	1.43
II A-2	90	57.7±4	40	2.07	405	77.0	95.7	70.67	11.77	2.97	25.45	0.92
II A-3	60	55.1±4.5	40	2.00	450	81.0	89.1	70.0	15.17	7.42	22.39	0.21
IV A	206	52.3±1.5	22	1.62	520	75.1	96.0	48.28	18.80	1.87	48.95	0.90

a: final dilution represents the total amount of water and aqueous alkali added to alloy.

7 and 8 from Table 2.2 it can be seen that if the hydrogen evolved was correctly measured, an extra amount of hydrogen was held by the catalyst. Most of this hydrogen is released during washings and in the first 24 hours of storage. However, for the Raney nickels the extra amount of hydrogen calculated in this way (about 130 cc (STP)/g) seems to be too large compared with the hydrogen content of the catalysts determined by other methods. Extended extraction times, high concentration of alkali and large NaOH/alloy ratios lead to catalysts of lower Al and alumina content (II A with ∿ 17.3 wt % $Al_2O_3 \cdot 3H_2O$). The alumina trihydrate in the IV A sample was identified by X-ray diffraction as crystalline bayerite. A smaller alumina content is obtained by extraction with boiling alkali at 107°C. The commercial catalysts prepared in this way by W. R. Grace Co. and termed COM Raney nickels contain about 7-10 wt % alumina trihydrate.

To minimize the hydrolysis of sodium aluminate to aluminum hydroxide, Sassoulas[13] washes the activated catalysts first with boiling 2N NaOH solution and then with decreasing concentrations (from 2N to N/32) of aqueous sodium hydroxide, followed by distilled water to a pH near 6. He obtained a catalyst with 0.2% alumina.

CHAPTER 3

EXAMINATION OF THE CATALYSTS

3.1 GENERAL

The physicochemical properties of a catalyst are important in determining its structure and usefulness for both laboratory and industrial applications.

The following sections describe the chemical composition of different types of Raney nickel, their X-ray powder diffraction patterns and adsorption properties. The Raney nickels used in this study were commercial catalysts, COM I and COM, (Davison Grade 28) supplied by the Grace Chemical Company and stored in distilled water at room temperature. The other catalysts examined were II A and IV-A types, the preparation of which was described in the preceding chapter. These samples were stored under ethanol at 0°C. All the Raney nickels were pyrophoric and they were kept wet with water or ethanol to prevent oxidation.

3.2 CHEMICAL ANALYSIS

3.2.1 Introduction

Most samples of catalysts were evacuated at room temperature for 24 hrs to remove the storage liquid from the catalyst; some samples were evacuated at 107-120°C. Nickel was analysed by standard gravimetric and volumetric methods and in some cases the results were checked by atomic absorption spectroscopy (AAS).

Aluminum was analyzed by standard volumetric methods and in some cases by AAS and iron was analyzed only by AAS. The analytical data are based on the weight of sample after evacuation. In estimating the composition of catalysts, nickel was assumed to be present as metallic nickel, aluminum as either metal or $Al_2O_3.3H_2O$ and iron as Fe_2O_3. Any difference between the total weight and the sum of the weights of total nickel, total aluminum and Fe_2O_3 was taken as the "$O_3.3H_2O$" component of the trihydrate provided that the estimated amount of aluminum calculated as present in the trihydrate did not exceed the total aluminum content[15]. Nickel and bayerite were identified by X-ray diffraction analysis (see next section). It has been shown that bayerite does not dehydrate appreciably during evacuation at 100-130°C[68].

3.2.2 Experimental Procedure

The gravimetric analytical procedure for nickel used in this study was the dimethylglyoxime method[69]. Nickel and aluminum were also determined by chelatometry using an analytical procedure supplied by W. R. Grace Co.[70]. Chelatometry provides an elegant technique for quick and easy determination of nickel in the presence of aluminum and iron without separation of nickel from the other metals. Samples containing 2 to 100% nickel and 1 to 100% aluminum can be analyzed by this method. The principle of the nickel chelatometric analysis is the following: the Raney nickel is dissolved by sodium hydroxide digestion, which dissolves the alumina and aluminum, followed by a nitric acid

treatment. An aliquot is reacted with triethanolamine to eliminate both aluminum and iron interferences[71] and nickel is titrated with EDTA in an ammonia medium using murexide as indicator. To determine Al by chelatometry an aliquot of the dissolved Raney nickel sample is treated with excess EDTA to complex both Al and Ni metals[72]. Excess EDTA is eliminated with a lead salt. Ammonium fluoride[71] is added to liberate all EDTA previously complexed with aluminum. EDTA is then titrated with lead nitrate to a xylenol orange end point.

To determine nickel by gravimetry, an aliquot from the Raney nickel solution is treated with tartaric acid to prevent precipitation of iron and aluminum by ammonia, and nickel is precipitated by an alcoholic solution of dimethylglyoxime from the hot, slightly ammoniacal solution. The sensitivity of the method is 4-5 ppm. The detailed description of the analytical procedures is given in Appendix A. The chemical analysis data of the various types of Raney nickels are given in tables 3.1 and A-1.1 and A-2.1. Most of the chemical composition data are based on the gravimetric Ni and volumetric Al analysis. For cases where 2 or 3 samples of the same type of Raney nickel were analyzed and the composition of one sample was significantly different than the others, the values obtained from volumetric and/or atomic absorption spectroscopy (AAS) Ni analysis and AAS values for Al were used to obtain the final chemical composition. The elemental Al content of the IV A catalyst has large

Table 3.1

Analysis of Catalyst Samples

Sample	Weight percent				
	Ni	Total Al	Elemental Al	$Al_2O_3 3H_2O$	Fe_2O_3
COM I	90.2± 0.3	6.1± 0.2	4.3± 0.3	5.3± 0.6	0.29± 0.02
COM I	90.5 "	6.2 "	4.6 "	4.6 "	0.29 "
COM	89.4 "	5.6 "	3.1 "	7.2 "	0.28 "
COM	89.2 "	5.9 "	3.5 "	7.0 "	0.29 "
[a]IIA-1	76.8 "	10.5 "	4.5 "	17.3 "	1.43 "
IIA-2	70.3 "	11.7 "	2.7 "	26.1 "	0.92 "
IIA-2	71.1 "	11.8 "	3.1 "	24.9 "	0.92 "
[b]IIA-3	69.9 "	14.9 "	7.1 "	23.0 "	0.22 "
[b]IIA-3	70.1 "	15.4 "	7.9 "	21.8 "	0.18 "
IV A	48.0 "	19.0 "	2.2 "	48.8 "	1.11 "
IV A	48.1 "	19.5 "	2.7 "	48.5 "	0.80 "
[c]IV A	49.5 "	17.9 "	1.0±0.1	48.7 "	0.80 "
Alloy A	50.1± 0.1	48.7± 0.1	-	-	0.97 "
Ni/SiO_2	8.63± 0.04	-	-	-	-

a: sample evacuated at 120°C

b: sample evacuated at 107°C

c: sample evacuated at 117°C

uncertainties, probably due to the nonhomogeneity of the sample and large alumina trihydrate content. Another source of error comes from the storage liquid which cannot be removed completely by evacuation at room temperature and leads to a higher weight of the sample than the actual weight. In this case the experimental Ni and total Al content is lower than the actual content.

3.3 X-RAY ANALYSIS

3.3.1 Introduction

In addition to nickel, Raney nickel contains small to moderate amounts of alumina trihydrate, aluminum metal and hydrogen, the last two presumably as solid solutions in nickel. X-ray powder patterns of the unactivated 50% Ni-Al alloy are those expected for a mixture of Ni_2Al_3 and $NiAl_3$[25]. A partly activated catalyst shows a diffraction pattern corresponding to the intermetallic phases present in the initial alloy and the nickel phase[13]. Free aluminum metal was not detected by X-ray diffraction, even in the partially activated Raney nickels. In a completely activated sample only face centered cubic nickel was detected[14,25] and alumina trihydrate[15,25] which is better crystallized than nickel. Mars et.al.[29] found in all the Raney nickel samples distinct lines of Al_3Ni_2 (or AlNi), but could not ascertain the presence of $Al_2O_3 \cdot 3H_2O$. The lattice constant of the cubic cell was determined by different authors and it was found to be slightly in excess of the a_o for pure nickel reported as 3.5238 Å, but significantly smaller than the

lattice constant of NiH, reported as 3.721 Å[66].

In this section X-ray powder data for COM and IV A Raney nickel are given, the phases identified and the cubic cell constant, a_o, calculated.

3.3.2 Experimental Procedure and Results

X-ray powder spectra (Debye-Scherrer method) were taken with a Philips Debye-Scherrer Powder Camera with a diameter of 114.83 mm (type PW 1024). A catalyst sample was transferred from its storage medium into a glass capillary which was sealed at the ends. The specimen was irradiated for 3 hours with molybdenum radiation monochromatized by using a zirconium filter (50 KV and 12 mA being the tube voltage and current, respectively). If the number of crystallites irradiated is sufficiently great, some crystals will, by chance, be at just the right orientation for Bragg reflection:

$$n\lambda = 2\ d\ \sin\theta \qquad (1)$$

where n is the order of reflection, λ is the wavelength of the monochromatic radiation in Å, d is the interplanar spacing (Å) and θ is the angle of reflection.

The reflected X-ray beams appear on cones centred on the direction of the incident beam, with 2θ as the semivertical angle of each cone. The 114.83 mm camera is designed so that 2 mm measured on the film is equal to 1° Bragg angle. The distance between the diffracted lines on the film are read on the film measuring instrument and using the Bragg law (1) the interplanar spacings d, are calculated. The X-ray wavelength λ used in calculations was 0.71069 Å.

COM Raney nickel presented strong but broad lines, characteristic to face centered cubic nickel. No other phase was detected. IV A catalyst had faint, but sharp lines, due to alumina trihydrate and stronger and broader lines, characteristic of nickel. The X-ray spectra are shown in Fig. 3.2 and the interplanar spacings are presented in Table 3.1. The diffraction lines for Ni, Al, NiO and several Ni-Al intermetallic phases are given in Table 3.3; gibbite and bayerite interplanar spacings are found in Table 3.4[65].

3.3.3 Discussion

The X-ray diffraction spectrum of the COM sample evacuated at 23°C shows the lines characteristic of face-centered-cubic nickel with a lattice constant of the cubic cell of 3.532±0.003Å. The lattice constant was calculated using the first 9 interplanar spacings in the COM X-ray spectrum and the formula:

$$a_o = d(h^2 + k^2 + l^2)^{1/2} \qquad (2)$$

where a_o is the lattice constant of the cubic cell in Å, d is the interplanar spacing in Å and h,k,l are the Miller indices for the respective reflective plane. The a_o for the COM catalyst is higher than a_o for a pure nickel sample (3.5238 Å) but this is to be expected for samples in which there is a solid solution with Al. Lattice spacings for solid solutions of Al in Ni increase about linearly with Al content; the work of Taylor and Floyd[63] leads to a linear relationship between the lattice

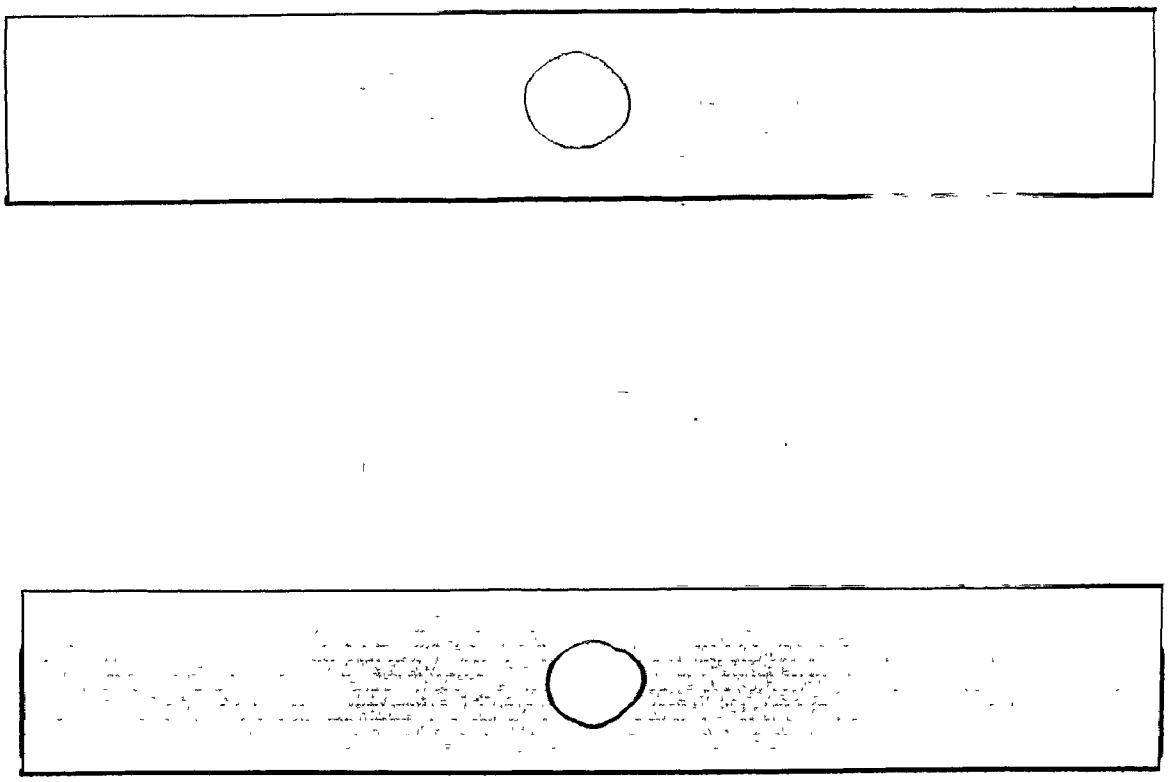

Figure 3.1. X-ray spectra of Raney nickels: upper figure - COM sample, lower figure - IV A sample.

Table 3.2

X-Ray Diffraction Analysis of the COM and IV A types of Raney Nickel

*COM type Observed Interplanar d Spacing (Å)	Nickel Interplanar d Spacing (Å)	Miller Indices hkl	*Type IV A Observed Interplanar d spacing (Å)	Bayerite $Al(OH)_3$ Interplanar d spacing (Å)	Miller Indices hkl
			4.72±0.46	4.72	001
			4.34±0.42	4.35	110,020
			2.19±0.31	3.20	111,021
			2.222±0.21	2.222	201,131
2.041±0.20	2.034	111	2.037±0.13		
1.763±0.17	1.762	200	1.767±0.17		
			1.725±-.17	1.723	202,132
			1.448±0.14	1.445	060
			1.392±0.13	1.392	331,160
			1.330±0.13	1.333	161,203
1.245±0.12	1.246	220	1.245±0.12		
			1.169±0.12	1.170	004,421
1.064±0.10	1.062	311	1.064±0.10		
1.019±0.10	1.017	222	1.018±0.10		
0.885±0.07	0.881	400			
0.811±0.07	0.808	331			
0.789±0.07	0.788	420			
0.720±0.07	0.719	422			
0.679±0.07	0.678	333			

*Error expressed as percent relative error

TABLE 3.3

X-ray diffraction data for Al, Ni, Al_3Ni, Al_3Ni_2, AlNi, and NiO.

Al	Ni C.F.C.	Al_3Ni	Al_3Ni_2	AlNi	NiO
			4,88 (11)		
		4,02 (40)			
		3,89 (70)			
		3,68 (50)			
			3,49 (12)		
		3,44 (100)			
		3,01 (60)			
			2,84 (10)	2,87 (40)	
		2,71 (3)			
		2,55 (30)			
		2,46 (40)			
		2,40 (20)			2,41 (91)
2,338 (100)					
		2,26 (5)			
		2,18 (70)			
		2,16 (80)			
		2,07 (100)			2,088 (100)
2,024 (47)	2,034 (100)	2,01 (40)	2,01 (100)	2,02 (100)	
		2,00 (90)			
		1,97 (70)			
		1,93 (100)			
		1,88 (30)	1,86 (7)		
		1,84 (30)			
	1,762 (42)	1,76 (20)	1,78 (3)		
			1,64 (3)	1,655 (20)	
			1,48 (3)		1,476 (57)
1,431 (22)			1,42 (20)	1,434 (20)	
			1,32 (2)		
			1,28 (3)	1,285 (10)	
					1,259 (16)
	1,246 (21)				
1,221 (24)			1,22 (2)		
			1,19 (2)		1,206 (13)
1,169 (7)			1,16 (65 B)	1,171 (70)	
			1,13 (3)		
	1,0624 (20)		1,05 (9)		1,044 (8)
			1,03 (4)		
1,0124 (2)	1,0172 (7)		1,01 (33 B)	1,015 (20)	
			0,983 (3)		
					0,9582 (7)
0,9289 (8)					0,9338 (21)
0,9055 (8)					
	0,8810 (4)				
					0,8527 (17)
0,8266 (8)					
	0,8084 (14)				0,8040 (7)
	0,7880 (15)				

TABLE 3.4

X-ray diffraction data for gibbsite and bayerite.

12-460

d	4.82	4.34	4.30	4.82	α-Al(OH)$_3$
I/I$_1$	100	40	20	100	ALPHA ALUMINUM HYDROXIDE (Gibbsite)

Rad CuKα λ Filter Ni Dia
Cut off I/I$_1$ DIFFRACTOMETER
Ref H. C. STUMPF, RESEARCH LABS., ALUMINUM CO. OF AMERICA, NEW KENSINGTON, PENNSYLVANIA.

Sys MONOCLINIC SG $P2_1/n$ (14)
a_o 8.641 b_o 5.070 c_o 9.719 A 1.704 C 1.917
α β 94°34' γ Z 8 Dx 2.44
Ref MEGAW, Z. KRIST. 87 185 (1934)

εα nωβ εγ Sign
2V D mp Color
Ref

SAMPLE PRECIPITATED FROM HOT SODIUM ALUMINATE SOLUTION; CONTAINS UP TO 0.3% Na_2O.

d Å	I/I$_1$	hkl	d Å	I/I$_1$	hkl
4.82	100	002	1.65	4	420
4.34	40	110	1.63	2	421
4.30	20	200	1.58	4	313,422
4.35	10	202	1.57	2	132
4.31	6	112	1.55	2	404
4.17	8	21$\bar{1}$,112			
4.08	4	10$\bar{3}$,202			Indexed by LGB
2.44	16	311,021			
2.42	4	004			
2.37	20	213,311			
2.28	4	21$\bar{2}$			
2.23	6	022,213			
2.15	8	312			
2.09	12	31$\bar{3}$,204			
1.98	10	025			
1.95	2	12$\bar{3}$			
1.90	8	411			
1.79	10	31$\bar{4}$			
1.74	10	024			
1.67	10	33$\bar{3}$,304			

20-11

d	2.22	4.71	4.35	4.71	Al(OH)$_3$
I I$_1$	100	90	70	90	Aluminum Hydroxide (Bayerite)

Rad CuKα λ 1.5418 Filter Ni Dia
Cut off I I$_1$ Diffractometer
Ref Rothbauer, Zigan and O'Daniel, Z. Krist., 125 317-31 (1967)

Sys Monoclinic SG $P2_1/a$ (14)
a_o 5.062 b_o 8.671 c_o 4.713 A 0.5837 C 0.5435
α β 90 27° γ Z 4 Dx 2.504
Ref Ibid V 206.86

εα nωβ εγ Sign
2V D mp Color
Ref

Synthetic.
d values calculated from cell dimensions, averaged for lines with multiple indices (hkl).

See following card

d Å	I I$_1$	hkl	d Å	I/I$_1$	hkl
4.71	90	001	1.969	2	041
4.35	70	110,020	1 917	2	122
4.14	<2	011	1 904	<2	230
3.29	<2	120	1 835	2	141
3 20	30	111,021+	1.826	2	032
2.699	4	121	1.765	<2	231
2.531	<2	200	1.723	40	202,132+
2.510	<2	130	1.695	2	212
2.464	2	031	1.688	2	212
2.430	<2	210	1.656	2	310
2.356	4	002	1.646	2	240
2.274	2	012	1.641	2	150
2.222	100	201,131+	1.628	<2	051
2 186	<2	220	1 600	10	222,042+
2 168	<2	040	1.572	2	320,003
2.164	<2	211	1.554	8	311,241+
2.156	2	211	1.523	<2	142
2.073	2	112,022+	1 520	<2	142
1.993	<2	140	1.492	2	321
1.983	4	221	1.484	<2	232

20-11A

d	2.22	4.71	4.35	4.71	Al(OH)
I I$_1$	100	90	70	90	Aluminum Hydroxide (Bayerite)

Rad λ Filter Dia
Cut off I/I$_1$
Ref

Sys SG
a_o b_o c_o A C
α β γ Z Dx
Ref

εα nωβ εγ Sign
2V D mp Color
Ref

See preceding card

d Å	I I$_1$	hkl	d Å	I/I$_1$	hkl
1.478	2	232,023+	1.242	<2	332
1.457	12	330	1.237	<2	332
1.445	8	060	1.235	<2	143
1.431	<2	250	1.233	<2	143
1.420	<2	123	1.232	<2	062
1.416	<2	124	1.225	2	252,401+
1.397	<2	052	1.212	8	420,261+
1.392	6	331,160+	1.199	2	170,071+
1.381	2	061,033	1.170	6	004,421+
1.370	<2	251	1.161	<2	342
1.368	<2	251	1.159	<2	430
1.358	<2	312	1.157	<2	342
1.348	2	312,242+	1.137	2	313,024+
1.333	18	161,203+	1.127	<2	251
1.320	<2	213	1.125	<2	431
1.311	<2	322	Plus 16 lines to 1.084		
1.305	<2	322			
1.277	2	341,223+			
1.265	<2	400			
1.254	<2	260,410			

constant a_o and the Al content in a Ni-Al solid solution:

$$a_o = 3.524 + 0.181 \cdot X_{Al} \quad (3)$$

where a_o is the lattice constant in Å of a Ni-Al solid solution with X_{Al} aluminum atom fraction. The aluminum content for the COM catalyst calculated by formula (3) gives a value of 2.08 wt % Al, compared with 3.47 wt % given by chemical analysis. Similarly for the IV A Raney nickel a_o was 3.530±0.005 Å

This value leads to 1.55 wt % Al, compared with 2.30 wt % obtained by chemical analysis. However, these values have moderately large uncertainties inherent to the Debye-Scherrer method used. Greater accuracy is possible than with film methods by using a diffractometer, since the diffraction peaks are recorded directly by a proportional counter.

The strong but broad diffraction lines characteristic to Ni presented by both COM and IV A X-ray spectra suggested small Ni crystallites. The faint but sharp lines characteristic to bayerite, $Al(OH)_3$, suggested that this material was present as fairly large crystallites in the IV A Raney nickel, in agreement with the findings of Robertson and Anderson[15].

The lattice constant a_o was 3.530-3.532 Å, much smaller than a_o for NiH, 3.721 Å; undoubtedly, there was no nickel hydride present in the Raney nickels analysed. Also, no nickel oxide was detected by X-ray analysis.

However, Janke and Michel[67] found by X-ray diffraction of a nickel cathodically charged with hydrogen, different combi-

nations between hydrogen and nickel. These compounds decompose easily at room temperature.

3.4 ADSORPTION STUDIES

3.4.1 General

A conventional glass vacuum system[45] was used to measure the surface area of the catalysts by the BET method and to perform chemisorption experiments. Each sample was placed in an adsorption tube and evacuated at room or higher temperatures overnight using a mercury diffusion pump backed by a conventional rotary oil pump. When the McLeod gauge indicated a pressure of less than 10^{-5} torr, the sample was ready for adsorption measurements. Adsorption data were calculated per gram of sample after this treatment.

3.4.2 Nitrogen Adsorption

The BET equation[46] was used to determine the surface area of the catalysts from the nitrogen adsorption isotherm at 77 K over a range of relative pressures from 0.05 to 0.3. The surface areas of different Raney nickel preparations are given in Table 3.5. All samples (except Ni/SiO_2) were stored in ethanol at 0°C or water at 25°C. The commercial Raney nickel showed a very good stability, as far as surface area is concerned; even after 3 years of storage in water the surface area remained virtually constant. Evacuation of the COM preparations at temperatures above 550°C sintered the catalyst decreasing the surface area by as much as 77 %.

Table 3.5

Summary of Surface Areas Determined from Nitrogen Adsorption Isotherm

Sample notation	Temperature of Evacuation (°C)	Storage Medium	Storage Time (months)	BET Area (m^2/g)
COM	23	Water	6	80.1
COM	23	Water	6	81.5
COM	23	Water	12	84.9
COM[a]	530	Water	18	15.0
COM[a]	537	Water	18	19.5
COM[a]	570	Water	18	7.5
COM[b]	580	Water	36	22.2
II A-1	23	Ethanol	19	34.8
II A-1	23	Ethanol	19	29.2
II A-1	570	Ethanol	* 6	10.1
II A-2	23	Ethanol	12	58.1
II A-2	23	Ethanol	12	59.7
II A-3	23	Ethanol	* 5	76.3
IV A	23	Ethanol	20	60.5
Ni/SiO_2	23	-		329.3

a: sample used in a thermodesorption experiment

b: sample used in determining a hydrogen isobar

*: days

Raney nickels II A and IV A stored under ethanol had a lower surface area after 2 years of storage, the area decreasing from 76.3 m^2/g to 32 m^2/g in 2 years of storage for the II-A catalyst. A possible explanation for the decreasing of the surface area with storage is the diffusion of oxygen from the atmosphere into the layer of Raney nickel. From simple considerations on diffusion transport in an absorbing layer Mars et.al.[47] calculated that for a Raney nickel stored in cyclohexane for 13 months, the oxidized layer is 1 cm deep. Experimentally they found 0.8 cm. For the samples stored under ethanol there is also the possibility of acetaldehyde formation and adsorption on Raney nickel decreasing in this way the surface area[64].

3.4.3 Surface Area of Nickel Metal

In addition to the nickel phase, Raney nickel may also contain unreacted alloy, β-alumina trihydrate and trace amounts of residual alkali. Several investigators have attempted to measure the amount of metallic nickel present in the surface. Kokes and Emmett[48] report a nickel area about 20% of the BET value; Huff et.al.[49] found 50% of the total area being nickel; Mars et.al.[29] concluded that 90% of the catalyst surface was metallic; Freel et.al.[50] found that the nickel area varied between 16% and 85% of the total BET area, depending on the type and treatment of the Raney nickel used. The surface area of metals can be determined by the chemisorption of a gas such as H_2 or CO, a brief evacuation period, to remove the weakly chemisorbed gas, followed by a second chemisorption[51-54]. The method used in this

study to determine the fraction of the surface as nickel was taken from ref. 50: a hydrogen isotherm H_2^I was done at -196°C, then the sample was evacuated at the same temperature for 30 minutes, and a second H_2^{II} isotherm determined. When CO is chemisorbed, the intermediate evacuation is done at -78°C. The difference in the volumes adsorbed in the two chemisorption experiments, $H_2^I - H_2^{II}$ and/or $CO^I - CO^{II}$ are used to calculate the the metallic surface area. The nickel metal area as m^2/g catalyst is given by the relation:

$$S_{Ni} = \frac{VN\sigma}{(2.24\times10^4)(10^4)} \qquad (4)$$

where V is $H_2^I - H_2^{II}$ or $CO^I - CO^{II}$ in cc/g; N is Avagadro's number and σ is the effective molecular coverage area as cm^2 per adsorbate molecule. The values used for σ were 13×10^{-16} cm^2 per molecule for carbon monoxide[48] and 12×10^{-16} cm^2 per molecule for hydrogen[53,17]. In the case of hydrogen it is considered that dissociative adsorption has occured, yielding a value of 6×10^{-16} cm^2 per hydrogen atom. If it is assumed that equal portions of most densely packed (111,110,100) planes of nickel are exposed and that 1 hydrogen atom is adsorbed on each nickel atom on the surface, then 1 cc of chemisorbed hydrogen will correspond to 3.64 m^2 of nickel surface [29, 35 page 24]. One nickel atom will have a surface of 6.77 $\mathring{A}^2$.

Surface nickel per g of catalyst is given by:

$$S_{Ni} = \frac{2V(58.7)}{2.24\times10^4} . \qquad (5)$$

It is assumed, again, that dissociative hydrogen adsorption occurs with one hydrogen atom for each surface nickel atom or molecular adsorption of CO occurs with a bridged orientation between two nickel atoms. For the situation where one molecule of CO adsorbs with a linear orientation on each surface nickel atom the factor 2 is omitted from the numerator in eq. (5). V is the chemisorbed gas as cm^3 (STP) per gram of catalyst and 2.24×10^4 is the molar volume in cm^3 (STP) of an ideal gas a 1 atm. and 0°C. The type of isotherms obtained for CO and H_2 chemisorption on a COM preparation is illustrated in Fig.3.2 and Fig. 3.3. Both isotherms are almost parallel and the volume of chemisorbed CO and H_2 are 19.8 and 8.0 cc/g,respectively. Using these values and eq. (4) nickel surface area is calculated for the commercial preparation. The data are presented in Table 3.6. A ratio of 2 will be expected between the volumes of CO and H_2 adsorbed, if CO is chemisorbed in the linear form Ni-C=O and H_2, dissociatively. The actual ratio is 2.47, probably due to the fact that hydrogen chemisorption is decreased by the hydrogen already present on the surface of nickel. The chemisorption of CO is decreased to a smaller extent by the hydrogen layer. The Dutch group[29] suggested that about 1/2 of the chemisorbed hydrogen remains on the Raney nickel after evacuation at about 90°C, and more hydrogen is left when the sample is evacuated at 23°C. On this basis the area estimated from hydrogen adsorption for the COM sample evacuated at 23°C

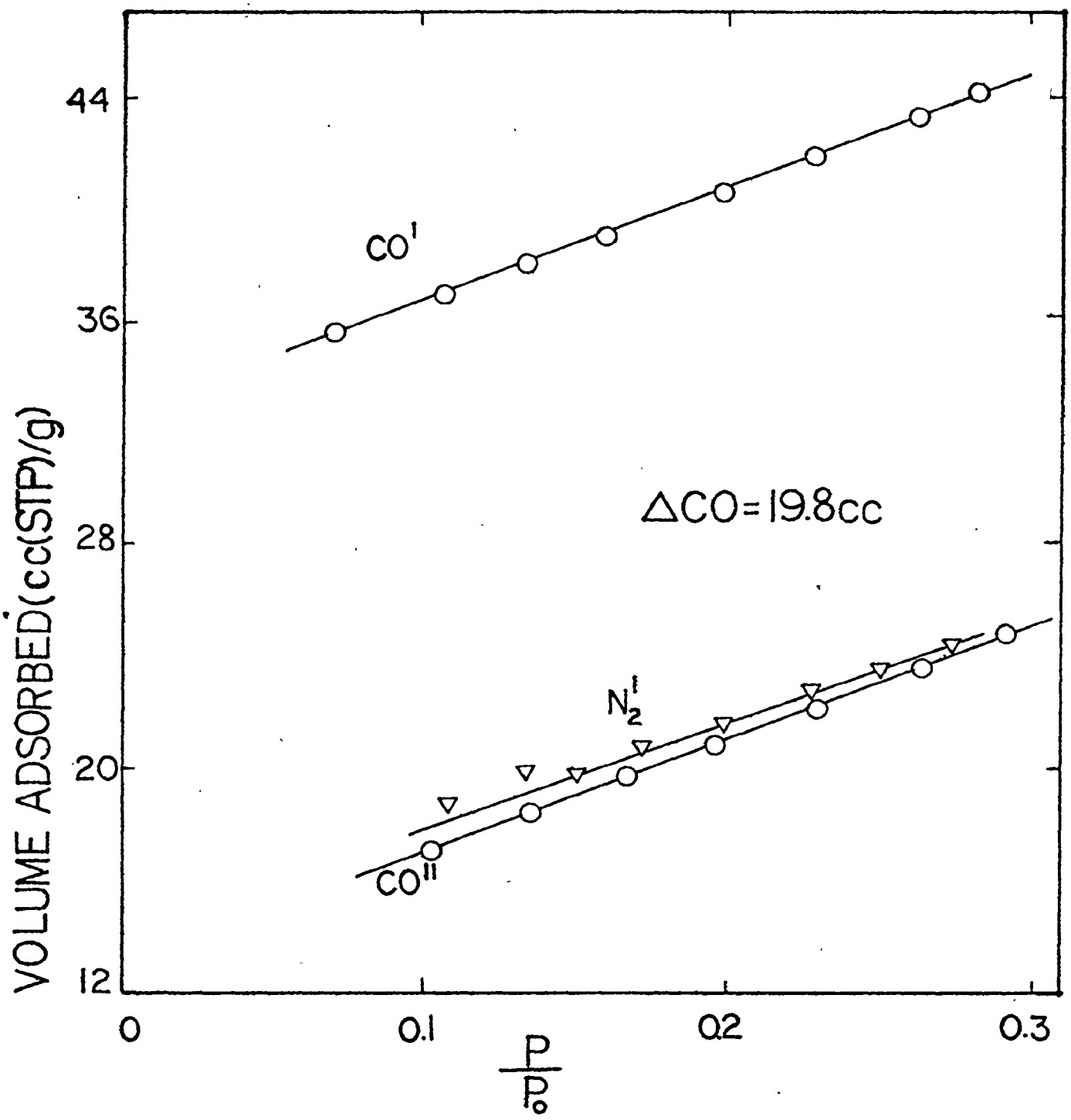

Figure 3.2 Adsorption of CO and N_2 on COM Raney nickel at -195°C : a) CO on sample evacuated at 23°C, CO^{I}; b) CO on previous sample after evacuation at -78°C, CO^{II}; c) N_2 at -195°C on fresh sample evacuated at 23°C, N_2^I.

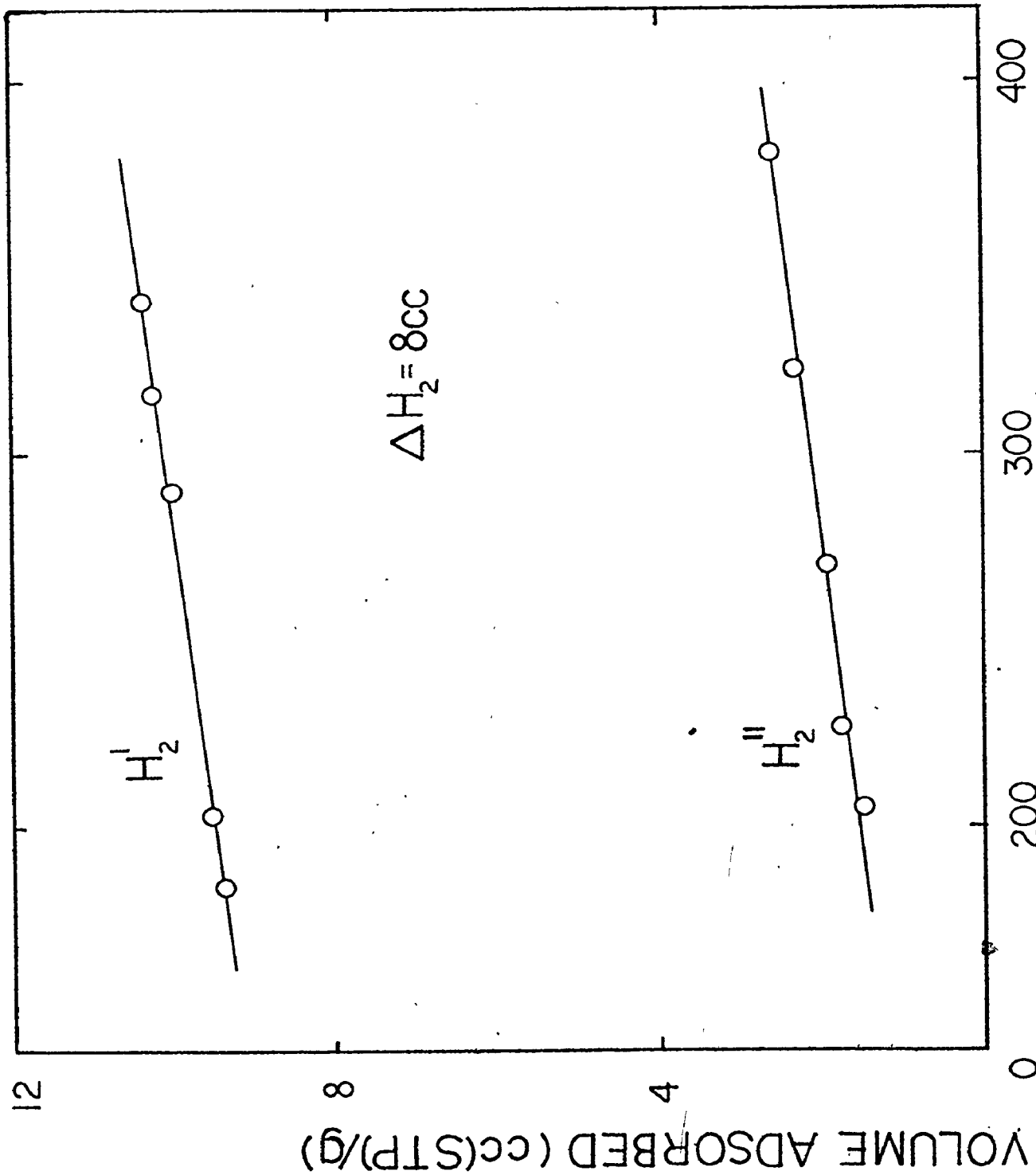

Figure 3.3 Adsorption of hydrogen on COM Raney nickel at -195°C: a) on catalyst evacuated at 23°C, H_2^I; b) previous sample after evacuation at -195°C, H_2^{II}.

Table 3.6

*Nickel Area from CO and H_2 Chemisorption at -196°C

Catalyst	Temperature of Evacuation (°C)	N_2-V_m (cc STP /g)	BET Area (m^2/g)	Total Nickel Content ($\frac{gNi}{gcat.}$)	ΔCO Chemisorbed $\frac{cc(STP)}{gcat.}$	ΔH_2 Chemisorbed $\frac{cc(STP)}{gcat.}$	Nickel Area $\frac{m^2Ni}{gcat.}$	Nickel Area % of BET	Surface Nickel wt % of total Ni
COM	23	18.3	80.1	0.905	19.8	-	69.2	86.3	5.73
COM	23	18.3	80.1	0.905	-	8.0	29.1	36.3	4.63
COM[a]	580	5.07	22.2	0.892	-	2.4	8.74	39.5	1.41
COM	570	1.7	7.5	0.905	1.07	-	3.72	49.6	0.31
Ni/SiO_2	23	75.2	329.3	0.0866	-	0.3	1.1	0.33	1.82

a: sample was used in an isobar adsorption experiment and was treated thermally in a different way than the others.

V_m: nitrogen monolayer

*: the precision of the adsorption measurements is ± 0.05cc(STP)/g

should be increased by, at least, a factor of 2. This correction substantially improves the agreement between values of fraction of surface as nickel determined from CO chemisorption (69.2 m^2/g) and H_2 chemisorption (29.1 m^2/g). Brooks and Christopher[53] found an average ratio of 2.64 between the volumes of CO and H_2 chemisorbed on a Ni/Al_2O_3 catalyst and Anderson et al.[50] report an average ratio of 1.7 (1.97 for the COM catalyst) for different Raney nickel catalysts. It should be mentioned that the chemisorption of both gases may be influenced by residual hydrogen remaining on the Raney nickel after evacuation at 23°C. Also the presence of residual alumina and the interaction of the catalyst and storage liquid occuring during storage could affect the chemisorption of CO and H_2.

3.4.4 Hydrogen Adsorption Isobars

3.4.4.1 Experimental Results

After examining the composition of the Raney nickel surface by the low temperature chemisorption of hydrogen and carbon monoxide, determination of isobars for hydrogen from -195°C to 580°C in both increasing and decreasing temperature sequences was done. The purpose of this work was to find out if the hydrogen adsorbed at higher temperatures decreases the chemisorption at -195°C. Two different samples were used in these experiments: II A and commercial Raney nickel, grade 28. The properties of these two catalysts are summarized in Table 3.7.

Table 3.7

Adsorption Data for COM and II A Raney Nickels

Catalyst	Storage Liquid	Age	BET area (m^2/g)	ΔH_2 cc(STP)/g	ΔCO cc(STP)/g	% Nickel[a] Area
COM	Water	3 years	80.1	8	19.8	69.2
II A[b]	Ethanol	2 months	92	9.4	14.4	59.3

a: nickel areas were estimated from CO chemisorption

b: adsorption data from ref. 50

The experimental procedure used for the COM sample was the following: Raney nickel was transferred under water into the adsorption tube and the storage liquid removed by evacuation. When no more liquid was left on the sample, the adsorption tube was heated to 106°C and evacuated for 40 hrs. This precaution was taken in order to prevent an explosive reaction occurring between the storage liquid and the catalyst during evacuation. When the McLeod gauge indicated a vacuum of about 10^{-5} torr, the sample was weighted (0.9134 g) and the experiment was started. The dead space was measured with helium. An amount of hydrogen of about 78 cc(STP) was introduced over the sample at a pressure of about 300 torr and a temperature of -196°C (liquid nitrogen bath). The "equilibrium" was reached in 3 minutes but 2 more hours were allowed to see if any further adsorption occured. Then the temperature was increased to -77°C (dry ice and acetone

bath) and, successively to 0°C, 25°C and 106°C; the same procedure was used in decreasing the temperature from 106°C to -196°C. The catalyst was evacuated overnight at 251°C and another isobar was taken. The same procedure was repeated for evacuation temperatures of 400°C and 580°C. The isobar for the evacuation temperature of 23°C was done with a fresh sample evacuated for 24 hrs at room temperature. The adsorption data for the II A Raney nickel were taken in an increasing temperature sequence from -196°C to 0°C and then back to -196°C. The isobar was then continued to higher temperatures, the maximum adsorption temperature being the temperature of the evacuation of the catalyst. The adsorption data for the hydrogen isobars are presented in Tables 3.8 and 3.9. The amounts of hydrogen adsorbed per gram of catalyst after a maximum equilibration time of 2 hours at 300 torr for COM and 140 torr for II A Raney nickel as the temperature is raised in steps from the lowest temperature, i.e., -196°C are shown in the third column. The 4th column in each case gives the data for adsorption as the temperature is lowered in steps from the highest temperature to -196°C. The corresponding adsorption isobars are plotted in Figs. 3.4 and 3.5.

3.4.4.2 Discussion of the Hydrogen Isobars

The hydrogen isobars 1 and 2 (Fig. 3.4) for the COM Raney nickel are similar to those of Benton and White[55] for Ni powder catalysts and Taylor and Sadek[56] for nickel on kieselguhr. The ascending temperature isobars show a minimum at -77°C and a sharp rise in adsorption from -77°C to 0°C. The descending

Table 3.8

Hydrogen Adsorption Isobars on COM Raney Nickel at $P_{H_2} \approx 300$ Torr

Temperature of Evacuation (°C)	Temperature (°C)	Volume of H_2 adsorbed cc(STP)/g	
		Increasing Temperature	Decreasing Temperature
23	-196	5.31	10.02
	- 77	3.56	7.74
	0	6.85	6.98
	23	6.89	
106	-196	8.25	13.90
	- 77	6.55	11.58
	0	8.95	10.86
	25	9.63	10.72
	106	10.08	
251	-196	9.21	11.28
	- 77	7.46	9.03
	0	6.62	8.02
	25	6.47	7.85
	82		7.25
	106	6.32	
	250	5.42	
400	-196	4.50	7.62
	- 77	5.05	5.72
	0	4.35	4.71
	25	4.17	4.55
	117		3.73
	197	3.06	
	357	2.09	
580	-196	2.58	3.64
	- 77	1.82	2.34
	0	1.82	1.97
	24	1.72	1.93
	102		1.63
	105	1.47	
	237	1.01	
	537	0.32	

Table 3.9

Hydrogen Adsorption Isobars on II A Raney Nickel at $P_{H_2} \approx 140$ torr

Temperature Evacuation (°C)	Temperature (°C)	Volume of H_2 adsorbed cc(STP)/g	
		Increasing Temperature	Decreasing Temperature
0[a]	-196	3.11	8.07
	- 77	5.52	5.98
	0	5.01	
204	-196	4.48	10.37
	- 77	7.29	8.51
	0	6.91	
	27	7.08	
	198	5.68	
302	-196	7.38	10.95
	- 77	7.00	7.31
	0	6.00	
	27	5.55	
	113	4.79	
	201	4.15	
	300	3.17	

a: sample evacuated at 0° for 96 hrs.

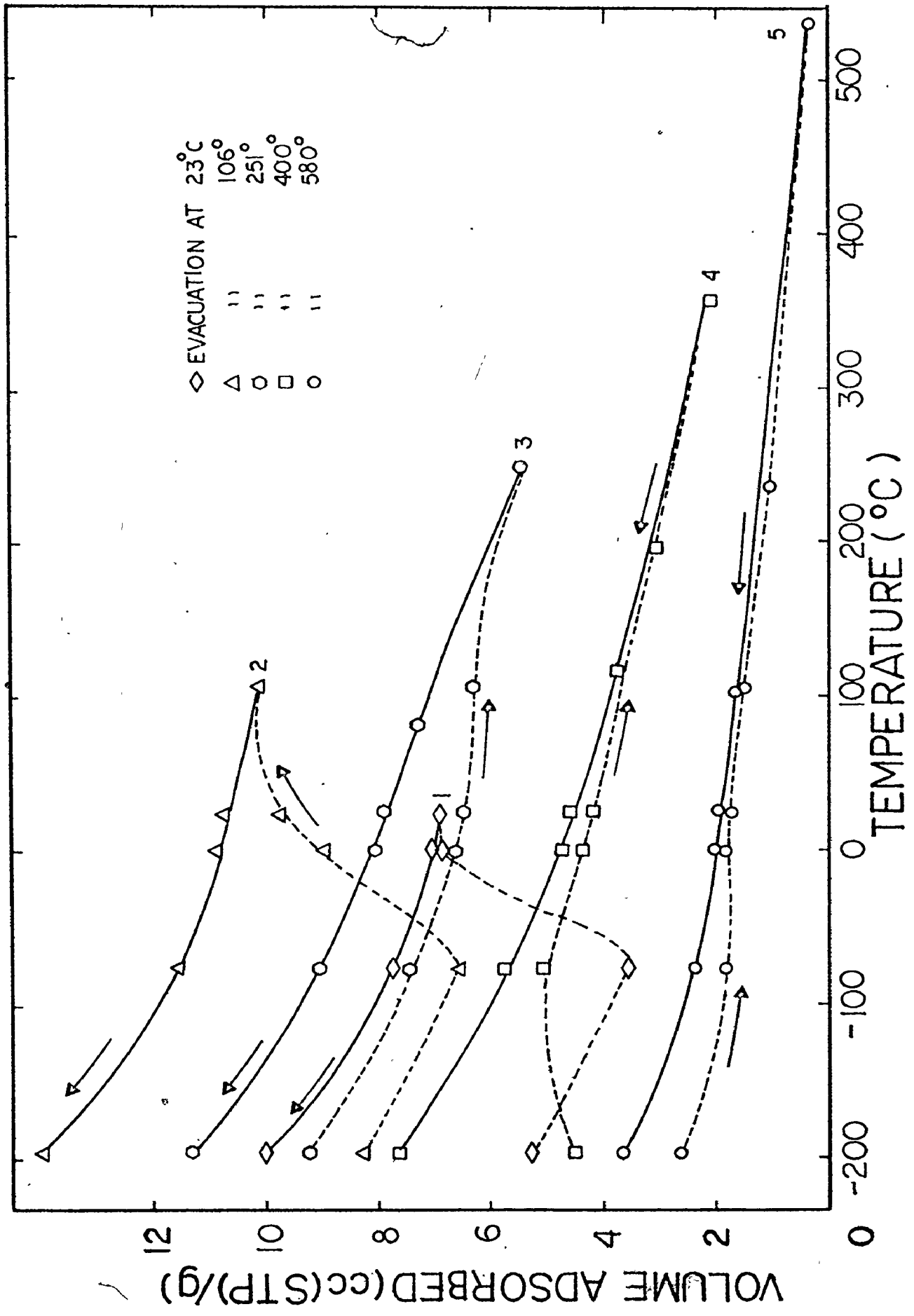

Figure 3.4 Hydrogen adsorption isobars on COM Raney nickel.

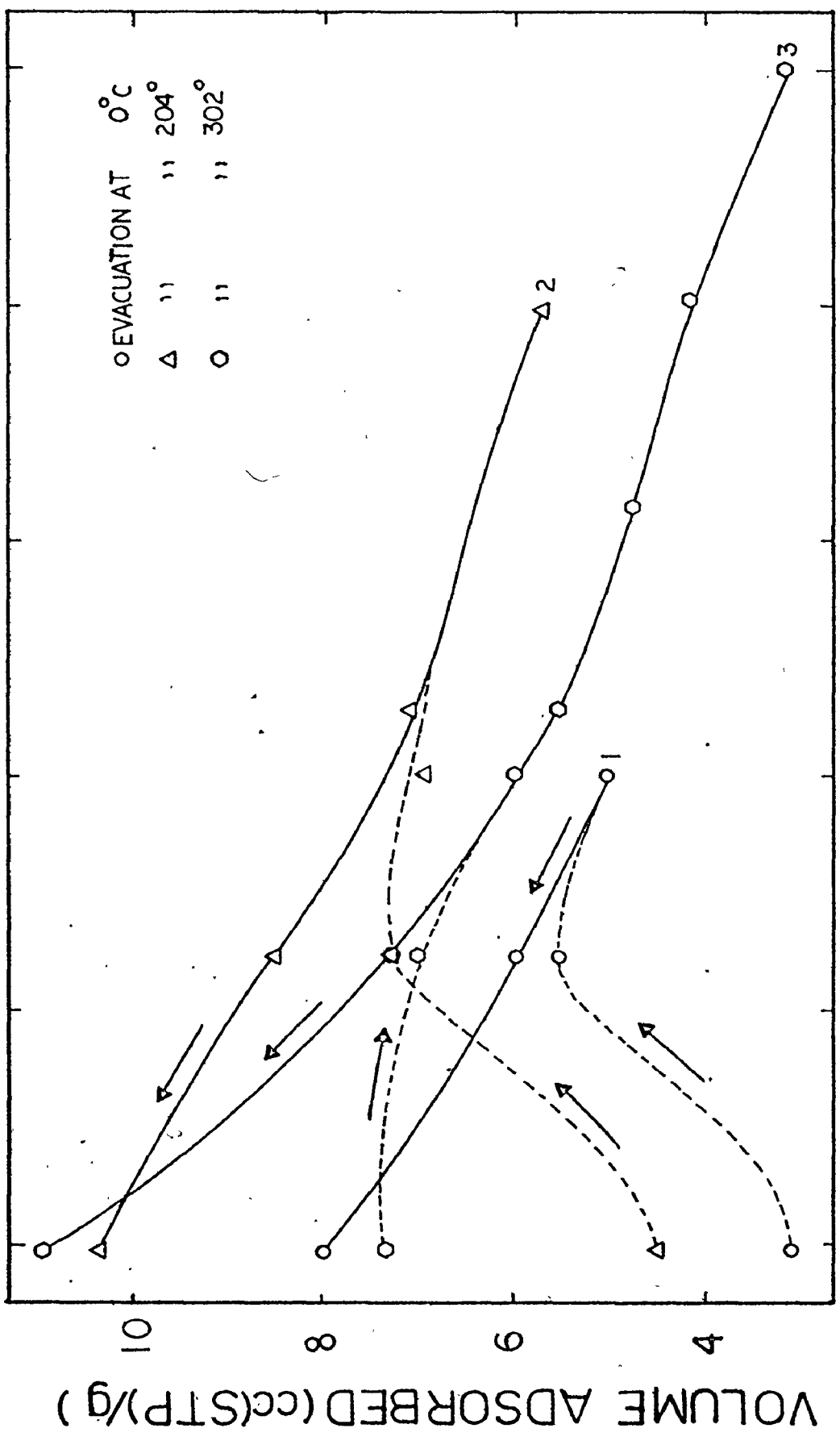

Figure 3.5 Hydrogen adsorption isobars on II A Raney nickel

temperature isobars 1 and 2 deviate progressively from the ascending temperature isobars, the maximum deviation being at -77°C and -196°C. The other isobars (4 and 5) do not have a minimum, but they also show a maximum deviation for the descending temperature isobars at -196°C. The descending temperature isobar 3 has an almost constant (∿ 21%) higher adsorption than the ascending one. The maximum deviation between the ascending and the descending temperature isobars for the II A catalyst occurs at -196°C for all three curves. The minimum in the isobars 1 and 2 for the COM catalyst can be explained as follows.

Chemisorption frequently has an activation energy and proceeds at a limited rate which increases with increasing temperature. The rate only becomes measurable above some minimum temperature. One therefore encounters the anomaly that the amount chemisorbed may increase with increasing temperature. Taylor[57] discussed this kind of isobar with the aid of a diagram similar to Fig. 3.6. The curve ABCD represents the isobar for the measured, or total, adsorption. The curve ABB' is the equilibrium curve for low temperature adsorption or type C chemisorption (ref. 58, page 93) and the curve C'CD is the equilibrium curve for chemisorption, each falling monotonically with increasing temperature. At low temperature the rate of chemisorption is so slow that the amount taken up within the period of each measurement is negligible. At B the rate is high enough to produce an appreciable contribution to the total adsorption. The contribution of the chemisorption to the total adsorption increases along the line BC and at C the equilibrium is reached. The curve BC represents a false equilibrium and adsorption continues to increase as a function of time along BC. Along CD the contribution of the low temperature adsorption becomes negligible.

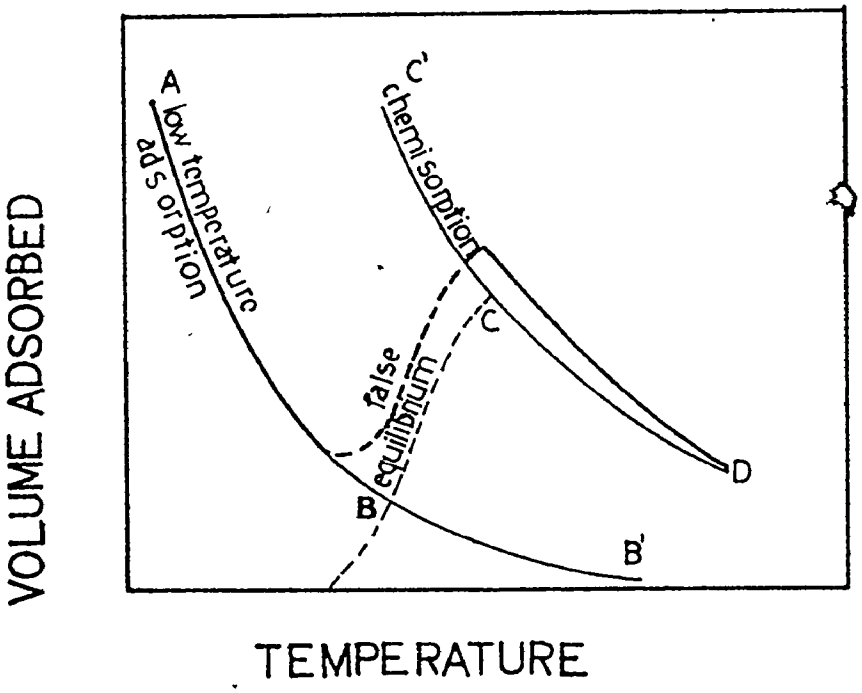

Figure 3.6 Adsorption isobar

As the critical temperature of hydrogen (-241°C) is significantly lower than the lowest temperature at which the adsorption measurement was done (-196°C), it is not likely that the physisorption of hydrogen occurred on the COM Raney nickel, but only a low temperature chemisorption took place in the range -196°C → -77°C. On evaporated nickel films the processes of chemisorption were rapid and complete down to temperatures of liquid nitrogen[59] and on reduced nickel catalysts Euken and Hunsmann[60] found that at liquid air temperatures and higher the process occurring was chemisorption with a heat of adsorption of ∿ 20 Kcal/mole.

A second feature presented by all isobars is that adsorptions with decreasing temperatures lie above the isobar for increasing temperatures, a phenomenon which was not observed with nickel films. As Taylor pointed out in 1947[61] this phenomenon is due to the non-uniformity of the nickel surface, i.e., that due to a combined operation of the heat of adsorption and the activation energy of adsorption, there might result conditions at a given temperature, under which only a fraction of the available surface might be involved in the activated adsorption. Because of the nonuniformity of the surface, on increasing the temperature, desorption occurs and, on cooling in the same temperature range there is an increased adsorption compared to the ascending isobar.

By increasing the evacuation temperature of the Raney

nickel the surface becomes more uniform, the difference between the ascending and the descending temperature isobar being smaller. The total amount of hydrogen adsorbed at -196°C for the COM sample decreases from 13.9 cc(STP)/g for the catalyst evacuated at 106°C to 3.64 cc/g for the evacuation temperature of 580°C, indicating that sintering has occurred (Fig. 3.7). Also, the total surface area decreased from 80.1 m^2/g to 22.2 m^2/g.

The highest adsorption capacity for hydrogen was presented by the COM catalyst evacuated at 106°C due to the removal of part of the hydrogen already present on Raney nickel (which starts to be evolved at ∿ 70°C) and of traces of storage liquid (water) which are probably still present on samples evacuated at 23°C. In determining the metallic surface area for COM Raney nickel evacuated at 23°C, an amount of 8 cc/g of hydrogen was found compared with 13.9 cc/g on the COM sample evacuated at 106°C. The adsorption of the extra 5.9 cc/g can be explained as follows:

1) The evacuation at 106°C created new adsorption sites for H_2 and/or removed some of the "adherent" water and hydrogen, or
2) the hydrogen was "absorbed" into the nickel lattice, probably as hydrogen atoms.

Freel et al.[50] found a maximum amount of chemisorbed H_2 at -196°C on a COM sample evacuated at 130°C of 9.6 cc/g. The total surface area of their Raney nickel was 82 m^2/g. This argument favors the hypothesis of hydrogen being present as a substitutional nickel-hydrogen solid solution. The solubility of hydrogen in

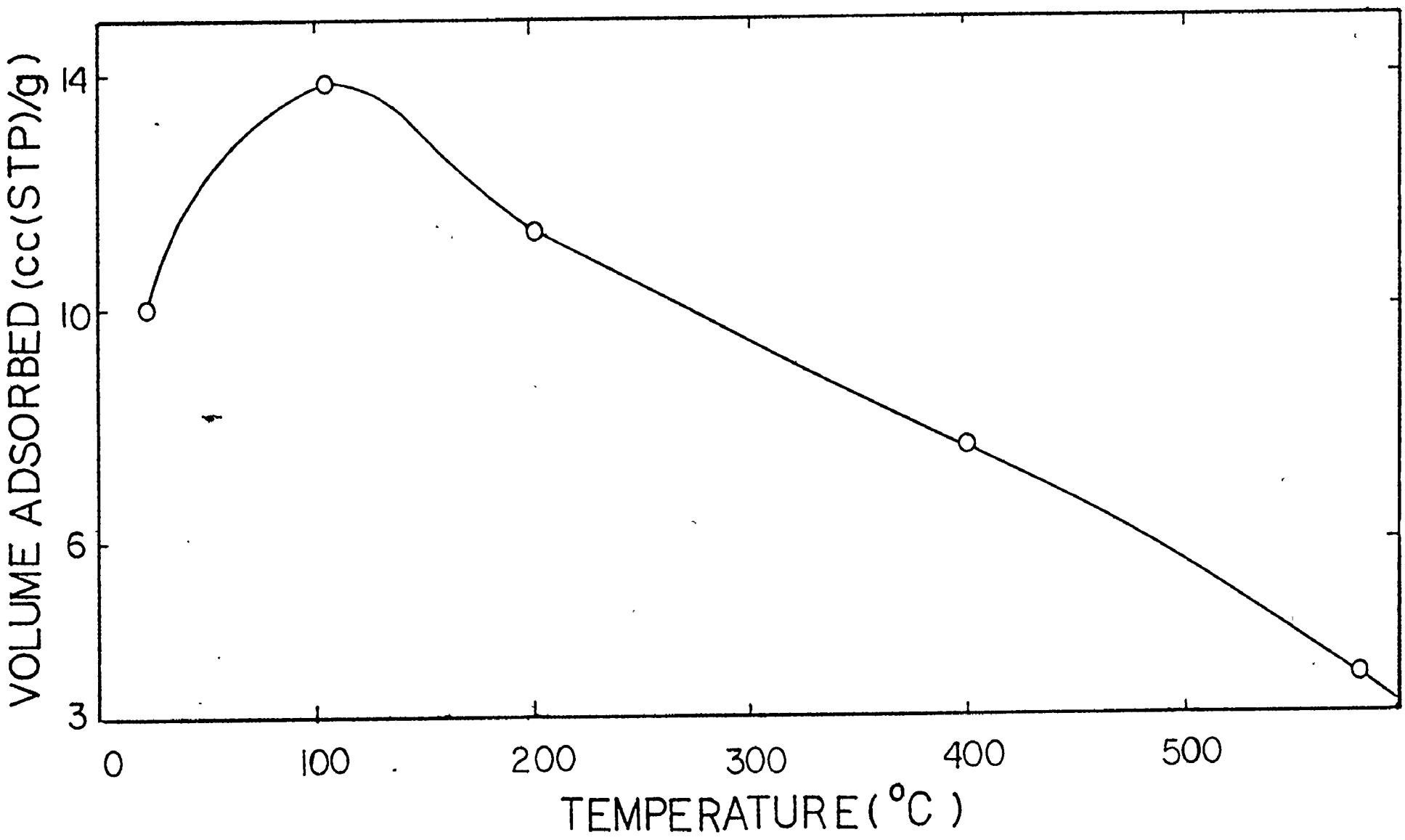

Figure 3.7 Hydrogen chemisorption at -196°C on commercial Raney nickel as a function of pretreatement.

the lattice or exothermic entry of hydrogen into the nickel lattice at temperatures between -195°C and -77°C was suggested by Beeck et. al.[62].

The II A Raney nickel evacuated at 302°C showed a maximum in adsorption of hydrogen at -196°C, but the rest of the isobar was below that of the curve 2 (see Fig. 3.5). Thus the II A evacuated at 204°C showed the maximum adsorption for hydrogen. In this case sintering started to occur after 300°C.

3.4.4.3 Conclusions

The isobars for COM Raney nickel showed a minimum and a maximum for the sample evacuated at 23°C and 106°C. The minimum and maximum were eliminated from the isobars at higher evacuation temperatures. There was a difference between the ascending and descending temperature isobars and the maximum in the adsorption of hydrogen at -196°C was noted for evacuation temperatures of 106-204°C.

The surface of Raney nickel is heterogeneous; evacuation at temperatures higher than 204°C favors a reduction in the heterogeneity of the surface and sintering.

The evacuation at temperatures between 106°C-204°C removed part of the adsorbed hydrogen and/or storage liquid from the catalyst surface, increasing the adsorption of hydrogen at -196°C.

CHAPTER 4

HYDROGEN EVOLUTION ON SOLUTION OF CATALYSTS IN HYDROCHLORIC ACID

4.1 GENERAL

One of the earliest methods of determining the hydrogen content of Raney nickel[76] is by dissolving it in acids and measuring the amount of hydrogen evolved. The equivalent amount of hydrogen formed by solution of the metal components is calculated from the concentration of metal ions in the acid solution assuming all were present as metals in the catalyst. The difference between the amounts evolved and calculated gives the hydrogen content of the catalyst. This method would seem ideal for measuring the hydrogen content of the catalyst, i.e., the hydrogen chemisorbed and dissolved in Raney nickel. The method eliminates the disadvantages of thermodesorption, i.e., the possibility of oxidation of elemental aluminum at higher temperatures by the storage liquid or water associated with the alumina trihydrate and producing additional hydrogen. However, the accuracy of the method is low due to several factors which will be discussed later. This chapter presents the hydrochloric acid dissolution of commercial catalysts to determine their hydrogen content and the amalgamation of Raney nickel with evolution of hydrogen.

4.2 EXPERIMENTAL PROCEDURE AND RESULTS

The hydrogen evolved during the dissolution of Raney nickel in hydrochloric acid was measured in a volumetric adsorption apparatus equipped with a manostat and a calibrated burette. The description of the apparatus will be given in the next chapter. The adsorption bulb was large enough (37 mm diameter) to accomodate HCl solution required for the complete dissolution of the catalyst. The samples were evacuated overnight at 23°C until the vacuum reached 10^{-5} torr and then the weight of the dry sample was determined. Correction for the error introduced by the weight of the air removed by evacuation was made. The void space of the apparatus, a liquid nitrogen trap and adsorption tube was determined with helium at 23°C. The procedure is identical with that used for the thermodesorption and described in Appendix B. An aqueous solution of HCl was poured into the funnel b (see Fig. 4.1) making sure that no air bubbles were formed. To slow down the violent reaction between Raney nickel and hydrochloric acid, the adsorption bulb c was immersed in a liquid nitrogen bath. The teflon stopcock a was then opened carefully to allow small amounts of aqueous HCl to reach the sample. The acid solution froze instantaneously and it was allowed to melt and react with the catalyst first in an ice bath and finally at 23°C. In some cases a hot water bath was used or the bulb was gently heated with a flame to dissolve as much Raney nickel as possible. A liquid nitrogen trap was used

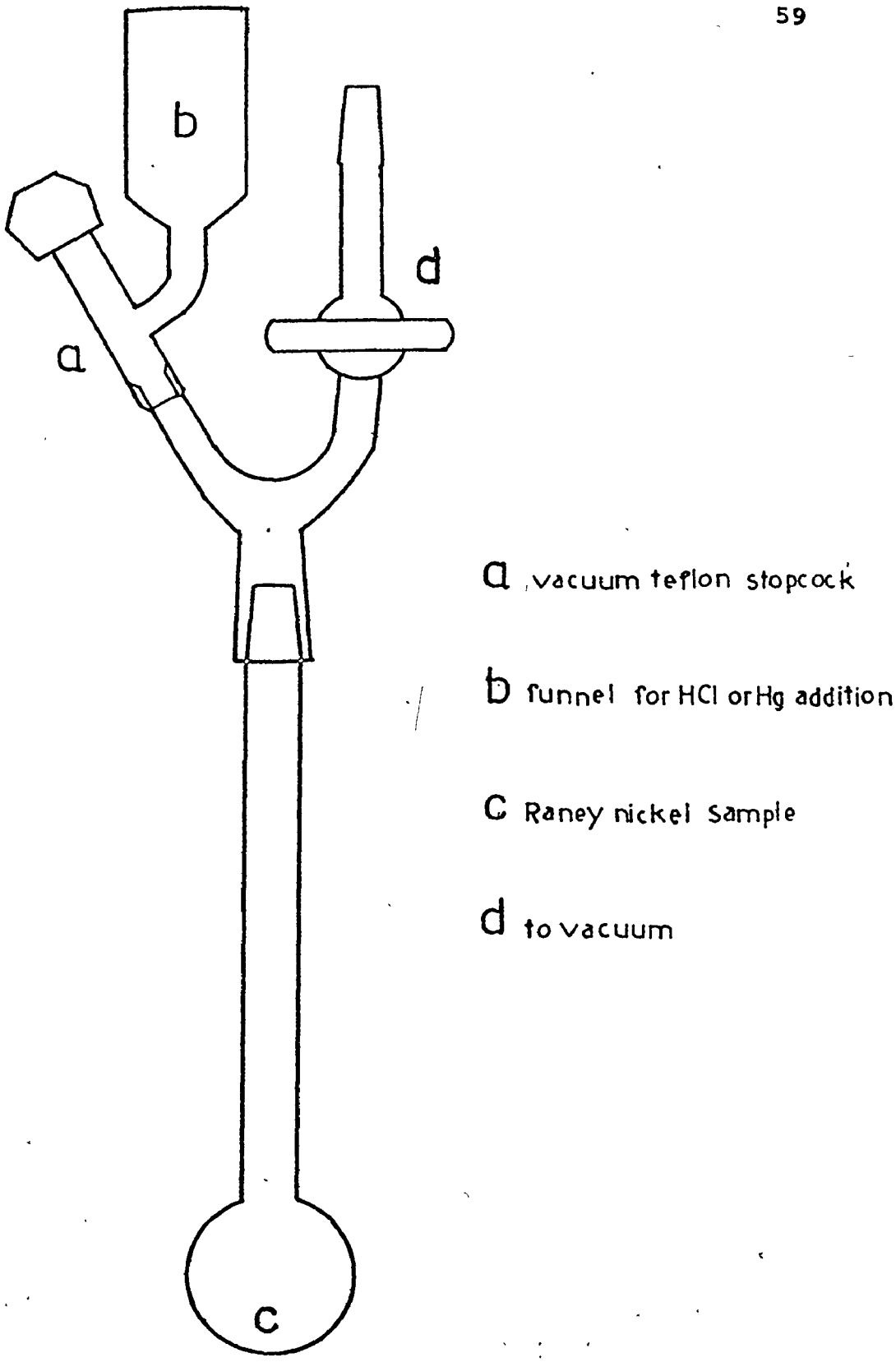

Figure 4.1 Adsorption tube for hydrochloric acid dissolution and amalgamation of Raney nickel.

between the adsorption bulb and the rest of the adsorption apparatus to condense water vapor and HCl. After all or most of the Raney nickel was dissolved, the volume of hydrogen was determined making the correction for the volume of acid solution in the adsorption bulb. The Raney nickel solution was transferred into a 250 ml beaker and filtered through a medium porosity fritted-disc crucible. The insoluble material was dried at 100°C to constant weight, and the Raney nickel solution diluted to 500 ml in a volumetric flask. 50 ml aliquots were taken for chemical analysis: nickel was analyzed by the dimethylglioxime method and by titration with EDTA. Al was analyzed volumetrically by chelatometry. In calculating the amount of hydrogen corresponding to the concentration of Ni^{+2} and Al^{+3} ions in solution an important factor to be considered is the solubility of the alumina trihydrate in hydrochloric acid. Aubry[76] considers that alumina trihydrate is practically insoluble in aqueous 1:20 HCl solution. Mars et.al.[29] removed soluble Al_2O_3 with a caustic soda solution before the Raney nickel sample is dissolved in 6N HCl. The author of the present thesis believes that neither one of these methods is adequate. 1:20 hydrochloric acid has a normality slightly less than 0.6 N. As can be seen from Table 4.1, 11.32% of $Al_2O_3 \cdot 3H_2O$ is soluble in 1N HCl. When a Raney nickel sample is dissolved in hydrochloric acid not only metallic Al is soluble in acid, but also a fraction of alumina, leading to a larger calculated amount of hydrogen. On the other hand, removing soluble Al_2O_3 by washing

Table 4.1

Solubility of Gibbsite ($Al_2O_3 \cdot 3H_2O$) in Hydrochloric Acid

Sample Weight (G)	Acid Dissolution	Treatment	Aluminum soluble in HCl		
			Volumetric (mg)	AAS [a] (mg)	wt % of [b] $Al_2O_3 \cdot 3H_2O$
1.4276	71.4 ml of 4N HCl	3 hrs at 23°C and 2 hrs on a hot plate	324.2±3	321.5	65.34
1.2506	64 ml of 1N HCl	Same as above	50±2	48.1	11.32

a: AAS - Atomic Absorption Spectroscopy

b: in calculating the weight percent of $Al_2O_3 \cdot 3H_2O$ soluble in hydrochloric acid an average between the volumetric and AAS determinations was taken.

Raney nickel with alkali changes the metallic aluminum content of the catalyst and might change the hydrogen content of that particular sample. The method used in this study was to compare the aluminum content of the Raney nickel solution with the elemental Al content from the chemical composition of that Raney nickel sample. In most cases part of the alumina was dissolved by HCl. For example, by dissolving 0.2903 g of COM I Raney nickel in 4N HCl, 126.1 cc(STP) of hydrogen was evolved. The amount of nickel found in solution was 260.7±0.7 mg and Al was 15.7±0.1 mg or 5.41 wt %. The corresponding amount of hydrogen (1.246 cc(STP)/mg Al and 0.382 cc(STP)/mg Ni) is 119.1±0.4 cc(STP), leading to a hydrogen content of 24.2±1.4 cc(STP)/g of catalyst. However, the metallic Al content of COM I Raney nickel is estimated to be 4.43±0.25%, the remaining 0.98±0.25% being aluminum from alumina trihydrate. The corrected amount of hydrogen due to Ni and Al is 115.6±1.2 cc(STP). This calculation gives a hydrogen content of 36.2±4.1 cc(STP)/g of catalyst. A summary of the results is presented in Table 4.2.

4.3 DISCUSSION AND CONCLUSIONS

A comparison between the corrected and uncorrected hydrogen content of the commercial catalyst determined by dissolution in acids and the hydrogen content determined by thermodesorption is given below:

Table 4.2

Summary of Hydrogen Content Data of Commercial Raney Nickel Determined from Dissolution in Acids

Type of Raney Nickel	Sample Weight (g)	Nickel Content gravimetric (mg)	Nickel Content volumetric (mg)	Aluminum Content volumetric (mg)	Aluminum Content wt %	Hydrogen Found cc(STP)	Hydrogen Calc. (uncorr) cc(STP)	Hydrogen Calc. (corr) cc(STP)	Hydrogen Content (uncorr) cc(STP)/g catalyst	Hydrogen Content (corr) cc(STP)/g catalyst
COM I	0.2903	257.2 ± 0.9	260.7 ± 0.7	15.7 ±0.1	5.41	126.1	119.1 ± 0.4	115.6 ± 1.2	24.2 ±1.4	36.2 ±4.1
[a] COM I	0.4268	392.8 ± 0.3	-	23.2 ±0.1	5.45	186.2	178.9 ± 0.2	173.6 ± 1.5	17.2 ±0.5	30.0 ±3.5
[a] COM I	0.3742	338.2 ± 0.1	-	19.6	5.24	148.0	153.5	149.8 ± 1.1	-	0
COM	0.0964	78.6	81.8	3.7	3.84	38.4	35.8	35.2 ±0.4	27.0	33.2 ±4.2
[b] COM	0.3174	277.6	-	15.4 ±0.1	4.84	130.5	125.2 ± 0.1	119.1 ± 1.1	16.8 ±0.3	35.9 ±3.5

Al_{met} content of COM I sample is 4.43 wt % ± 0.25 and of COM sample in 3.30 wt % ± 0.28

a: sample heated to 500°C and dissolved in 1:20 HCl

b: sample dissolved in 1N HCl; all the other samples were dissolved in 4N HCl.

(Uncorrected) Hydrogen Content by Acid Dissolution cc(STP)/g	(Corrected) Hydrogen Content by Acid Dissolution cc(STP)/g	Hydrogen Content by Thermodesorption cc(STP)/g
21.3±5.1	33.8±7.7	22.0±1.2

It can be seen that the precision of the results obtained by HCl dissolution is quite low (± 24% error for the uncorrected hydrogen content). The main disadvantage is due to the solubility of the alumina in hydrochloric acid and the correction introduced because of this factor is approximate. Another disadvantage of the method leading to low accuracy is that the amount of hydrogen contained by the catalyst is small compared to the total amount of hydrogen evolved during the dissolution process. Samples with higher hydrogen content as determined by thermodesorption, could not be used in these experiments because of their high alumina content, between 17.3-49.0 wt %, compared to 5-7 wt %, the alumina content of the commercial Raney nickel.

Even if one considers the lower limit of the hydrogen content (uncorrected), 16.2 cc(STP)/g catalyst, this value represents more hydrogen than the surface can accomodate by chemisorption at room temperature. The largest amount of hydrogen chemisorbed at -196°C by a commercial preparation evacuated at 23°C and 10^{-5} torr, was 10.02 cc(STP)/g (see Table 3.8). The strongly chemisorbed hydrogen by the same type of Raney nickel at -196°C was 8 cc(STP)/g (see Table 3.6).

The conclusion is that part of the hydrogen is dissolved in Raney nickel, probably as a nickel-aluminum-hydrogen solid solution. However, Mars et.al.[29] found 27±1 cc(STP)/g of hydrogen by dissolving Raney nickel in HCl and claim that it is all chemisorbed hydrogen.

4.4 IMMERSION OF RANEY NICKEL IN MERCURY

In these experiments, the catalysts were evacuated at 23°C and 10^{-5} torr in the adsorption tube provided with a funnel (see Fig. 4.1) and then Hg was added to the catalyst. A variable amount of hydrogen was measured in the adsorption apparatus, between 7.5 and 14 cc(STP)/g if the determination was made at 23°C for a commercial preparation. When the adsorption bulb was heated gently in a flame, the amount of hydrogen evolved increased to 16.1±0.4 cc(STP)/g. In similar experiments II A Raney nickel evolved 12.0 cc(STP)H_2/g and 13.1 cc(STP)H_2/g at 23°C. Aubry[76] and Moreau[27] found that 17 cc(STP)/g H_2 were evolved by amalgamation of Raney nickel at room temperature. Moreau postulates the formation of a ternary amalgam (Hg,Ni,H) containing 2% nickel.

As the nickel amalgam is formed, the chemisorbed hydrogen is displaced from the surface of the catalyst.

Hackspill and Rohmer[77] found that aluminum reacts with water vapor in the presence of traces of mercury at temperatures between 0°C and 90°C.

As Raney nickel contains metallic aluminum and water bound

to aluminum trihydrate and "adherent" water, it is conceivable that hydrogen can also be produced by the reaction of Al and H_2O when mercury is added to the Raney nickel.

It was interesting to note that the COM catalyst reacted with mercury faster and easier than II A. Hydrogen started to evolve immediately after mercury was added to the COM sample. The II A Raney nickel needed some time to react with mercury and the sample tube had to be tapped to increase the rate of hydrogen evolution at room temperature.

A possible explanation for the different behaviour of COM and II A Raney nickels towards mercury is their different bulk and surface composition. Larger amounts of alumina trihydrate present in II A catalyst could block the pores and prevent the formation of a Ni-H-Hg alloy. Also, acetaldehyde and ethanol adsorbed on the catalyst surface would make the reaction between mercury and nickel more difficult.

CHAPTER 5

THERMODESORPTION

5.1 GENERAL

Thermodesorption is a physical method of determining the hydrogen content of Raney nickel catalysts. It consists mainly of hydrogen desorption during heating of catalyst and determining the hydrogen volumetrically by measuring gas volumes or by means of a thermal conductivity cell in the dynamic system. Compared to the chemical methods of determining the hydrogen content it has the advantage of a better precision and accuracy. However, the reproducibility of the results is a function of the evacuation procedure and temperature of the sample, the heating rate, storage liquid and age of the catalyst. During thermodesorption, the storage liquid and water bound to the alumina trihydrate contained by the sample can react with the Ni and Al components of the Raney nickel and form additional hydrogen and other products. This chapter describes thermodesorption experiments with different types of Raney nickel, the analysis of gases evolved by gas chromatography and discusses the possible correlations between the amount and composition of gases evolved and the chemical composition and storage conditions of various types of catalysts.

5.2 EXPERIMENTAL

5.2.1 Sample Preparation

The samples used in the present experiments were the following types of Raney nickel: II A, II A-1, II A-2, II A-3, III A and IV A, all stored under absolute ethanol at 0°C for intervals between 1 day and 2 years. The preparation of II A Raney nickel was described in Chapter 2. III A catalysts were prepared by adding alloy A to a 20% aqueous solution of boiling alkali. The resulting catalyst was similar to COM Raney nickel: large pore volume, BET surface area of about 70 m^2/g and a chemical composition quite similar to the COM sample. Also, the commercial preparations stored under water at room temperature for periods of several months/up to 30 months were used. The preparation of the sample was done in the same way as in the hydrochloric acid dissolution experiments. The samples were placed in an adsorption tube and were evacuated overnight or for longer periods of time at 23°C until a "sticking" vacuum was obtained on the McLeod gauge, indicating a pressure of less than 10^{-5} torr. The sample was then ready for adsorption and the storage liquid was assumed to be removed from the catalyst. Hydrogen evolution data were calculated per gram of sample after this treatment.

5.2.2 Adsorption Apparatus

The description of the adsorption apparatus and its diagram was adapted from ref. 79. The Pyrex volumetric apparatus equipped with a manostat and a calibrated burette (Fig. 5.1) is a constant pressure, variable volume system. It consists of

5 bulbs of calibrated volumes [80] of 4.597, 16.308, 22.756, 49.424 and 135.057 cc; a calibrated graduated burette of 100 cc capacity and a mercury manometer, all connected by capillary tubing to the sample tube and to a vacuum system and gas storage section. A liquid nitrogen trap prevents water vapor entering the adsorption system and affecting experimental results. The volume of gas in the burette could be altered continuously by the raising or lowering of a mercury levelling bulb connected to it by rubber tubing. Air which diffused through this tubing accumulated in a sealed trap which is not shown, and thus could not leak into the burette. During hydrogen evolution experiments the levelling bulb was automatically lowered in small steps by a reversible 3 rpm motor which was activated when mercury in the left leg of the manometer breaks the electrical contact at the reference mark to maintain constant pressure. Similarly, as gas is removed from the burette system by adsorption; the mechanism can be set to raise the levelling bulb. The gas bulbs and the burette have water jackets through which water from a constant temperature bath is circulated at 25°C. A McLeod gauge (not shown) is included in the system to check the vacuum obtained prior to introducing He into the system and before starting a thermodesorption experiment. A vacuum of at least 10^{-5} torr is obtained with a mercury diffusion pump in series with a rotary vacuum pump. The void space (V_v), the volume of the capillary tubing to the right of S_2 (not accounted for by the burette and gas bulb) in Fig. 5.1, the volume between S_2 and S_3 including

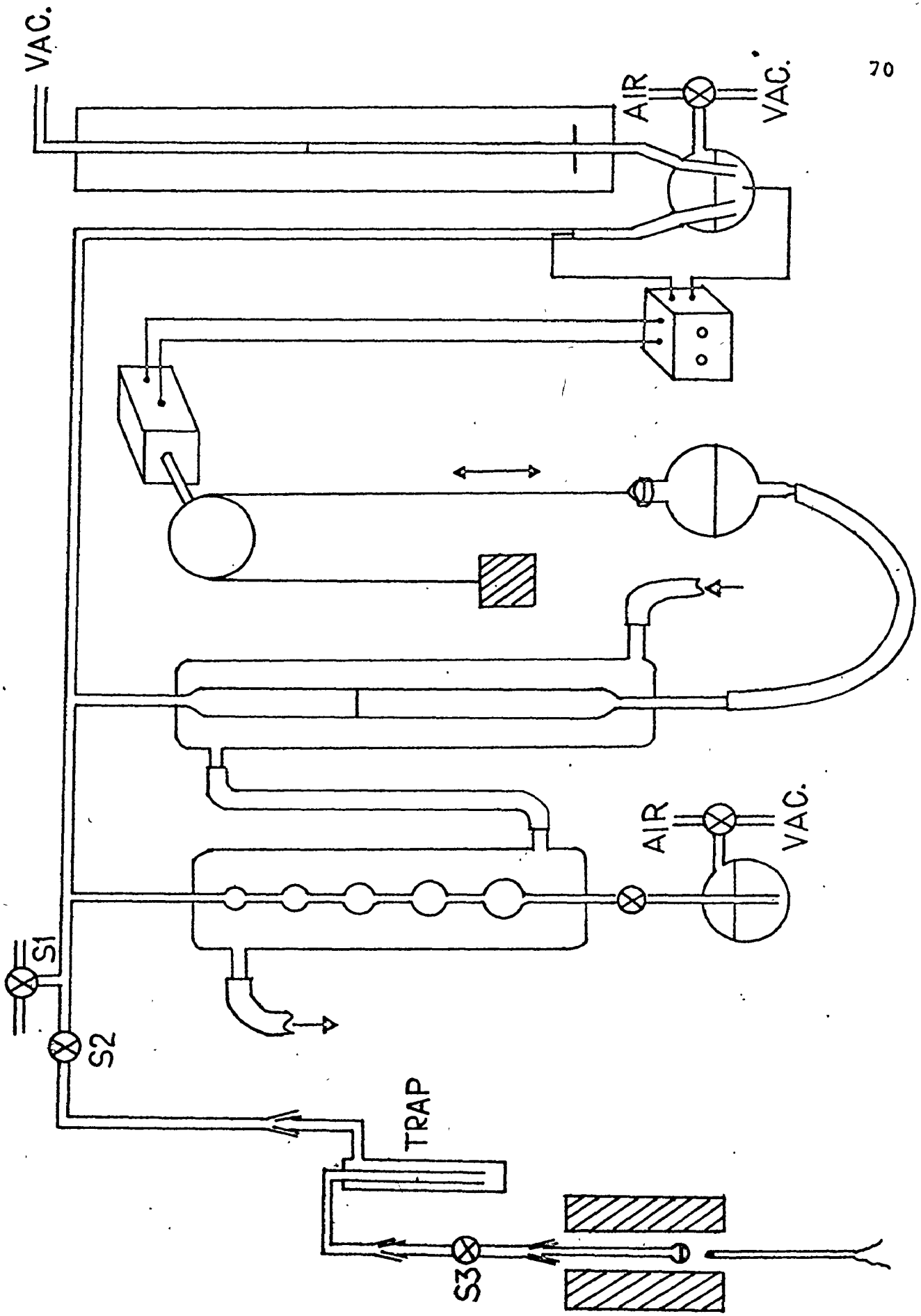

Figure 5.1 Adsorption apparatus.

the trap and the volume below S_3 including the adsorption tube, was determined with helium as 108.10±1.72 cc at room temperature with the trap immersed in liquid nitrogen. The method of determining the void volume is given in Appendix B. The void space for two different adsorption tubes when no liquid nitrogen trap was used was 29.69±0.78 cc and 23.25±0.76 cc. The volume of the capillary tubing to the right of S_2 was 11.86 cc at room temperature. The weight of the catalyst and the rate of heating were chosen such that the rate of hydrogen evolution allowed the mercury to reach a stable level after each adjustment by the manostat, as it was difficult to obtain a true reading during or immediately after a mercury level adjustment. After the void volume was determined with He, the adsorption system had been evacuated and the sample heated by means of a furnace at a heating rate of about 2°C/min to 700°C. The evolved hydrogen built up pressure in the calibrated sections to a pre-set level and thereafter the manostat motor operated in the usual way. Volume measurements could be made after reaching this pressure. The volume of hydrogen per gram of catalyst can be calculated as follows:

$$V_{cc\,(STP)\,H_2/g} = (273.16 \times V_1 \times P)/(760 \times 298.16 \times \text{weight of catalyst (g)}) + (273.16 \times V_2 \times P)/(760 \times T \times \text{weight of catalyst (g)}) \quad (1)$$

where $V_1 = (V_B + V_{GB} + V_v) - V_2$ in cm^3, V_B is the volume of gas bulbs, V_{GB} is the volume of the graduated burette, V_v is the void volume, V_2 is about 5 cc and T is the temperature of the adsorp-

tion tube in K.

The volume of the adsorption tube in the furnace was about 5 cc, the rest of the adsorption system was at 25°C with the exception of the liquid nitrogen trap. In calculating the volume of hydrogen evolved a correction was made for the temperature differences between the part of the adsorption tube at the furnace temperature and the rest of the adsorption system at 25°C. Pressure readings were corrected for mercury expansion from 0°C. 24 hours after the end of the experiment when there was no further volume change, another measurement of the volume of gas was made at room temperature and the amount of the readsorbed gas was calculated. The sample was weighed and the weight loss used in mass balance calculations.

5.2.3 The Composition of the Evolved Gases in Thermodesorption and of the Storage Liquid

5.2.3.1 The Action of Raney Nickel on Alcohols

Paul[64] noticed that a Raney nickel stored under absolute ethanol develops, after a certain period of time, a distinctive smell of acetaldehyde. If a small amount of Raney nickel is added to a few milliliters of ethanol at room temperature, after 3 hours the acetaldehyde is detected with Schiff's reagent. 5 g of Raney nickel in 50 ml of absolute ethanol produce in three months a concentration of 1 g/l of acetaldehyde and has its characteristic smell.After 4 years the concentration of acetaldehyde was 1.3 g/l. Paul claimed that acetic acid was also formed and it dissolved nickel, diminishing the catalytic activity.

After 4 years the concentration of nickel salts was 11.1 g/l and the color of the storage ethanol became pale green. The main reaction taking place was the dehydrogenation of ethanol to acetaldehyde:

$$\underset{\text{ethanol}}{CH_3\text{-}CH_2\text{-}OH} \xrightarrow{RNi} \underset{\text{acetaldehyde}}{CH_3\text{-}CHO} + H_2 \quad . \qquad (2)$$

If allylic alcohol, $CH_2=CH\text{-}CH_2\text{-}OH$ is distilled over Raney nickel, propionaldehyde, CH_3CH_2CHO, is formed and the following gases are evolved: carbon monoxide (23%), ethylene and propylene (25%) and hydrogen (52%).

Alcohols can decompose in three ways[81]:

1) dehydrogenation to an aldehyde, $C_2H_5OH \rightarrow CH_3CHO+H_2$
2) deformylate to an olefin or paraffin with a carbon number one less than that of the alcohol, $C_2H_5OH \rightarrow CH_4+H_2+CO$
3) dehydrate to the corresponding olefin

$$C_2H_5\text{-}OH \rightarrow CH_2 = CH_2 + H_2O \ .$$

In the presence of nickel catalysts[82] at 150°C-190°C and atmospheric pressure, hydrogenolysis of aliphatic alcohols includes reductive dehydroxylation, reductive dehydroxymethylation and formation of ethers. Hydrogenolysis of ethanol in these conditions can lead to the formation of acetaldehyde, ethane, methane and carbon monoxide.

Kokes and Emmett[25] showed that samples of Raney nickel stored under CH_3OH and C_2H_5OH yielded large amounts of methane when degassed and heated to evolve hydrogen. Mars et.al.[29]

found only traces of methane by mass-spectrometer analysis in the hydrogen evolved by Raney nickels stored under organic solvents. Surprisingly no other researchers reported any impurities in the hydrogen evolved by heating Raney nickels stored under ethanol.

5.2.3.2 The Composition of the Storage Liquid. Experimental

The storage ethanol of three different types of Raney nickels stored for different periods of time was analyzed by gas chromatography. A model A90P-3 Varian Aerograph chromatograph with a thermal conductivity detector was used. The conditions of the analysis were the following: impregnated celite 1/4 inch o.d. copper tubing column at 105°C, temperature of the katharometer was 135°C, injector temperature was 135°C, hydrogen flow rate was 93 cc/min and the filament current was 200 mA. 100 µl syringe was used to inject the ethanol samples. The only impurity in the fresh absolute ethanol used as storage liquid was benzene, about 2 wt %, unexpectedly high. However, in the storage liquid the benzene was 0.02 wt %, suggesting that it was adsorbed on Raney nickel during storage and/or participated in a reaction. The storage ethanol contained acetaldehyde between about 0.1 to 1 wt %. The analytical data for the formation of acetaldehyde are given in Table 5.1. These values are approximate but they indicate clearly an increase in the concen-

Table 5.1

Analytical Data for the Formation of Acetaldehyde in Storage Ethanol at 0° C

Catalyst	Storage Time (months)	Acetaldehyde in Ethanol	
		wt %	g/g Ni
IV A	24	1.01± 0.03	$5.11 \times 10^{-2} \pm 1.52 \times 10^{-3}$
II A-1	21	0.46± 0.01	$3.95 \times 10^{-2} \pm 0.86 \times 10^{-3}$
II A-3	3	0.016±0.003	$0.55 \times 10^{-2} \pm 0.15 \times 10^{-3}$

tration of acetaldehyde in ethanol with storage time.

Acetaldehyde and ethanol are strongly adsorbed on the surface of Raney nickel and cannot be removed by evacuation at room temperature and 10^{-5} torr even after a period of several days. The liquid frozen in the liquid nitrogen trap during a thermodesorption experiment and analyzed by gas chromatography showed the presence of C_2H_5OH and CH_3CHO, the ratio C_2H_5OH/CH_3CHO being equal to 2.3 for II A-3 Raney nickel.

5.2.3.3 Analysis of Gases Evolved in Thermodesorption. Experimental

At the beginning of thermodesorption experiments, gas samples of the evolved gases in the adsorption apparatus analyzed by mass spectroscopy showed only traces of organic ions. However, a mass balance could not be established after a "hydrogen" evolution experiment and a gas chromatographic (G.C.) analysis of the evolved gases was done. Details of the GC analysis are given in Appendix B. Type II catalysts were characterized by a much greater volume of gas evolved and by evolution starting at 70°C compared with 100°C for the COM catalysts. The rate of gas evolution had a maximum at about 220°C for COM and 200°C for II A Raney nickels. At this temperature water vapor and possibly ethanol started to condense on the walls of the adsorption tube

Alumina trihydrate loses most of its water at 220°C[77]. Gas composition data are given in Table 5.2, gas evolution, analytical and adsorption data on fully extracted catalysts are given in Table 5.3 and on partly extracted Raney nickels in Table 5.4.

5.2.4 Interpretation of Results and Discussion

Table 5.2 shows that Raney nickels stored in ethanol for at least four months evolved H_2, CO and CH_4 on heating to 700°C. The source of these gases is in the ethanol and acetaldehyde adsorbed on Raney nickel that is not removed by evacuation at room temperature. The following reactions are likely to take place:

$$\underset{\text{ethanol}}{C_2H_5OH} \xrightarrow{\text{dehydration}} C_2H_4 + H_2O \qquad (3)$$

$$C_2H_4 \xrightarrow{H_2,\ \text{hydrogenation}} C_2H_6 \xrightarrow[\text{hydrogenolysis}]{H_2} 2CH_4$$

$$C_2H_5OH \xrightarrow{\text{dehydrogenation}} CH_3CHO + H_2 \qquad (4)$$

$$CH_3CHO \xrightarrow{\text{decarbonylation}} CH_4 + CO$$

The series of reactions (3) and (4) can be synthesized as follows: Ethylene is obtained by the dehydration of ethanol and is further converted to CH_4 by hydrogenation

$$2H_2 + C_2H_5OH = 2CH_4 + H_2O \qquad (5)$$

The ethanol is also dehydrogenated to acetaldehyde which can be decomposed to CO and CH_4.

Table 5.2

Gas Composition Data for Different Raney Nickels

Catalyst	Storage Medium	Storage Time (months)	Gas Evolved cc(STP)/g of cat.	Composition of Gas Evolved vol %			Expected Weight loss wt %	Experimental Weight Loss wt %	H_2O Bound to $Al_2O_3 \cdot 3H_2O$ wt %
				H_2	CO	CH_4			
II A-1	Ethanol	23	65.5	19.28	18.67	62.06	10.52	11.89±0.91	5.97
II A-2	Ethanol	18	62.4	23.38	17.36	59.26	*10.30±0.37	9.32±0.07	6.17
II A-3	Ethanol	4	71.0	70.04	9.32	20.74	10.07±0.28	9.65±1.0	7.75
IV A	Ethanol	24	63.3	50.00	5.00	45.00	19.65±0.12	19.57±0.63	16.94
COM	Water	30	30.9	96.33	0.0	3.67	between 2.07±0.16 and 2.81±0.07	0.86±0.09	between 1.72 and 2.46

*$Al_2O_3 \cdot 3H_2O$ content of this sample was corrected from 25.45 wt % to 17.83 wt %.

Table 5.3

Gas Evolution to 550-700°C, Adsorption and Analytical Data for Different Types of Raney Nickel

Catalyst	Storage Medium	Storage time	cc(STP) of gas per g of catalyst	cc(STP) of gas per g of Ni	BET Area (m^2/g)	Surface Nickel (% BET area)	Readsorption of gas at 23°C		Chemical Analysis			
							cc(STP)/g cat.	Vol % of Total	Ni wt %	Al wt %	$Al_2O_3 \cdot 3H_2O$ wt %	Fe_2O_3 wt%
II A	Ethanol	11 d	83.3	99.2	92.0	[a]59.0	3.8	4.6	84	4.1	11.9	-
III A	Ethanol	1 d	14.7	16.5	86.0	-	7.07	48.1	89	3.9	7.1	-
COM I	Water	2 m	20.9	23.1	80.1 15 after heating to 540°C	86.3	3.4	16.3	90.32	4.43	4.96	0.29
COM I	Water	2 m	21.0	23.3	80.1 7.5 after heating to 570°C	86.3	*2.9	14.0	90.32	4.43	4.96	0.29
COM	Water	5 m	20.8	23.3	81.5	86.3	3.6	17.1	89.33	3.30	7.10	0.29
COM	Water	5 m	22.4	25.1	81.5	86.3	2.8	12.5	89.33	3.30	7.10	0.29
COM	Water	19 m	24.3	27.2	81.5	86.3	-	-	89.33	3.30	7.10	0.29
COM	Water	30 m	30.9	34.6	81.5	86.3	-	-	89.33	3.30	7.10	0.29

*This sample chemisorbed 1.07 cc CO/g after heating to 570°C;
[a]Nickel surface area obtained from CO chemisorption (ref. 50).

Table 5.3 (continued)

Catalyst	Storage Medium	Storage time	cc(STP) of gas per g of catalyst	cc(STP) of gas per g of Ni	BET Area (m^2/g)	Surface Nickel (% BET area)	Readsorption of gas at 23°C		Chemical Analysis			
							cc(STP)/g cat	Vol % of Total	Ni wt %	Al wt %	$Al_2O_3 \cdot 3H_2O$ wt %	Fe_2O_3 wt %
II A-1	Ethanol	8 d	26.4	34.4	32.0 10.1 after heating to 570°C	[a]59.0	4.7	17.8	76.79	4.52	17.26	1.43
II A-1	Ethanol	2 y	65.5	85.3	32.0	[a]59.0	5.1	7.8	76.79	4.52	17.26	1.43
II A-2	Ethanol	6 m	22.4	31.7	58.9	59	1.1	5.1	70.67	2.97	25.45	0.92
II A-2	Ethanol	18 m	62.4	88.3	58.9	59	2	3.2	70.67	2.97	25.45	0.92
II A-3	Ethanol	4 m	71.0	101.4	76.3	59	-	-	70.00	7.42	22.39	0.21
IV A	Ethanol	7 d	82.4	170.7	60.5	38.5	3.5	4.3	48.28	1.87	48.95	0.90
IV A	Ethanol	8 d	67.6	140.0	60.5	38.5	2.4	3.6	48.28	1.87	48.95	0.90
IV A	Ethanol	2 y	63.3	131.1	60.5	38.5	7.1	11.2	48.28	1.87	48.95	0.90

*Nickel surface area obtained from CO chemisorption (ref. 50)

Table 5.4

Gas Evolution to 550°C and Analytical Data* for the Partially Activated Raney Nickels

Catalyst	Extent of Activation (%)	cc(STP) of gas per g of cat.	cc(STP) of gas per g of Ni	Storage Time (months)	BET Area m^2/g	Aluminum Oxidation (%)	Chemical Analysis			Readsorption of gas at 23°C		Surface Nickel (% BET) area
							Ni wt %	Al_{met} wt %	$Al_2O_3 \cdot 3H_2O$ wt %	cc(STP/g cat	Vol % of Total	
II A	25	11.6	21.7	-	18	28.29	53.52	37.17	9.31	1.3	11.2	14.15
I A	50	16.0	25.1	7	46	55.33	63.66	27.54	8.80	-	-	48.00
I A	75	74.0	105.3	16	73	79.25	60.27	14.12	15.61	12.8	17.2	25.72
I A	100	95.3	113.7	-	87	93.44	83.79	5.32	10.89	11.9	12.5	63.00
I B	25	26.2	58.8	7	43	33.32	44.58	43.67	11.75	4.5	17.2	4.46
I B	50	42.8	92.5	-	51	62.27	46.25	25.64	28.11	3.9	9.2	8.55
I B	75	76.2	138.3	1.5	99	81.75	55.09	14.77	30.14	7.0	9.2	13.75
I B	100	49.4	51.9	-	115	96.80	85.31	4.01	10.68	9.2	18.7	48.86

*: Analytical data and surface area derived from the weight of catalyst after evacuation at 130°C for 24 hours and obtained by S.D. Robertson (78).
a: Metallic surface area determined by CO chemisorption using a cross-sectional area of CO = 13 $Å^2$
b: % aluminum oxidation calculated from the chemical composition of the catalysts. wt % Ni (alloy A) = 50.8±0.1; wt % Ni (alloy B) = 40.5±0.1

$$C_2H_5OH = CH_4 + CO + H_2$$

By adding the equations (5) and (6) we obtain finally:

$$2C_2H_5OH + H_2 = 3CH_4 + CO + H_2O. \qquad (7)$$

Reaction (7) was suggested by an experimental ratio CH_4/CO of about 3 (see Table 5.2)

The amount of methane evolved per gram of nickel in cc(STP) is 59 for IV A catalyst, 53 for II A-1, 49.5 for II A-2 and 21 for II A-3, i.e., the oldest sample evolves a larger amount of methane, in agreement with the data given in Table 5.1. The oldest sample had the largest concentration of acetaldehyde in the storage liquid. Reaction (7) shows that for every three moles of methane produced, one mole of hydrogen is consumed. This means that the actual amount of hydrogen evolved in the thermodesorption was higher than the amount indicated by Table 5.2. For example, the II A-1 Raney nickel evolved 65.5 cc of gas (STP)/g catalyst: 12.62 cc H_2, 12.23 cc CO and 40.65 cc CH_4. If the hydrogen consumed in the reaction was about one third the amount of methane produced (see reaction (7)), then 40.65 cc/3 is 13.55 cc which added to 12.62 cc H_2 gives 26.17 cc(STP) H_2/g of catalyst. This value agrees well with the hydrogen content found in a thermal desorption experiment immediately after the preparation of the catalyst, 26.4 cc(STP)/g and with the hydrogen content found by the hydrogen-deuterium exchange method, 27.5 cc(STP)H_2/g. It is not likely that on a freshly prepared sample acetaldehyde forms and adsorbs in large enough quantities to produce significant amounts

of methane and carbon monoxide on heating the catalyst, thus we can regard the gas evolved by thermodesorption from a fresh catalyst as mainly hydrogen. A similar explanation can be given for the II A-2 catalyst (see Table 5.3). Mass balance calculations showed discrepancies between expected and experimental weight loss of 0.4% to 11.5% which can be considered acceptable. The expected weight loss was calculated on the basis of the $Al_2O_3 \cdot 3H_2O$ content and the amount of H_2, CO and CH_4 evolved. It was assumed that all three molecules of water bound to alumina were lost during thermodesorption to 700°C. The II A-2 catalyst (see Table 5.2) had an expected weight loss 38% higher than the experimental weight loss. It appeared that $Al_2O_3 \cdot 3H_2O$ content was about 7% too high. The chemical composition of the catalyst, the composition of gases evolved and the experimental weight loss were checked again. The only possible error was the weight of catalyst on which basis the chemical composition was calculated. Because some acetaldehyde and ethanol were adsorbed on the catalyst and could not be removed by evacuation at 23°C, the actual weight of the catalyst was lower than the weight used in chemical analysis calculations. The correction of the weight of II A-2 sample was done in this way: 36.98 cc(STP)CH_4/g evolved on heating were formed by 50.7 mg of ethanol (see reaction (7)) adsorbed on the surface of Raney nickel, so the actual weight of the II A-2 sample was about 5.07% lower than the value obtained by weighing the sample before and after evacuation. This correction brings

the alumina trihydrate content down from 25.45 wt % to 17.83 wt % and the expected weight loss agrees within 10.5% with the experimental weight loss (see Table 5.2). Possible explanations for the discrepancies in mass balance calculations shown by COM catalyst are an incorrect alumina trihydrate content or removal of only part of the water bound to alumina on heating the catalyst. Kokes and Emmett[25] reported an alumina trihydrate content of about 1 wt % for the COM catalyst and analyses for COM catalyst done by W. R. Grace Co. showed about 3.2 wt % of $Al_2O_3 \cdot 3H_2O$. It is not known in which form the alumina hydrate is present in the COM catalyst as the X-ray diffraction pattern showed only lines characteristic to face centered cubic nickel (see Fig. 3.1).

The source of methane in the commercial Raney nickel could be traces of carbon in the nickel-aluminum alloy used for the preparation of the activated catalyst. During the hydrogen evolution on heating the catalyst methane can be formed. Another possible source of methane could be sodium carbonate formed from the atmospheric carbon dioxide diffusing through the storage water and reacting with the alkali, present on Raney nickel even after repeated washings. As shown in Table 5.3, COM I catalyst yielded quite reproducible results for the hydrogen content, 21±0.07 cc(STP)g/ The hydrogen content of COM sample increased from 21.6±1.1 cc(STP)g after 5 months of storage to 24.3 cc after 19 months of storage and finally to 30.9 cc of gas after 30 months of storage, the last value including 1.13 cc CH_4.

The same trend was found in temperature programmed desorption experiments.

A feature common to Raney nickels stored under ethanol is the decrease with time of the hydrogen content of the freshly prepared samples. Moreau[27] found that for catalysts stored in water and exposed to the air their hydrogen content decreased from 135 cc/g Ni to 9 cc/g in 41 days. Table 5.3 shows in the case of IV A catalyst a decrease of 14.8 cc H_2/g in 24 hours. Most of this gas was probably hydrogen for reasons shown earlier. There is a further decrease of about 27 cc(STP)H_2/g in about two years of storage for the IV A Raney nickel. The highest hydrogen content of a II A type of Raney nickel was about 54.6 cc(STP)/g for a 4 month old II A-3 sample and about 41 cc(STP)/g for a 2 year old IV A catalyst. The hydrogen content was calculated by adding to the amount of hydrogen evolved, one third of the amount of methane evolved, for reasons shown earlier. These values are significantly larger than the maximum amount of chemisorbed hydrogen accomodated by the nickel surface.

Thermal desorption experiments were made to establish a correlation between the amount of gas evolved and the extent of activation of partly extracted Raney nickels (see Table 5.4). As all these catalysts were stored under ethanol for at least 1.5 months it is very likely that the gases evolved contained not only hydrogen, but also methane and carbon monoxide. Analytical data shows that the extent of aluminum oxidation exceeds that from hydrogen evolution in preparation of catalysts as given in Table 5.4. These differences could arise from retention of

hydrogen in the Raney nickel and from failure to arrest the activation process instantaneously. The nickel content increased with increasing aluminum oxidation, whereas the concentration of alumina trihydrate was greatest at 75% activation. In both series II A and II B the amount of gas evolved per gram of catalyst was proportional to the degree of aluminum oxidation, with the exception of II B 100% activated catalyst. There was a large increase in the amount of gas evolved in going from II A 50% activated to II A 75% activated catalyst. The readsorption of gas at 23°C was in some cases 10-13 cc/g of catalyst, much more than the nickel surface could accomodate by chemisorption, even if one considers that the metallic surface area remains unchanged by heating the catalyst to 550°C. The II A catalysts readsorbed larger amounts of gas than the II B catalysts, except for II A 25% activated, in agreement with larger metallic surface areas of II A samples than II B samples. However II B Raney nickels exhibited larger total surface areas than the II A series. It is very likely that the amount of hydrogen evolved by II A 75%, II A 100% and II B 75% preparation exceeded substantially the hydrogen chemisorbed on these Raney nickels.

5.2.5 Conclusions

Most type II catalysts evolved more hydrogen than could possibly be adsorbed on the surface, suggesting that the remaining hydrogen was contained by the mass of nickel as a Ni-Al-H solid solution or was formed in the reaction between

aluminum and alcohol or water bound to bayerite.

Thermodesorption done with fresh Raney nickels stored under water is an accurate method of determining the hydrogen content. However, it does not avoid the reaction between elemental aluminum and water with the formation of hydrogen. Thermodesorption cannot distinguish between an interstitial hydrogen and hydrogen formed in a chemical reaction.

Readsorption experiments represent an argument in favor of a Ni-Al-H solid solution present in Raney nickel, as in some cases the amount of hydrogen readsorbed was larger than the amount of hydrogen which could be accomodated by the nickel surface.

CHAPTER 6

HYDROGEN-DEUTERIUM EXCHANGE

6.1 GENERAL

The hydrogen isotopes offer various possibilities of investigating both the properties of catalytic surfaces and the mechanisms of catalytic reactions[98,58,56,99]. The process in which an isotope is adsorbed and the other is initially entirely in the gas phase are described as exchange reactions. Equilibration reaction is reserved for processes in which H_2 and D_2 are initially in the gas phase[58]. The kinetics of equilibration reactions at constant pressures are always simple. The kinetics of exchange reactions are on the contrary quite complex.

The present chapter describes and discusses the application of the hydrogen-deuterium exchange reaction to determine the hydrogen content of Raney nickel catalysts.

6.2 APPARATUS

Different types of Raney nickel were evacuated in an adsorption tube of about 100 cc at room temperature to 10^{-5} torr for at least 24 hours. After evacuation, the sample tube was transferred to a BET adsorption apparatus where the hydrogen-deuterium exchange experiments were performed. The dead space factor of the adsorption tube was determined with helium, the

detailed procedure of which is given in Appendix C. After the He was pumped from the system and the vacuum reached 10^{-5} torr, a deuterium inlet was admitted to the catalyst. Deuterium gas supplied by Matheson of Canada Ltd. was 99.5 atom. % pure. The catalyst was in contact with deuterium at room temperature for periods of time varying between 20 and 70 hours. During this period and at its end the gas was homogenized by raising and lowering the mercury in the gas burettes thermostatted at 25°C. At the end of an "equilibration" period, gas samples were taken from the BET adsorption system and transferred to the gas chromatograph (GC) for analysis. The sample tube consisted of a U tube attached to a 4-way capillary vacuum stopcock which could be connected to the GC system and BET apparatus by ground glass joints.

A schematic diagram of the GC system is shown in Fig. 6.1. It consisted of a modified A90-P3 Varian Aerograph gas chromatograph with a thermal conductivity cell. A rerouting of the carrier gas was necessary to allow the chromatographic column to operate in a liquid nitrogen bath. Helium, supplied by Matheson of Canada Ltd., 99.995% purity, was used as carrier gas. The helium from the gas cylinder was split into two streams, one stream going directly through a needle valve to the reference side of the katharometer. The other stream of helium was directed through another needle valve to the U-sample tube, chromatographic column, copper oxide tube and finally to the measuring side of the thermal conductivity cell. The 11.5 ft $Al_2O_3/MnCl_2$ chromatographic column made of 1/4" copper tubing was immersed

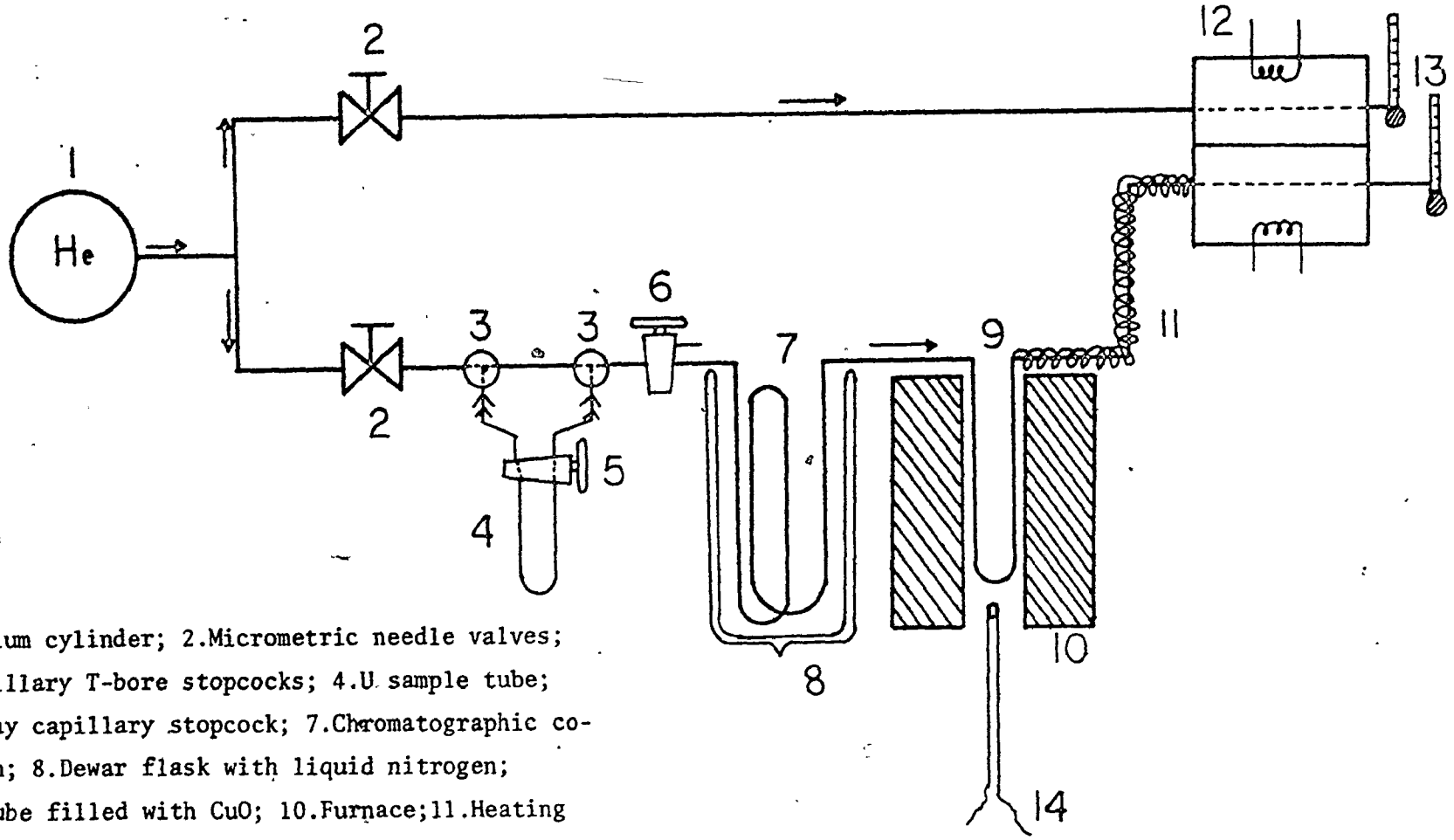

1.Helium cylinder; 2.Micrometric needle valves;
3.Capillary T-bore stopcocks; 4.U sample tube;
5.4-way capillary stopcock; 7.Chromatographic column; 8.Dewar flask with liquid nitrogen;
9.U tube filled with CuO; 10.Furnace;11.Heating tape;12.Thermal conductivity cell;13.Flowmeters;
14.Thermocouple;

Figure 6.1 Schematic diagram of the gas chromatograph.

in a liquid nitrogen bath at constant level. The U-tube 9 filled with CuO was used to oxidize H_2, HD, and D_2 at 600°C to H_2O, HDO and D_2O. The tubing between the CuO furnace and the entrance to katharometer was wrapped in heating tape to prevent the condensation of water vapor. The thermal conductivity cell was maintained at 116°C. A Texas Instrument Servoriter II recorder with disc integrator was used for measuring the response from the thermal conductivity detector of the gas chromatograph. The recorder was connected to a HP3373B Hewlett Packard digital integrator which printed the peak area in units of microvolts-seconds (μV-sec). A Watford Controll Instruments Ltd. A/C voltage stabilizer, model SF-3-L-R, was used to eliminate variations in the 117 V line voltage. The output of this regulator was fed to the gas chromatograph and furnace.

6.3 HYDROGEN AND DEUTERIUM ADSORPTION ON COM RANEY NICKEL

The detailed procedure of GC calibration is given in Appendix C. It was assumed that the hydrogen isotopes are not selectively adsorbed on Raney nickel. To prove this point, separate experiments were made to find the amount of hydrogen and deuterium adsorbed at room temperature on Raney nickels evacuated in the same conditions as samples used in H_2-D_2 exchange experiments. The results are given in Table 6.1. On COM I sample adsorption of D_2 is between 10.3 and 13.3 cc/g. Adsorption of H_2 is 8.3-9.1 cc/g COM sample, which is a different batch of commercial catalyst and which shows a slightly lower adsorption

Table 6.1

Adsorption of Hydrogen and Deuterium on Commercial Raney Nickel at Room Temperature and P = 150-200 torr

Sample #	Catalyst	Gas	Volume Adsorbed cc(STP)/g	Time (hours)
1	COM I	D_2	13.3	16
2	COM I	D_2	12.0	9
3	COM I	D_2	10.3	5
4	COM I	H_2	9.1	24
5	COM I	H_2	8.3	72
6	COM	D_2	8.9	72
7	COM	D_2	9.2	20

Table 6.2

Adsorption of Hydrogen and Deuterium on Nickel on Kieselguhr at 110°C (Data of Pace and Taylor, ref. 99)

Run	Gas	Volume Adsorbed cc(STP)/g	Time (min)
1	H_2	7.87	47
2	H_2	7.93	60
3	D_2	8.02	60
4	D_2	8.05	76
5	H_2	8.02	63

for D_2, 8.9-9.2 cc/g. It can be concluded from these data that, within the experimental error, the adsorption of hydrogen and deuterium is practically the same on commercial Raney nickel. 85-90% of the gas is adsorbed in the first five minutes and after about 20 hours the volume of gas adsorbed becomes constant.

Table 6.2 shows adsorption data of hydrogen and deuterium on supported nickel at 110°C obtained by Pace and Taylor[99]. Between each run the catalyst was evacuated at 450°C. The authors found that there was no difference at all in the rates of adsorption of hydrogen and deuterium on nickel and also on chromium oxide and zinc oxide catalysts.

Deuterium adsorption on COM Raney nickel was followed by a readsorption experiment. After it adsorbed 12 cc(STP)D_2/g (sample #2, Table 6.1) COM I catalyst was evacuated for 72 hours to 10^{-5} torr at room temperature and a second deuterium adsorption experiment was made. This time only 6.23 cc/g were adsorbed after 4 hours and 6.54 after 21 hours compared with 12.0 initially. These data suggest a heterogeneous nickel surface with about 45% of the deuterium being strongly adsorbed. These preliminary adsorption experiments indicated a nonselective adsorption of D_2 and H_2 on a heterogeneous surface of Raney nickel.

6.4 CALCULATION OF THE HYDROGEN CONTENT OF RANEY NICKELS FROM GAS COMPOSITION DATA

We know the composition of each of the gas samples containing H_2, HD and D_2 and wish to calculate the amount of hydrogen in Raney nickel which exchanged with deuterium.

We assume that there is no preferential adsorption for any one of the three isotopes and that the deuterium used in the exchange reaction is 100% pure. If V_D is the volume of deuterium inlet in cc.(STP), V_H is the amount of hydrogen in cc.(STP) contained in the catalyst and equilibrium is assumed between deuterium and all the hydrogen in the solid, then

$$\frac{V_D}{V_H} = \frac{1-h}{h} \qquad (1)$$

where h is the fraction of hydrogen in the gas phase calculated from H_2 and HD present in the gas phase. For example, if the gas phase composition is 28.33% H_2, 47.41% HD and 24.26% D_2, then h is

$$0.2833 + \frac{0.4741}{2} = 0.5204 \ .$$

Now a sample V_{s_1} (cc(sTP)) of hydrogen content h_1 is removed for the first analysis. For the second sample the expression (1) becomes

$$\frac{V_D - V_{s_1}(1-h_1)}{V_H - V_{s_1} h_1} = \frac{1-h_2}{h_2} \qquad (2)$$

where h_2 is the hydrogen fraction in the second sample removed.

When n samples are analyzed, the relationship which gives the volume of hydrogen in the catalyst is:

$$\frac{V_D - V_{s_1}(1-h_1) - V_{s_2}(1-h_2) - \ldots - V_{s_{n-1}}(1-h_{n-1})}{V_H - V_{s_1}h_1 - V_{s_2}h_2 - \ldots V_{s_{n-1}}h_{n-1}} = \frac{1-h_n}{h_n} \qquad (3)$$

Here V_D, V_s and h are known quantities, so V_H is easily calculated.

Table 6.8 gives the values for V_s, h and the hydrogen content calculated for each gas sample, V_H.

6.5 RESULTS AND DISCUSSION

The results of the GC analysis of the exchanged mixtures of H_2, HD and D_2 for different Raney nickels are shown in Tables 6.3-6.7. The hydrogen content data are given in Tables 6.8-6.9. The gas composition data of COM catalyst (Tables 6.3 and 6.4) indicated that ratios of H_2:HD:D_2 were those of thermodynamic equilibrium, after 18.5 hours. The amount of hydrogen in Raney nickel which exchanged with deuterium was 26 cc(STP)/g in one experiment and 25.7 in another (Table 6.9). Equilibrium constants calculated for the reaction $H_2 + D_2 \rightleftharpoons 2HD$ at room temperature from gas composition data of IV A and II A-1 catalysts (Tables 6.4, 6.6 and 6.7) are between 6 to 12% larger than the literature values[83,58] suggesting a possible error in the GC analysis. The hydrogen content calculated for two IV A samples was an average of 12.8±1.2 cc(STP)/g and 26.5 cc per gram for II A-1 (Table 6.9).

Table 6.3

G.C. Analysis Data for the Deuterium Exchange with Hydrogen in Commercial Raney Nickel for 63.5 hours at 25°C. Run #1

Sample size cc(STP)	A_{H_2} μV-sec	A_{HD} μV-sec	A_{D_2} μV-sec	$A = \frac{A_{HD}^2}{A_{H_2} \cdot A_{D_2}}$	K_{eq}^{**}	Gas Composition (mole %) H_2	HD	D_2
0.736	6352	11940	5827	3.852	3.264	27.74	47.42	24.84
0.934	8384	15490	7307	3.917	3.319	28.32	47.59	24.09
1.070	10200	17990	9310	3.408	2.888	28.62	45.90	25.49
1.095	10100	18340	8849	3.763	3.188	28.52	47.09	24.39
0.899	8137	14890	7093	3.841	3.255	28.45	47.35	24.20
*0.622	138.4	259.5	125.9	3.865	3.275	26.76	49.49	23.75
0.609	5467	9998	4654	3.928	3.329	28.62	47.60	23.78

*Area of the peak determined by manual integration

**$K_{eq} = A \cdot \frac{S_{H_2}}{S_{HD}} \cdot \frac{S_{D_2}}{S_{HD}} = 3.272 \pm 0.051$;

Literature Value $K_{eq}^{25°C} = 3.225$ (ref. 83)

$K_{eq}^{25°C} = 3.268$ (ref. 58)

Average gas composition (mol %): H_2 28.33±0.35

HD 47.41±0.21

D_2 24.26±0.39

Table 6.4

G.C. Analysis Data for the Deuterium Exchange with Hydrogen in Commercial Raney Nickel for 18.5 hours at 25°C. Run #2

Sample size cc(STP)	A_{H_2} μV-sec	A_{HD} μV-sec	A_{D_2} μV-sec	$A = \frac{A_{HD}^2}{A_{H_2} \cdot A_{D_2}} K_{eq}$		Gas Composition (mole %) H_2	HD	D_2
0.768	6752	12590	6237	3.764	3.189	27.80	47.14	25.06
1.016	8639	15800	7716	3.745	3.173	28.29	47.05	24.66
-	9864	17990	8821	3.720	3.152	28.32	46.97	24.71
1.092	10020	18180	8980	3.674	3.113	28.37	46.81	24.82
0.879	7889	14480	7126	3.735	3.165	28.16	47.03	24.81
0.631	5514	10240	4952	3.840	3.254	28.05	47.37	24.58

Average calculated $K_{eq}^{25°C} = 3.175 \pm 0.047$;

Literature value $K_{eq}^{25°C} = 3.225$ (ref. 83)

$K_{eq}^{25°} = 3.268$ (ref. 58)

Average gas composition (mol %): H_2 28.16±0.21

HD 47.06±0.19

D_2 24.78±0.17

Table 6.5

G.C. Analysis Data for the Deuterium Exchange with Hydrogen in IV A Raney Nickel for 19 hrs. at 25°C. Run #1

Sample size cc(STP)	A_{H_2} μV-sec	A_{HD} μV-sec	A_{D_2} μV-sec	$A = \frac{A_{HD}^2}{A_{H_2} \cdot A_{D_2}} K_{eq}$		Gas Composition (Mole %) H_2	HD	D_2
1.276	1488	13930	31620	4.124	3.495	3.31	28.14	68.55
1.598	2043	18000	39870	3.977	3.370	3.56	28.56	67.88
1.328	1624	14660	32760	4.040	3.423	3.46	28.41	68.13
1.629	1973	18200	40110	4.186	3.547	3.42	28.70	67.88

Average calculated $K_{eq}^{25°C} = 3.459 \pm 0.078$;

Literature value $K_{eq}^{25°C} = 3.225$ (ref. 83)

$K_{eq}^{25°C} = 3.268$ (ref. 58)

Average gas composition (mol, %): H_2 3.44±0.10

HD 28.45±0.24

D_2 68.11±0.32

Table 6.6

G.C. Analysis Data for the Deuterium Exchange with Hydrogen in IV A Raney Nickel for 44.5 hours at 25°C
Run #2

Sample size cc(STP)	A_{H_2} μV-sec	A_{HD} μV-sec	A_{D_2} μV-sec	$A = \frac{A_{HD}^2}{A_{H_2} \cdot A_{D_2}} K_{eq}$		Gas Composition (mole %) H_2	HD	D_2
0.986	725	9230	26980	4.355	3.690	2.05	23.68	74.27
1.409	939	11570	34090	4.182	3.544	2.10	23.52	74.38
1.443	1136	13750	39330	4.232	3.586	2.18	24.04	73.78
1.304	970	12240	35410	4.362	3.696	2.08	23.86	74.06

Average calculated $K_{eq}^{25°C} = 3.629 \pm 0.076$

Literature value $K_{eq}^{25°C} = 3.225$ (ref. 83)

$K_{eq}^{25°C} = 3.268$ (ref. 58)

Average gas compositon (mol %): H_2 2.10±0.06

HD 23.78±0.22

D_2 74.12±0.26

Table 6.7

G.C. Analysis Data for the Deuterium Exchange with Hydrogen in II A-1 Raney Nickel for 20 hours at 25°C

Time of Exchange (hrs)	Sample size cc(STP)	A_{H_2}	A_{HD}	A_{D_2}	$A = \frac{A_{HD}^2}{A_{H_2} \cdot A_{D_2}}$	K_{eq}	Gas Composition (mole %) H_2	HD	D_2
20.00	0.609	10280	25630	15160	4.215	3.572	21.25	48.18	30.57
20.42	0.779	13790	33080	19750	4.018	3.405	21.84	47.64	30.52
20.83	0.797	14130	33520	19910	3.994	3.384	22.08	47.60	30.34
21.25	0.829	14890	35530	20500	4.136	3.504	22.16	48.08	29.76
21.67	0.690	12130	29010	17010	4.078	3.456	22.01	47.87	30.12
22.08	0.692	12030	28940	16650	4.206	3.565	22.07	48.29	29.64
26.12	0.184	3107	6915	4139	3.718	3.152	23.13	46.81	30.06
68.00	0.283	6061	11580	6262	3.533	2.994	26.70	46.38	26.92

After 22.08 hrs: Average calculated $K_{eq}^{25°C} = 3.481 \pm 0.08$

Literature value $K_{eq}^{25°C} = 3.225$ (ref. 83) ; $K_{eq}^{25°C} = 3.268$ (ref. 58)

Average gas composition (mol %) H_2, 21.90±0.34 HD, 47.94±0.29 D_2, 30.16±0.39

Table 6.8

Hydrogen Content of COM, IV A and II A-1 Raney Nickel Determined for Each Gas Sample

Type of Raney Nickel	Volume of Sample V_S, cc(STP)		Fraction of Hydrogen h		Hydrogen Content V_H, cc(STP)/g	
	Run #1	Run #2	Run #1	Run #2	Run #1	Run #2
COM	3.292	3.371	0.5145	0.5130	25.8	25.8
	4.144	4.181	0.5212	0.5182	25.3	25.8
	4.756	4.730	0.5157	0.5181	25.8	25.8
	4.854	4.743	0.5207	0.5178	25.8	25.7
	3.879	3.749	0.5213	0.5168	25.3	25.7
	2.665	2.625	0.5151	0.5174	26.0	-
	2.509	-	0.5242			
IV A	5.717	4.428	0.1738	0.1389	13.7	11.8
	7.129	8.380	0.1784	0.1386	13.6	12.0
	5.935	6.351	0.1767	0.1420	13.6	11.9
	6.328	5.574	0.1777	0.1401		
II A-1	2.747		0.4534		23.2	
	3.459		0.4566		23.4	
	3.543		0.4588		23.7	
	3.637		0.4620		23.5	
	2.946		0.4595		23.7	
	2.697		0.4622		26.5	
	0.814		0.4989		-	

Table 6.9

Hydrogen Content of COM, IV A and II A-1 Raney Nickels Determined by the Hydrogen-Deuterium Exchange Method

Catalyst	Sample Weight (g)	Deuterium Inlet V_D, CC(STP)	Hydrogen Content V_H, cc(STP)/g catalyst
[a] COM	1.9944	47.381	26.0
[a] COM	1.9579	47.009	25.7
[b] IV A	0.9000	56.901	13.6
[b] IV A	0.6327	46.295	11.9
[c] II A-1	1.4620	40.431	26.5

a: catalyst 5 months old

b: catalyst 12 days old

c: catalyst 11 days old

The pressure in the adsorption system decreases with the removal of gas samples leading to a small decrease in the amount of the adsorbed gas. However, the decrease in pressure does not affect significantly the hydrogen content found after the removal of each sample for COM and IV A Raney nickel, implying a non-preferential adsorption of the three isotopes(Table 6.8). Table 6.7 shows a slight increase in hydrogen concentration in the gas phase, suggesting a release of adsorbed hydrogen. A corresponding small increase in the hydrogen content during a period of 6 hours and an increase from 23.7 to 26.5 cc(STP)/g after 42 hours is also seen from Table 6.8.

6.6 CONCLUSIONS

The IV A Raney nickel has the smallest hydrogen content of the catalysts analyzed. It also has the largest alumina trihydrate content, about 50 wt %, and probably some ethanol and acetaldehyde adsorbed on its surface.Apparently the H_2O bound to bayerite in Raney nickel and the ethanol and acetaldehyde adsorbed on the catalyst do not exchange with deuterium to any appreciable extent. The hydrogen content of IV A is about the amount expected for chemisorbed hydrogen. It is possible that the large amount of $Al_2O_3 \cdot 3H_2O$ in IV A prevents a further exchange by blocking the nickel surface. Thermodesorption gave about 75 cc gas/g for a 7-8 day-old IV A catalyst. The difference between the two values for the hydrogen content will be explained in the last chapter. For an 8 day old II A-1 sample, the hydrogen

content obtained by thermodesorption was 26.4 cc(STP)/g and for a several month old COM Raney nickel about 22 cc(STP)/g. Agreement between data for COM and II A-1 obtained by thermodesorption and hydrogen-deuterium exchange seems reasonably good.

For both catalysts (COM and II A-1) the hydrogen content seems too high to be attributed only to chemisorbed hydrogen. It is likely that part of this hydrogen is present as interstitial solid solution with nickel and aluminum in Raney nickel.

CHAPTER 7

TEMPERATURE-PROGRAMMED DESORPTION

7.1 GENERAL

With the exception of thermal desorption in a volumetric system, the method of studying the hydrogen in Raney nickel catalysts presented so far in this thesis could determine only the amount of hydrogen present in the catalyst.

The temperature-programmed desorption technique (TPD) applied to the study of hydrogen in Raney nickel leads to the determination of not only the amount of hydrogen but also its different forms of bonding. Thermal desorption in a volumetric system gives integral gas evolution data. TPD was applied to the study of hydrogen in nickel catalysts and Raney nickels by Zapletal et al.[37,101,102] and Lenfant[34]. Zapletal et al. found that the activity of a supported nickel catalyst for the hydrogenation of 1-octyne depends on the presence and is proportional to the amount of a definite "form" of hydrogen, i.e. hydrogen desorbed at a particular temperature. Lenfant used the TPD method to determine the nature of hydrogen in nickel-boron catalysts, the activation energy of desorption of different types of hydrogen and the volume of hydrogen present in the sample. This chapter describes TPD experiments made with Raney nickels stored in water and ethanol to determine the amount of gas evolved, the

maxima in the rates of desorption and elucidates the nature of hydrogen in Raney nickel catalysts.

7.2 BASIC PRINCIPLES OF TPD ANALYSIS

The flash-desorption technique has been used in catalysis to obtain kinetic information on adsorption and desorption of gases on metals. Studies have been done on metal filaments using ultra high vacuum techniques. The filament temperature is increased in vacuum to obtain a clean surface on which a gas is adsorbed. A rapid change in the filament temperature is obtained by an electrical discharge and the subsequent desorption of the gas is followed by measuring the changes in pressure by means of an ionization gauge.

In 1963 Amenomiya and Cvetanovic[103-105] adapted this technique to the study of solid powders for the systems alumina-ethylene, alumina-2-butene and alumina-propylene. The technique was termed temperature-programmed desorption (TPD) and it differs from the flash-filament desorption method in several respects. The conditions used in TPD are similar to those used in catalytic reactions and the technique is modified such that it is possible to study simultaneously a chemisorption process and the surface reaction which accompanies it. Also TPD is usually done at atmospheric pressure. The heating rate is considerably slower than in flash-desorption and is achieved in a furnace. The porous structure of the catalytic materials introduces complications in the TPD technique compared to the relatively simple theoretical treatment of flash-filament desorption. The principle of the TPD

technique applied in catalysis is relatively simple: a catalyst, on which a gas has been previously adsorbed, is heated in a flow of inert gas and its temperature follows a definite time schedule, often linear. The desorption of the gas from the catalyst surface is followed by using a thermal conductivity detector which allows one to obtain, at any time, the rate of desorption. If the heating law is known, the desorption spectrum (or sometimes the desorption chromatogram) can yield the following information:

- the number of desorbed phases
- the population of these phases
- the activation energy of desorption E_{des} for different adsorbed phases
- the reaction order of desorption.

There are three cases of desorption[106,107]:

1) desorption from sites with the same E_{des}
2) desorption from sites with different E_{des}, but changing in a discrete manner
3) desorption from sites with E_{des} varying continously.

For a simpler case when only monoenergetic sites are considered, and a linear heating schedule is applied

$$T = T_o + bt \qquad (1)$$

where $b = \frac{dT}{dt}$, T being the temperature and t, the time it can be shown[34] that if the flow rate of the carrier gas is sufficiently high so that readsorption occurs to a negligible extent, then:

$$2 \log T_M - \log b = \frac{E_d}{2.303R} \cdot \frac{1}{T_M} + \log \frac{E_d V_M}{R K_o} \qquad (2)$$

or for each b, (2 log T_M - log b) plotted as a function of $\frac{1}{T_M}$ gives a straight line. The activation energy for desorption E_d, can be determined from the slope. In expression (2), T_M is the temperature at which the rate of desorption reaches a maximum, V_M is the monomolecular layer in cc(STP) for a surface coverage equal to unity, K_o is a constant in cc sec^{-1} and R is the gas constant. The amount of gas desorbed in a TPD experiment is determined from the peak area (see Appendix D for details). If V is the volume of hydrogen desorbed in cc(STP), then the number of sites per cm^2, n_s, is:

$$n_s = 2 \frac{N}{V_o} \cdot \frac{V}{mA} \qquad (3)$$

where N is the Avogadro's number, V_o is the molar volume in c.c., m is the weight of catalyst in grams and A is the surface area in cm^2/g. Dissociative hydrogen chemisorption was assumed. For simpler cases, the shape of the peak can be used to determine the order of reaction for the desorption process. A nonsymmetrical peak indicates a first order reaction, while symmetrical peaks suggest a second order reaction[34].

Detailed review articles on the temperature-programmed-desorption technique were written by Cvetanovic and Amenomiya[108,109] and more recently by Smutek, Cerny and Buzek[110].

7.3 APPARATUS

A typical apparatus for TPD is basically similar to a gas chromatograph except that there is no chromatographic column and gas chromatographic separation does not occur. Fig. 7.2 shows schematically the experimental arrangement used in this laboratory. A carrier gas such as argon or hydrogen is passed from a cylinder through a molecular sieve column to remove traces of water. The carrier gas is split into two streams: one leading directly to the reference arm of the detector, the other passing, whenever desired, through a water saturator and through the quartz TPD cell containing the catalyst, to a dry ice trap which prevented the water vapor entering the detector and finally to the measuring arm of the detector.

The detector was a conventional thermal conductivity cell (Gow-Mac Instrument Co.) with rhenium-tungsten filaments of 30 ohms each and operated at room temperature. The bridge circuit design was kindly furnished by Dr. R. J. Cvetanovic from NRC Laboratories, Ottawa. The detector was connected to a Texas Instrument Servoriter II recorder with disc integrator used to measure the signal response in connection with a 3373B Hewlett-Packard digital integrator. The quartz TPD cell was surrounded by an electrical furnace with a quick response. The resistance of the furnace was wired on the inner surface of a ceramic tube. The TPD cell was provided with a chromel-alumel thermocouple which measured the temperature within the sample. A second thermocouple was connected to a 30 mV scale,

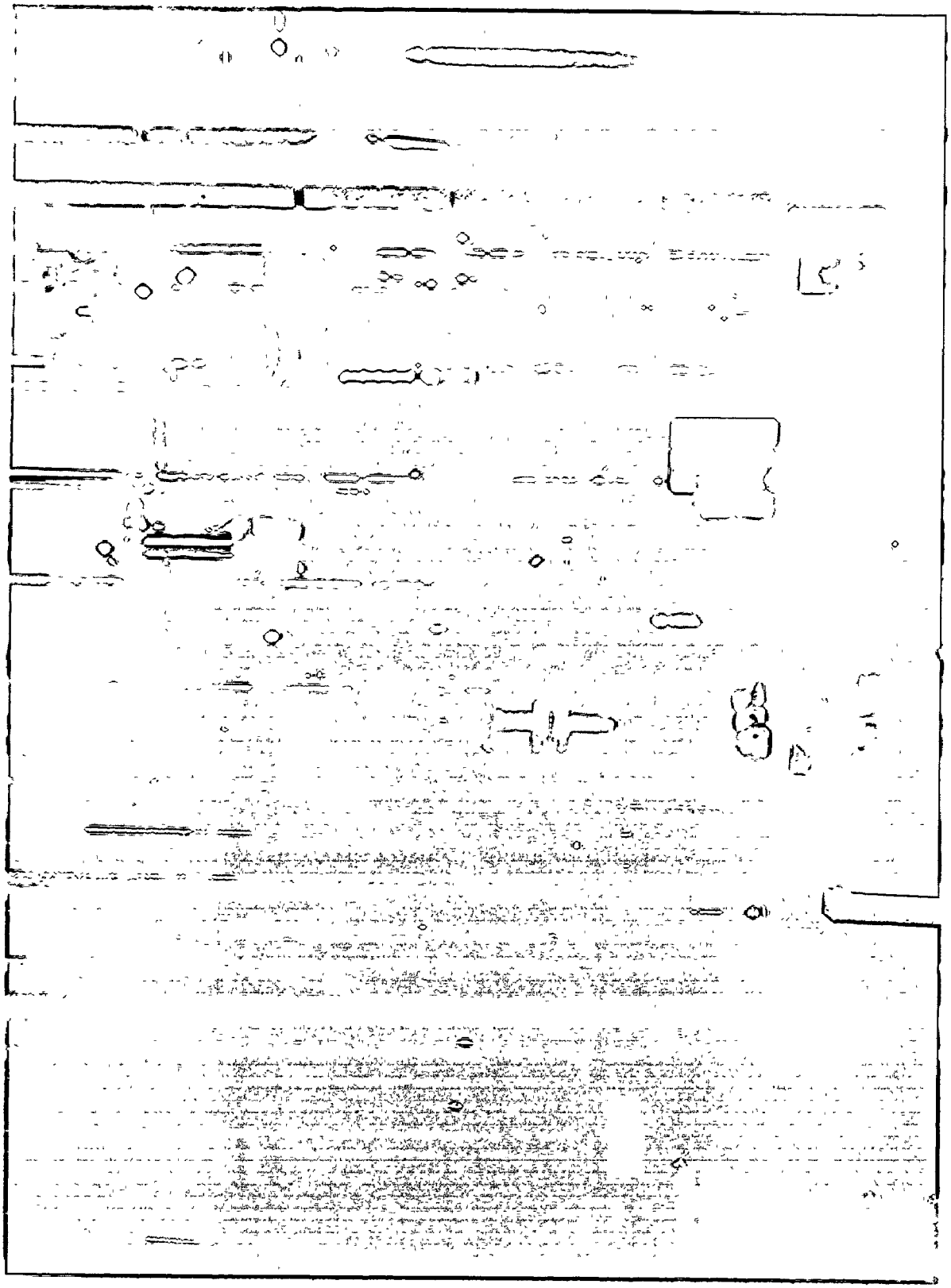

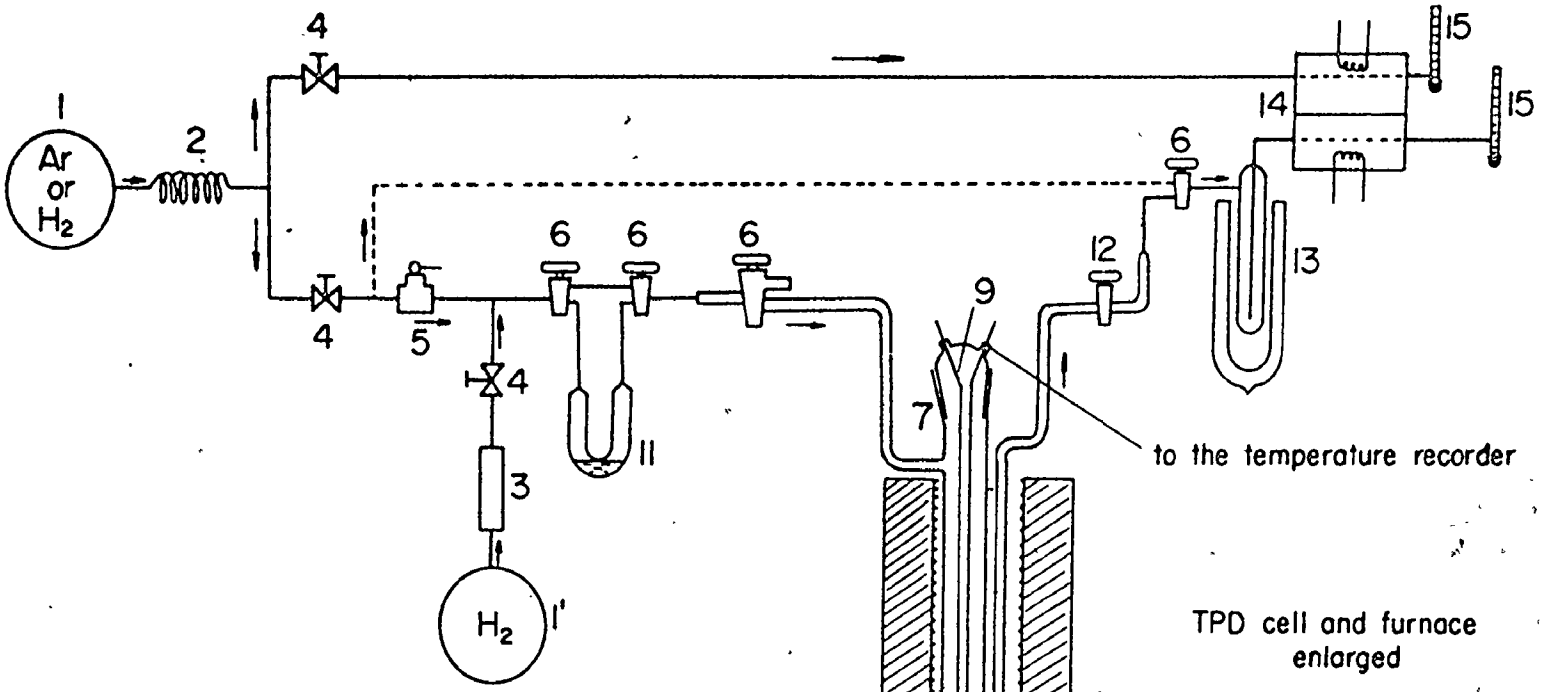

1 - argon or hydrogen cylinder,
2 - molecular sieve column, 3 - deoxo unit,
4 - micrometric needle valves, 5 - toggle valve,
6 - three-way stopcocks,
7 - quartz TPD cell,
8 - fritted disc,
9 - thermocouples, 10 - oven,
11 - water saturator,
12 - two-way stopcock, 13 - dry-ice trap,
14 - thermal conductivity detector,
15 - flowmeters.

Figure 7.2 Schematic drawing of the TPD apparatus.

24 point temperature recorder, model E 1124 made by Esterline Angus Instrument Co., Inc. This thermocouple recorded the temperature outside the TPD cell providing a measurement of the thermal effects occuring during desorption. A third thermocouple was connected to the temperature programmer. The temperature program was obtained by driving at a constant rate the potentiometer knob of a proportional band type temperature controller (Electronic Control Systems, Inc.) by a synchronous motor. Synchronous motors of different speeds of rotation and several interchangeable rubber driving wheels provided linear temperature rates of 4.2°C to 12.8°C per min. A Watford Control Instrument Limited A/C voltage stabilizer, model SF-3-L-R was used to eliminate variations in the 117 V line voltage. The output of this regulator was fed to the detector DC power supply to avoid variations in the filament current and through three resistances in parallel in series with the furnace.

The resistances could be used to make changes in the voltage supplied to the TPD cell heater. The catalyst temperature could be maintained to within 0.2°C. The deviation in the heating rate, i.e. in the linear increase in temperature with time was about 4.5% from one experiment to another. Temperature curves measured inside and outside the TPD reactor are shown in Fig. 7.3. The flow system and the reactor were designed to obtain smooth desorption peaks without base line drifts. The TPD reactor used initially, similar to a reactor designed by Cvetanovic and Amenomiya[107], had an inner tube jacketed, so that the rapid

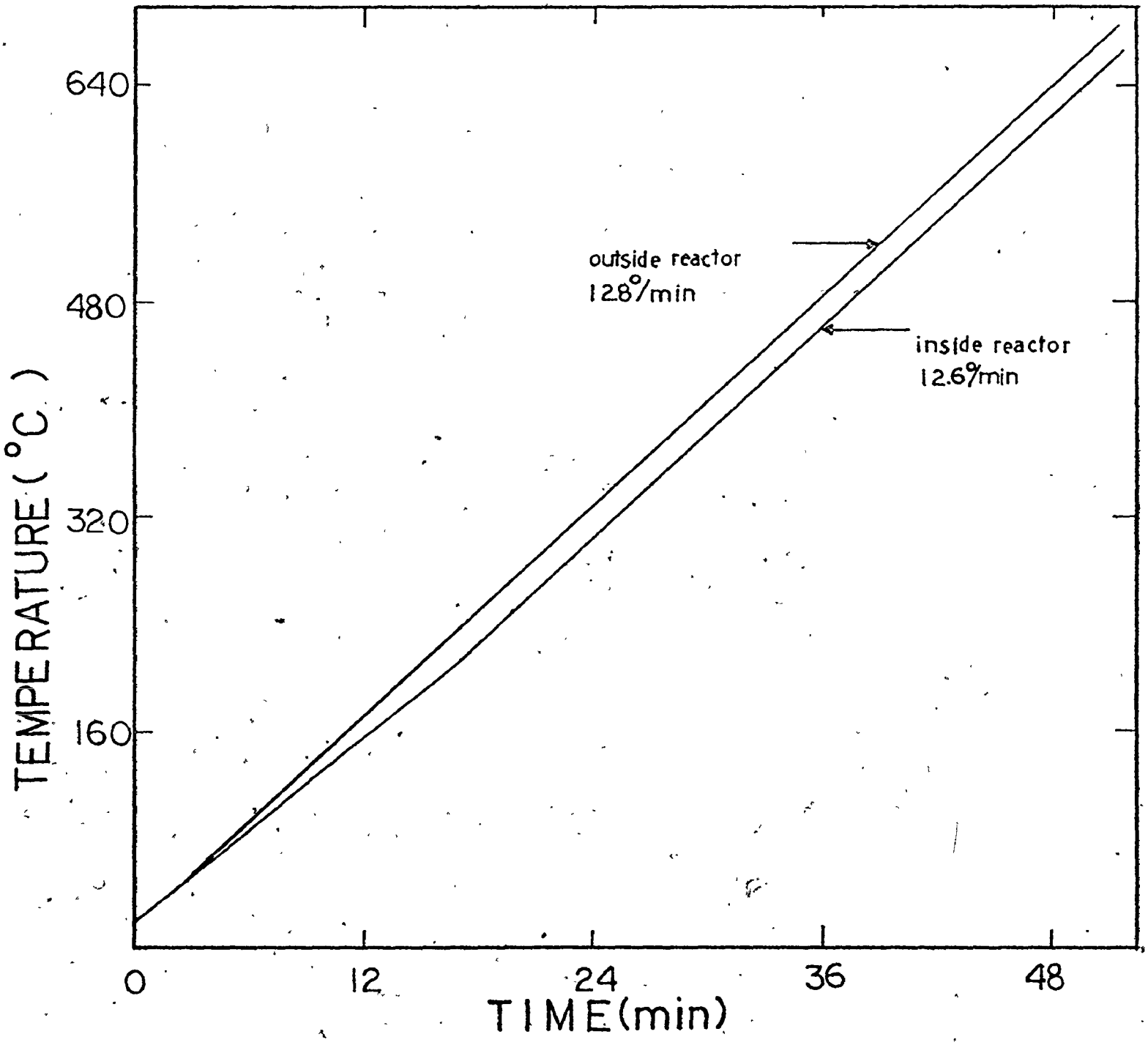

Figure 7.3 Temperature curves measured inside and outside the TPD reactor.

temperature fluctuations causing jagged peaks, were prevented. Subsequently, a simple reactor of lower volume was found to perform as well as the previous design. The temperature inside the sample, recorded on chart paper, was checked occasionally with a Croydon portable thermocouple potentiometer.

The TPD system was arranged so that hydrogen could be passed over the catalyst and reduction of oxidized samples took place. Calibration of the detector for hydrogen and other gases was made by replacing the TPD reactor with a gas sampling valve.

7.4 EXPERIMENTAL PROCEDURE

Raney nickel samples were transferred wet from the storage jar into the TPD reactor which was weighed and sealed with black wax. The solvent was removed by evacuation at 10^{-5} torr and room temperature for at least 24 hours. Dry Raney nickel samples weighed between 100 and 500 mg. After evacuation the reactor was connected to the TPD system by means of glass joints. The carrier gas which had been flowing in the meantime only through a bypass, was diverted to flow through the reactor. The three-way stopcock 6 belonging to the reactor (Fig. 7.2) was used to flush out the air accumulated in the lines. The recorder base line was disturbed when the carrier gas was switched to the reactor, but it became stabilized again after a few minutes. The temperature of the catalyst was then raised linearly by the temperature programmer. As the temperature increases the gas adsorbed on the catalyst or produced by a chemical reaction, desorbs and is carried by the carrier gas to the detector where it

produces a signal proportional to it's concentration in the carrier gas. The recorder will trace one or more peaks with the abscissa representing the time or temperature. The ordinate measures the rate of desorption. If there are molecules adsorbed on different types of active sites on the catalyst surface or different gases adsorbed on the sample, peaks will show up at different temperatures as a function of the activation energy of desorption. When the catalyst surface is depleted of gas, the recorder will trace the base line again.

Preliminary experiments were made with an empty TPD reactor to see if base line drifts occurreddue to the increase in temperature. Up to 800°C no base line drifts were noted. The heating rate and the amount of sample were selected such that the hydrogen concentrations remained in the linear range and no explosive gas evolution occured. Recorder chart speeds lower than 0.5 inch/minute made reading disc integrator counts difficult.

More than 100 TPD experiments were performed with different types of Raney nickels, nickel on silica, nickel-aluminum alloys, alumina trihydrate and nickel oxide. In the early stages of this work the gases evolved during thermodesorption were analyzed by mass spectrometry and only hydrogen with traces of organic molecules was found. Failure to establish a mass balance for ethanol-stored Raney nickels after a TPD experiment led to the idea that the gases evolved contained other gases in addition to hydrogen. Gas chromatographic analysis of the gases evolved in the thermodesorption showed important amounts of methane

and carbon monoxide in addition to hydrogen for Raney nickels stored in ethanol. The origin of CH_4 and CO was already discussed in Chapter 6. Lenfant[34] warns about the possibility of formation of dehydrogenation (acetaldehyde) and hydrogenation (methane) products due to the presence of ethanol in nickel catalysts stored in alcohol. However, gas chromatographic analysis of gases desorbed from nickel-boron catalysts stored in ethanol and evacuated in conditions similar to those used in this laboratory (20°C, 10^{-5} torr Hg, 15 hours) showed the presence of only hydrogen[34].

Therefore, TPD experiments with Raney nickels stored under ethanol should be regarded only as qualitative, because separation of products was not made during TPD and the exact amount of gas evolved could not be determined. However, approximate calculations will be presented later.

7.5 COMMERCIAL RANEY NICKEL

Commercial catalysts, supplied by W. R. Grace Co., are stored in water and are characterized by a surface area of 80 m^2/g and lower alumina trihydrate content (5-7 wt %) than other Raney nickels used in this work. The COM sample for the programmed desorption of hydrogen was prepared as described in Section 7.5. The sample was heated from room temperature to 700°C at 4.2, 6.2 and 12.8°C/min. Most experiments were done on the attenuation 32 of the recorder. On this attenuation the gas evolution started at about 70°C. However, on a more sensitive scale (attenuation 2) the hydrogen evolution was detected at 40°C.

A typical desorption chromatogram for a COM Raney nickel is shown in Fig. 7.4, curve a. There is only one maximum in the desorption rate at 207°C; the heating rate was 13.2°C/min and the amount of hydrogen evolved to 700°C was 23.7 cc(STP)/g of catalyst. When larger samples were used, a slight exothermic effect accompanied the maximum in the desorption rate. Most commercial catalysts produced TPD chromatograms with a peak at 206±10°C regardless of the different heating rates used: 4.2±0.2° C/min, 6.2±0.3°C/min and 12.8±0.5°C/min. Because the change in T_M, the temperature characteristic of the peak, with the heating rate was within 10°C, the activation energies for desorption of hydrogen could not be calculated. For about 10 months COM catalysts desorbed 21.8±1 cc H_2/g, the amount of hydrogen increasing to 23.2 after 17 months and to 29.1 after 23 months (Table 7.1). A second peak appeared at 485°C in the desorption chromatogram of a 23 months old COM Raney nickel. GC analysis of gases evolved in thermal desorption showed 3.67 vol % methane, the remainder being hydrogen. The source of methane could be carbon traces in the Ni-Al alloy or carbonates formed from the atmospheric CO_2 and alkali remaining in Raney nickel after washing with distilled water.

The peak at 485°C in the TPD spectrum is too large (about 5-6 cc/g) to be accounted only by the methane. The increase in hydrogen content determined by the TPD method parallels the values obtained by thermal desorption in a volumetric system.

TPD experiments were devised to determine the readsorption of hydrogen; the corresponding desorption spectra are shown in

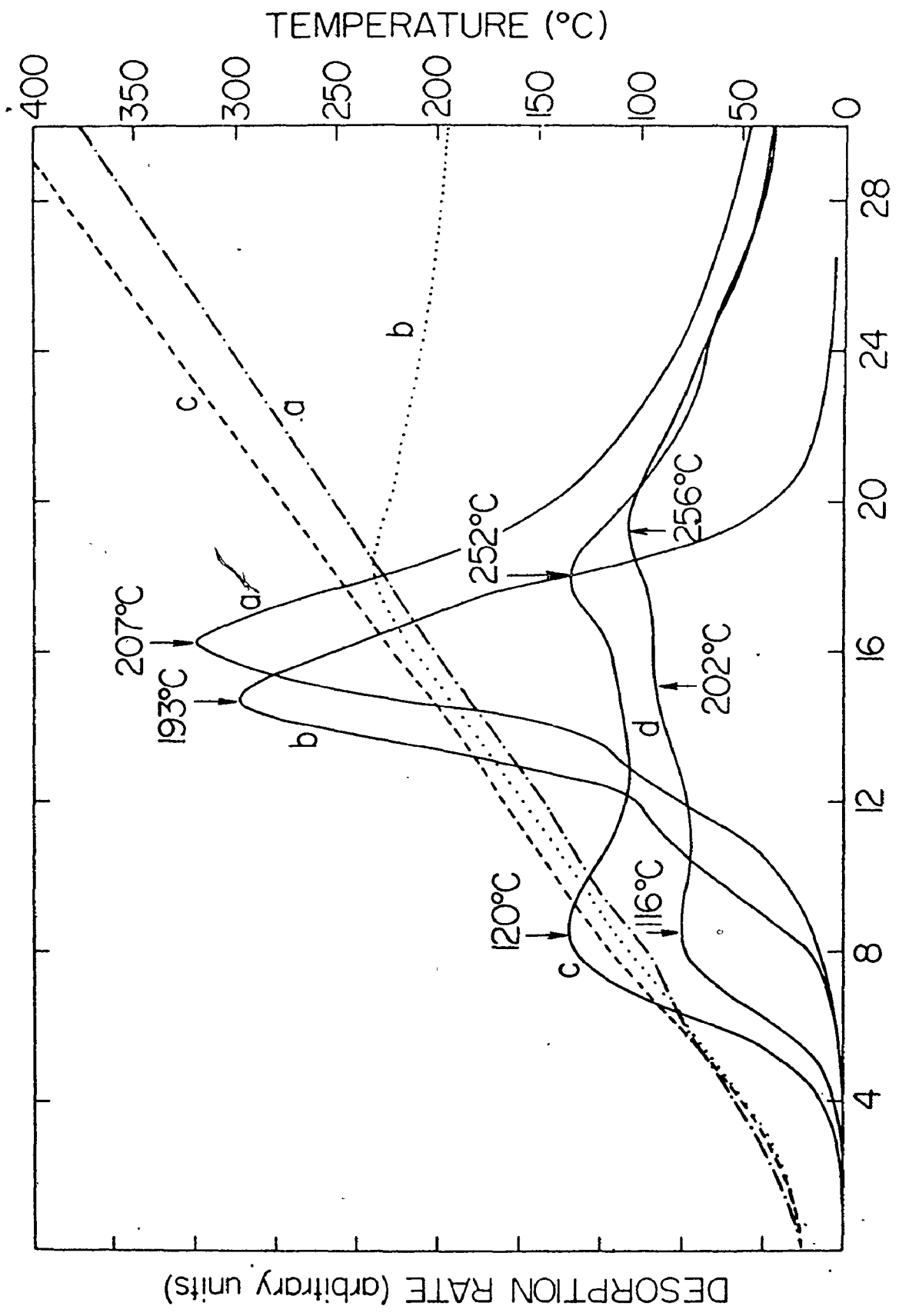

Figure 7.4 TPD curves for COM catalyst: a) regular experiment;b) heating stopped at 232°C; c) sample from b) after adsorption of H_2;d) different sample after adsorption of H_2 in the same conditions as in c).

Table 7.1

Hydrogen Content of COM Catalysts Obtained by Thermal Desorption and TPD as a Function of Catalyst Age

Catalyst Age (months)	*H_2 cc(STP)/g obtained in TPD	Catalyst Age (months)	*H_2 cc(STP)/g obtained in thermal desorption
10	21.8	5	20.5
17	23.2	19	23.4
23	29.1	30	29.8

*These values were corrected for the presence of 3.67 vol % CH_4

Fig. 7.4. A commercial catalyst was heated to 232°C at a heating rate of about 13°C/min, then cooled to room temperature in flowing hydrogen, held at 23°C for 20 hours in hydrogen, evacuated at 23°C to 10^{-5} torr and a second TPD experiment to 700°C was made (curve c, Fig. 7.4). This desorption spectrum had two small peaks: one at 120°C and another at 252°C. The nature of the readsorbed hydrogen, especially the peak at 120°C was different from that on the original catalyst. The peak at 120°C suggests adsorption sites with lower activation energies of desorption, probably weakly chemisorbed hydrogen. Curve d in Fig. 7.4 shows a small peak at 202°C for a similar readsorption experiment. The peak suggests that this hydrogen is the same as the hydrogen in the original sample. The peak at 252°C might be due to hydrogen bound stronger to nickel than the hydrogen corresponding to the peak at 193°C in the initial desorption experiment (curve b). The broken curve c shows the temperatures for both experiments, c and d. The amounts of readsorbed hydrogen are given in Table 7.2. In a regular experiment 22.5 cc H_2/g were evolved to 700°C. In a second experiment with another sample heated to 230°C, 14.11 cc H_2/g were evolved. After being treated with hydrogen, the same sample evolved 20 cc H_2/g instead of 8.39 cc (the difference between 22.5 and 14.11) which should have been evolved if no hydrogen was readsorbed. The extra hydrogen is 20 cc - 8.39 cc = 11.61 cc or 51.6 vol % of the amount of hydrogen evolved in a regular TPD, and it represents the readsorbed hydrogen. In a second experiment 61.3 vol % of the total

Table 7.2

*Readsorption Experiments with COM catalysts

H_2 evolved, cc(STP)/g			H_2 put back into catalyst	
Regular TPD to 700°C	To 230°C	To 700°C after read-sorption	cc(STP)/g	% of "total"
22.5	14.11	20.00	11.61	51.60
22.5	17.87	18.42	13.79	61.30
22.9	-	4.52	4.52	19.76

*In these experiments it was assumed that only hydrogen was evolved

hydrogen evolved by COM Raney nickel was put back into the catalyst. These values are larger than those corresponding to the hydrogen chemisorption on COM Raney nickel at room temperature. If in the initial experiment the sample is heated to 700°C instead of 230°C and a readsorption experiment follows, then the amount of readsorbed hydrogen is 4.52 cc/g or 19.76 vol % from total hydrogen evolved (see Table 7.2). Again the readsorbed hydrogen is larger than the amount accommodated by the surface area of a COM catalyst heated to 700°C. A similar conclusion was drawn from the following experiment[111]: 50 cc of the total 100 cc of hydrogen evolved by a Raney nickel catalyst heated to 1200°C were replaced by subjecting the sample to 2000 psi of hydrogen at 400°C. The authors interpreted this phenomenon as hydrogen existing in the lattice defects in the nickel.

To check the evolution of methane and water from the COM catalyst, hydrogen was used as carrier gas in a series of TPD experiments. In the first two experiments the dry ice trap placed before the detector was removed so that the water vapor could be detected. The GC signal started to increase at 40°C and reached a peak in the region 100-120°C and a small shoulder at 185-200°C accompanied by a slight exothermic effect. The signal returned to the base line at about 300°C. A third experiment was done with a liquid nitrogen trap before the detector to allow the methane to go through but to stop the water vapor. This time the evolution started at 108°C and a maximum was obtained at 208°C. As the only other component found in the evolu-

tion gases by GC was CH_4, the signal recorded with the liquid nitrogen trap in place was considered to correspond to methane. After the methane evolution ended, the dewar with liquid nitrogen was removed and the signal corresponding to H_2O, recorded. From these experiments, it was concluded that the water contained by the COM catalyst started to evolve at about 40°C with a maximum in the rate of desorption at 100-120°C. The desorption of water vapor ended at 300°C. The maximum in methane evolution occurred at 208°C coinciding with the peak in hydrogen evolution, suggesting that methane was formed mainly when the desorption rate of hydrogen reached its maximum. Bayerite loses most of its water at about 220°C, the decomposition being slow at 150°C. This means that the water vapor evolved from the COM catalyst is "adherent" water, i.e. water present in the sample and not removed by evacuation at 10^{-5} torr.

A mass balance calculation shows a good agreement between the experimental weight loss and the weight loss corresponding to the methane and water determined in the TPD experiment. The experimental weight loss for 0.1685 g of COM Raney nickel was 5 mg. The calculated water loss is:

Hydrogen, 17.7 cc(STP), 1.59 mg

Methane, 1.0 cc, 0.71 mg

Water, 2.82 mg

Calculated Weight Loss: 5.12 mg

Experimental Weight Loss: 5.0 mg

The methane determined by GC analysis of gases evolved in a volumetric apparatus was about 1.11 cc/g; the amount determined

by TPD using H_2 as carrier gas was 1.62 cc/g. The difference between the two values could be due to the fact that in the TPD experiment methane formation could be favored by an excess of hydrogen.

It should be mentioned that the presence of methane in the gases evolved during a TPD experiment when Ar is used as carrier gas does not affect significantly the desorption spectrum for two reasons:

1) the percentage of CH_4 is small, 3.67 vol %
2) the hydrogen calibration factor is about 5 times larger than the methane calibration factor.

7.6 RANEY NICKELS STORED UNDER ETHANOL

The TPD study of ethanol-stored catalysts contains experiments with the following samples: II A-1, II A-2, II A-3, and IV A. These samples are characterized by a relatively large alumina trihydrate content (17-49 wt %) and the gases evolved in thermal desorption in a volumetric apparatus contained 21 to 62 vol % methane plus 5-19 vol % carbon monoxide in addition to hydrogen. The separation and continuous determination of H_2, CH_4 and CO during TPD could have been done by using three sets of matched pairs of thermistors and absorption tubes. However, due to the fact that CH_4 and CO were detected at the end of this research, a different approach was used to determine approximately H_2, CH_4 and CO. The position of the peaks in the desorption chromatogram did not change appreciably when the heating rate increased from 2.3 to 12.8°C/min.

The heating rates used in the TPD were 2.3, 4.2, 6.2 and 12.8°C/min, but most experiments were done at 12.8±0.5°C/min because of the relatively short time required for the experiment. A TPD spectrum was characteristic to each of the four different samples studied. However the pattern changed as a function of the catalyst age and, to some extent, amount of sample. A feature distinguishing the ethanol-stored Raney nickels from commercial Raney nickel stored under water was the exotherm accompanying some peaks. For larger samples, the exothermic effect led in some cases to an instantaneous increase in temperature, ΔT of 70°C (or more), and gas evolution was very rapid. It is interesting to note that this explosive gas evolution occurred in the temperature range 150-220°C characteristic of the maximum in the rate of desorption of water vapor from bayerite. Water reacts with metallic aluminum present in the catalyst producing hydrogen

$$2/3\ Al + H_2O = 1/3\ Al_2O_3 + H_2 \qquad \Delta H^\circ_{298} = -70.5\ Kcal. \quad (4)$$

The reaction is highly exothermic. In the same temperature range the ethanol adsorbed on the catalyst and not removed by evacuation at 10^{-5} torr and 23°C undergoes a series of reactions in the presence of hydrogen. The stoichiometry of these reactions can be approximated by the following equation:

$$H_2 + 2C_2H_5OH = 3CH_4 + CO + H_2O \qquad \Delta H^\circ_{298} = -25.4\ Kcal. \quad (5)$$

Reaction (5) is also exothermic.

At the beginning of the TPD experiments it was believed that ethanol-stored Raney nickels evolved only hydrogen during

the desorption and the hydrogen content for different types of Raney nickels was calculated as such. (column 5, Table 7.3). The actual amount of gas evolved was determined volumetrically (column 4, Table 7.3) and the composition of the gas analyzed by GC (Table 5.2). The values given in column 5, Table 7.3 for the "hydrogen" content should be regarded only as relative numbers indicating a lower or larger volume of gas evolved. It is interesting to note that the ratios between the surface areas of the four types of Raney nickels discussed and between the "hydrogen" content are about the same (second and third rows, Table 7.4) suggesting that the desorption and/or formation of gas is a surface process. However, the ratios of the actual gas contents (4th row, Table 7.4) do not indicate this relationship.

The gas content from column 6, Table 7.3 was approximated in this way: it was assumed that the composition of the gases evolved during the TPD experiment was the same as that determined in a volumetric apparatus, where no carrier gas (argon) was present.

$$A = h.Y.f_{H_2} + m.Y.f_{CH_4} + c.Y.f_{CO} \qquad (6)$$

Here A is the total signal response obtained from the TPD chromatogram, h, m and c are the fractions of hydrogen, methane and carbon monoxide respectively determined by gas chromatography, f's are the calibration factors and Y is the unknown and represents the amount of gas evolved. Y is determined from eq. (6) where all the other quantities are known. Equation (6) is valid if there is a linear relationship between the concentration of

Table 7.3

Gas Content for Ethanol Stored Raney Nickels

Catalyst	Age (months)	Surface Area (m^2/g)	c.c. Gas/g Thermal Desorption	TPD	TPD and Gas Analysis	Δ % Between Columns 4 and 6
IV A	12–20	60.5	63.3	28.3	47.3	-25.3
II A-3	0–4	76.3	71.0	43.7	58.0	-18.3
II A-2	0–12	58.9	62.4	29.6	75.0	+20.2
II A-1	17	32.0	65.5	15.6	46.0	-29.8

Table 7.4

Ratios Between Surface Areas and Gas Contents of Ethanol Stored Raney Nickels

Ratio	II A-3:	IV A:	II A-2:	II A-1
Surface Area	2.4	1.9	1.8	1.0
TPD Gas Content	2.8	1.8	1.9	1.0
Thermal Desorption Gas Content	1.1	1.0	1.0	1.0
TPD and Gas Analysis Gas Content	1.3	1.0	1.6	1.0

each gaseous species and the signal response. The percent difference between the actual amount of gas evolved in thermal desorption and the amount calculated for TPD is about 25%. This figure seems too high for the admitted percent error, but one should consider the approximations involved in this calculation and the fact that the composition of the gases evolved in the presence of argon in a dynamic system might not be the same with that when argon is not present in a volumetric system. Also, the gas content depends on the age of the catalyst, usually decreasing with the time of storage, probably due to Al and/or Ni oxidation by the storage liquid and by the atmospheric oxygen diffusing through the liquid. The weakly adsorbed hydrogen, present in fresh preparations, is lost during storage. In eight months of storage the gas content of a IV A catalyst decreased by about 20%.

The TPD spectra of the four types of Raney nickels studied were similar. However it was possible to distinguish the catalysts by their TPD patterns. Temperatures of the maxima in the desorption rate for different types of Raney nickel stored under ethanol are given in Table 7.5. It was possible to obtain a good reproducibility (1-2°C) of the temperature of these maxima for a given type of catalyst, from one experiment to another. However, because the position of the peaks changed with storage time the overall precision in the peak temperatures was in some cases ±15°C. No significant shift of the peaks occurred when the heating rate was changed from 4.2°C/min to 12.8°C/min. A fresh sample has a TPD chromatogram with peaks at lower temperatures

Table 7.5

Temperatures of the Maxima in the Desorption Rate for Ethanol Stored Raney Nickels

Catalyst	Storage time (months)	Start in Gas Evolution (°C)	Temperature of Peaks (°C) I	II	III	IV
II A-1	17	103	151	213*	234	440
II A-2	0-12	63	170*	220		454
II A-3	0-4	50	122	183*	242	288
IV A	12-20	78	153	234*	267*	542

*indicates the largest peak in the desorption spectrum

than catalysts stored for different periods of time (II A-3 in Table 7.5). There is a tendency for some peaks to shift to higher temperatures with storage time. For example, a II A-3 sample had its peak at 113°C when the catalyst was fresh. In subsequent tests the peak was found at 117°C and 121°C after several days, and after four months at 138°C. The other peaks remained at the same temperature. This tendency could be explained in this way: a fresh sample has a large amount of weakly bound hydrogen which is desorbed at a relatively low temperature. This hydrogen is lost during the storage of the catalyst, so that the corresponding peak becomes gradually smaller.

Figure 7.5 shows TPD spectra for II A-2 catalysts. The spectrum in the upper figure was obtained with 0.1490 g of sample. The temperature curve measured in the sample did not show any thermic effects. The peaks at 176°C and 224°C are probably a mixture of hydrogen, methane and carbon monoxide as this temperature range is characteristic of both the dehydration of bayerite and reaction of water with aluminum on one side and the decarboxymethylation of ethanol on the other. When the temperature reached 427°C it is likely that all the ethanol adsorbed on Raney nickel was consumed or desorbed and the peak at 427°C might be due to hydrogen either desorbed from nickel or formed by the reaction of Al and water coming from the decomposition of a certain type of alumina hydrate. Also, hydrogen from the surface or mass of Raney nickel can be desorbed in the temperature range 30°C-700°C. The lower figure shows the TPD pattern of a larger sample of

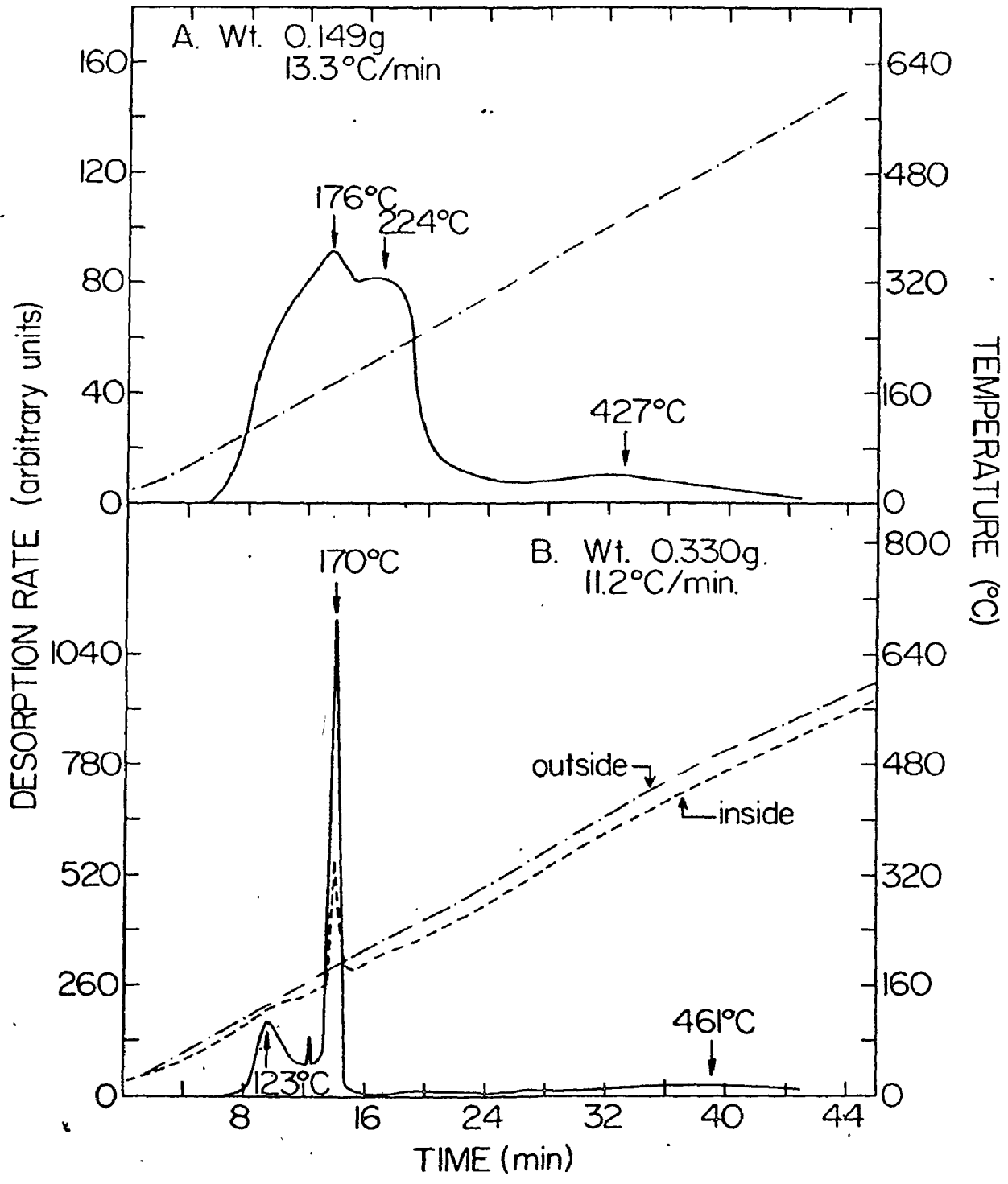

Figure 7.5 Desorption spectrum for type II A-2 Raney nickel.

Raney nickel and the temperature curves measured within the sample and outside the reactor. The peaks, at 123°C and 170°C, were accompanied by exotherms: the increase in temperature during the first peak was 12°C and for the second peak 130°C. The peak at 461°C was not accompanied by an exotherm. It was probably due to the desorption of strongly bound hydrogen, for the same reasons mentioned in the case of the peak at 427°C in the first TPD spectrum. The spectrum in Fig. 7.5-B was distorted by the overheating, i.e., the peaks appeared at lower temperatures than they did in an experiment when no large exothermic effect was found.

The II A-2 catalyst, when fresh, evolved a burst of gas in the temperature range 100-115°C accompanied by an increase in temperature. A 12 month old sample did not evolve gas as a burst in that temperature range, instead had a peak at 144°C and three others at 182°C, 232°C and 460°C.

An interesting TPD spectrum was produced by a IV A Raney nickel that contained about 49 wt % of alumina trihydrate. Eight months of storage did not change appreciably its TPD spectrum. The desorption spectrum is shown in Fig. 7.6, curve a. The peaks at 234-267°C are this time accompanied by an endothermic effect which leads to a decrease in the heating rate in that temperature range. The decrease in the desorption rate was then due to a change in heating rate and probably only one peak would be observed at 236-267°C if the heating rate remained constant. The endothermic effect was caused by the presence of a large amount

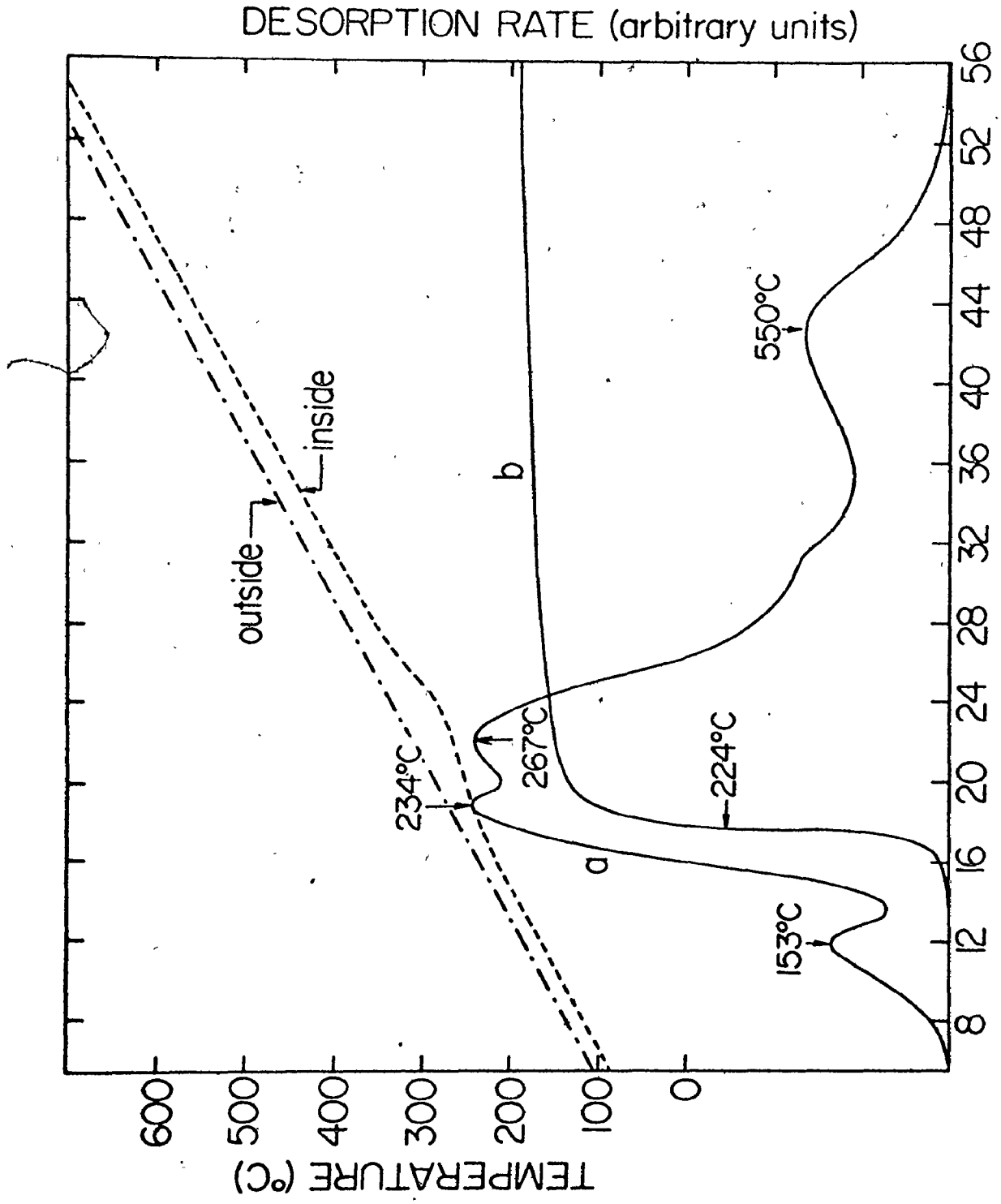

Figure 7.6 a) Desorption spectrum for type IV A Raney nickel (high alumina content).
b) Desorption spectrum of water vapor for $Al_2O_3 3H_2O$ (gibbsite).

of alumina trihydrate which loses most of its water at about 220°C. The dehydration reaction is endothermic[112]:

$$Al_2O_3 \cdot 3H_2O = Al_2O_3(c) + 3H_2O(g) \quad \Delta H^{\circ}_{298} = +70.4 \text{ Kcal/mol} . \quad (7)$$

The exothermic effect, usually present in the TPD chromatogram of ethanol-stored Raney nickels in the 150-220°C range was not observed because of the enthodermic reaction (7) and the net result was an endothermic effect. When large samples (0.7100 g) of IV A Raney nickel were used in a TPD experiment, an exothermic effect, $\Delta T = +32°C$ was observed in the 180°-200°C range followed by an endothermic effect, $\Delta T = -29°C$, at 250°-270°C.

Fig. 3.6-b shows the desorption spectrum of water vapor for an alumina trihydrate (gibbsite) sample with a particle size of about 5 μm. In this case hydrogen was used as a carrier gas and the dry-ice trap was not used. There is a rapid evolution of water above 220°C corresponding to a rapid evolution of gas (curve a) and an endothermic effect similar to that obtained with a IV A catalyst. The levelling of the curve b corresponds to the saturation vapor pressure of water at room temperature. For IV A Raney nickels the peak at 234-267°C is probably mostly hydrogen from reaction (4). At 550°C strongly adsorbed hydrogen is probably being desorbed.

One method of approximating the composition of the peaks evolved at different temperatures is to make TPD experiments with hydrogen as carrier gas using dry ice, or liquid nitrogen traps or no trap at all. In this way certain components in the effluent

are trapped and by comparing the desorption spectra obtained in different conditions, approximations of the composition of the peaks and mass balance calculations can be made. In addition to hydrogen, methane and carbon monoxide identified in the gases evolved in thermal desorption, ethanol and acetaldehyde were detected in a dry ice trap. Ethane is a likely product to be found as traces in the effluent. When no trap is placed before the detector in the TPD system and Ar used as carrier gas, all the above mentioned products plus H_2 can be detected. An adequate trap allows the detection of noncondensable gases from a mixture of condensable and noncondensable gases. For example, if hydrogen is used as the carrier and a dry ice trap prevents water, ethanol and acetaldehyde ($P_{CH_3CHO}^{-81.5°C}$ = 1 mm) to be detected, then the concentrations of a mixture of methane, carbon monoxide and ethane in hydrogen can be measured by the detector. A liquid nitrogen trap reduces the gases detected to CH_4 and CO.

Such an experiment with different traps and carrier gases was done with IV A Raney nickel. The TPD curves are shown in Fig. 7.7. The curve 1 is the chromatogram obtained in a regular experiment at an attenuation of 32 using argon as carrier gas and a dry ice trap. The peaks obtained were a mixture of H_2, CH_4 and CO. Table 5.2 gives the composition of the gases evolved in a volumetric apparatus in the absence of argon, 50 vol % H_2, 45% CH_4 and 5% CO. The curve 3 is the TPD spectrum obtained with a dry ice trap, but this time hydrogen was used as carrier gas and the attenuation was 2. The curve 2 was obtained without a trap in a hydrogen stream at attenuation 4.

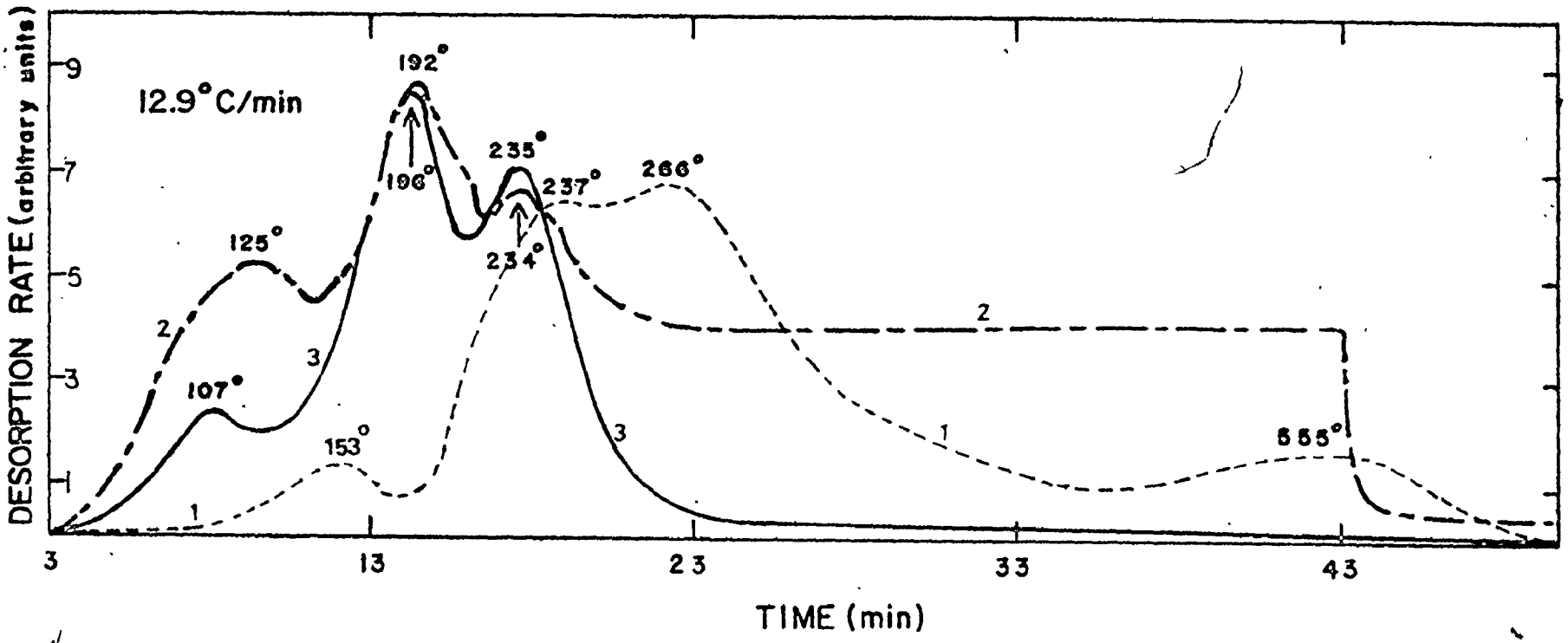

Figure 7.7 TPD spectra of IV A Raney nickels obtained with different traps and carrier gases.
1. Ar carrier gas, dry-ice trap.
2. H_2 carrier gas, no trap.
3. H_2 carrier gas, dry-ice trap.

The peak temperatures are indicated on the diagram. There are slight discrepancies between the peak temperature on the chart because the heating rate was not exactly the same in all three cases. Data from TPD tests made with different traps and carrier gases are presented in Table 7.6. Based on the information given in Table 7.6, the whole TPD spectrum in Fig. 7.7 can be interpreted in this way. The curve 3 shows three peaks at 107°C, 196°C and 235°C for the formation of CH_4 and CO (CH_4/CO = 9 from GC analysis). Beyond 235°C there is a sharp decrease in the rate of formation of these two products. The curve 2 almost parallels the previous curve showing maxima at 125°, 192° and 234°C corresponding to a mixture of CH_4, CO, C_2H_5OH and CH_3CHO. The larger signal is attributed to the presence of ethanol and acetaldehyde, which are the source of methane and carbon monoxide. After 234°C the dotted line becomes parallel to the base line at a height corresponding to the saturation vapor pressure of water at room temperature, the water being produced by the decomposition of alumina trihydrate. During this part of the TPD experiment liquid was condensed on the cool parts of the reactor and an endotherm was recorded. In this region the maxima recorded at 237° and 266°C (see curve 1) are probably due to hydrogen being formed in the oxidation of aluminum by water. The peak at 153°C could be a mixture of H_2, CH_4 and CO or of the last two gases only. The 200°C region of the TPD spectrum is exothermic as it was determined with large weights of catalysts. Obviously at 555°C hydrogen is evolved, either from the nickel surface or lattice or from the

Table 7.6

Summary of Data from TPD Tests at 12.8°C/min with IV A (curve 1,2,3) and II A-3 (curve A,B,C) Raney Nickels Using Different Traps and Carrier Gases

Curve	Sample Weight (g)	Attenuation	Trap Temperature (°C)	Carrier Gas	Molecules Detected	TPD Peaks at °C
1	0.3215	32	-78	Ar	H_2;CH_4;CO;	153(+);237;266(-);555;
2	0.2210	4	25	H_2	CH_4;CO;C_2H_5OH;CH_3CHO; H_2O;	125;192(+);234(+); (-) beyond 250;
3	0.2125	2	-78	H_2	CH_4;CO;	107;196(+);235; (-) beyond 260;
A	0.3470	32	-78	Ar	H_2;CH_4;CO	113(+);177(+);258(-); 300;
B	0.3705	2	-196	H_2	CH_4;CO;	164(+); (-) beyond 260;
C	0.1895	2	25	H_2	CH_4;CO;C_2H_5OH;CH_3CHO; H_2O	103;172(+);254; (-) beyond 260;

(+) denotes an exotherm and (-) an endotherm

oxidation of a metallic component of Raney nickel by water.

In a separate TPD experiment hydrogen was used as carrier gas and a liquid nitrogen trap allowed the detection of CH_4 and CO only. After the gas evolution ended, the dewar flask with liquid nitrogen was removed and the condensed mixture in the trap was detected too. For the mass balance calculations it was assumed that only water was present in the trap, although small amounts of ethanol and traces of ethane could have been present too. If the ratio CH_4/CO was 9, i.e., the same as in the gases evolved in the volumetric apparatus, then by using the equation (3) it is found that

$$178705.6 = (0.9).Y.(5606.8) + (0.1).Y.(5877.48) \quad (8)$$

Y = 31.72 cc/g, i.e., 28.55 cc(STP) of methane and 3.17 cc(STP) of carbon monoxide were evolved per gram of IV A Raney nickel. The gas chromatographic analysis of gases evolved in thermal desorption indicated 28.5 cc of CH_4 and 3.2 cc of CO, in excellent agreement with TPD values. The water content found by TPD was 182.1 mg H_2O/g of catalyst, about 7.5 wt % larger than the amount of water contained by the 48.95 wt % of alumina trihydrate in IV A Raney nickel. This discrepancy could be eliminated if one considers the fact that the condensed liquid in the liquid nitrogen trap contained not only water but small amounts of ethanol, acetaldehyde and traces of ethane which contributed to the total chromatographic signal. The calculated weight loss was 209.3 mg/g of catalyst, also about 7% higher than the experimental weight loss, 195.7±6.3 mg/g. Again there is good agreement

in the mass balance calculations if the correction mentioned above is introduced.

A similar series of TPD experiments were done with II A-3 catalyst immediately after its preparation and after four months. The corresponding TPD spectra are shown in Fig. 7.8 and a summary of data in Table 7.6. Curve A represents a regular experiment with 0.3470 g of sample using argon as carrier gas and a dry ice trap. The recorder attenuation was 32. Curve B is the TPD spectrum of 0.3705 g II A-3 Raney nickel on attenuation 2 with hydrogen as carrier gas and liquid nitrogen trap. Curve C (broken line) was traced on attenuation 2 of the recorder with hydrogen as carrier gas and no trap before the detector. The sample weight was 0.1895 g. The peaks in spectrum A at 113°C and 177°C were exothermic, ΔT reached a value of +42°C. The peak at 258°C was slightly endothermic due to the dehydration of alumina trihydrate. The peaks at 164-177°C in spectrum B were exothermic too indicating that the desorption of H_2, CH_4 and CO was an exothermic process. The constant height of the curve B is caused by CH_4 and/or CO condensing in the trap at -196°C ($P_{CH_4}^{-196°C}$ = 10 mm and $P_{CO}^{-196°C}$ = 400 mm). Spectrum C is produced by a mixture of C_2H_5OH, CH_3CHO, CH_4, CO, C_2H_6 and H_2O, the last component obtained from the decomposition of alumina trihydrate. After 254°C an endothermic effect caused by the dehydration of alumina trihydrate is recorded and curve C becomes almost parallel to the abscissa indicating that water was condensing on the room temperature parts of the system. In the same

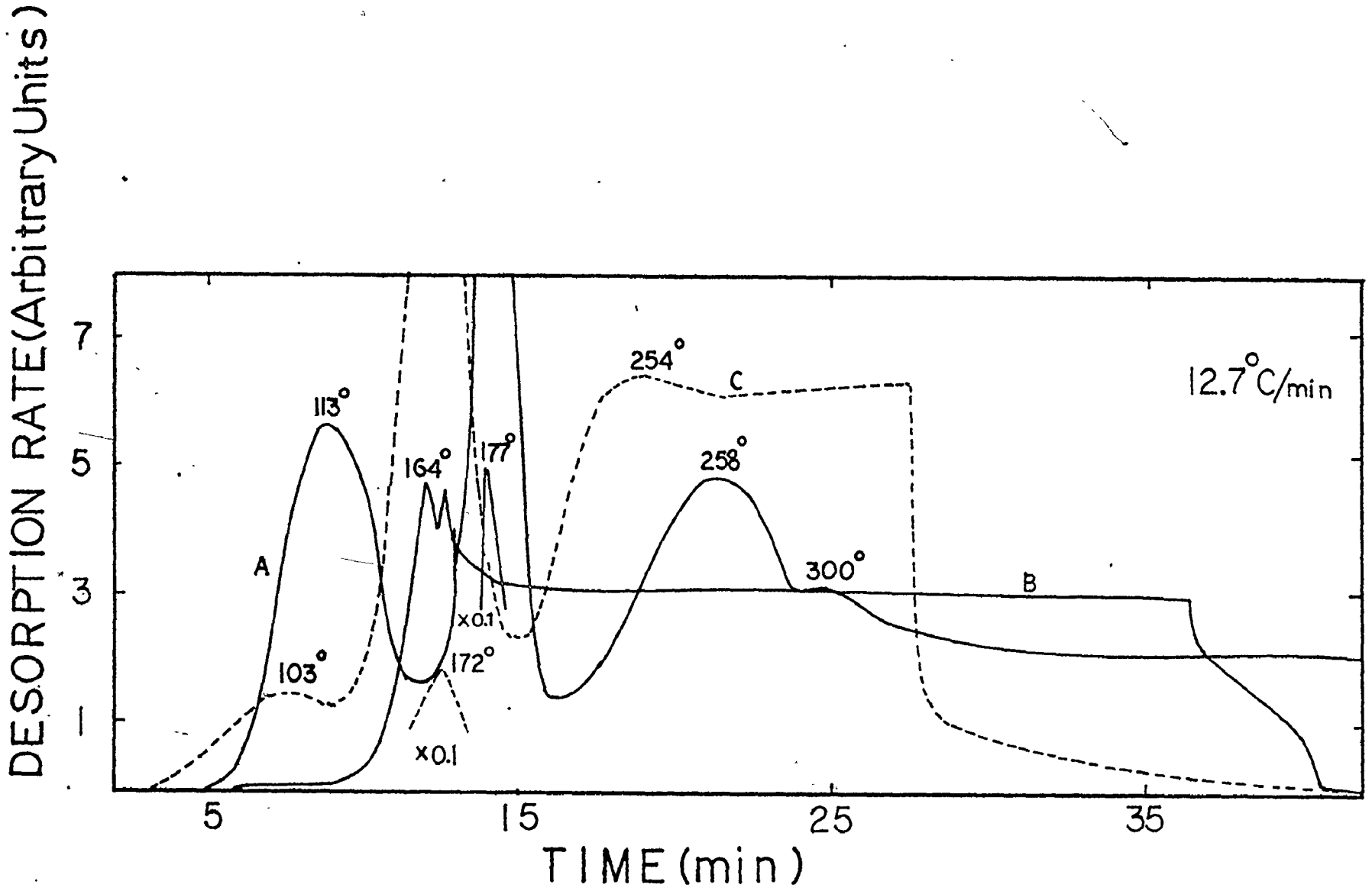

Figure 7.8 TPD spectra of II A-3 Raney nickels obtained with different traps and carrier gases.

A. Ar carrier gas, dry-ice trap.
B. H_2 carrier gas, liquid nitrogen trap.
C. H_2 carrier gas, no trap.

temperature range a peak is recorded on spectrum A at 258°C, this very likely corresponding to hydrogen formed in the reaction between water and Al. By comparing the size of the peaks at 113° and 103°C, we could say that most of the gas evolved at 113°C (spectrum A) is hydrogen, probably weakly chemisorbed. The desorption of hydrogen in the range 100-180°C is accompanied by the formation of methane and/or carbon monoxide. A mass balance calculation for the II A-3 sample, similar to the calculation done for IV A Raney nickel, determines from the amount of CH_4, CO and H_2O evolved an expected weight loss of 40.3 mg compared with an experimental weight loss of 41 mg.

Most Raney nickel samples were evacuated at room temperature prior to TPD experiments. When a II A-3 catalyst was evacuated at 110°C for 48 hours, the desorption spectrum consisted of one peak only at 278°C. The gas evolution started at 190°C and the amount of gas evolved per gram of catalyst to 700°C was about half the amount evolved in a regular TPD. It is likely that most of the ethanol and the species derived from it were evolved during the evacuation at 110°C and only hydrogen desorbed in the TPD, about 22 cc(STP)/g. The hydrogen source could have been the reaction between water from alumina trihydrate and aluminum. The experimental weight loss was 58.4 mg/g compared with 96.5±10 mg in a regular experiment. The water bound to alumina trihydrate in II A-3 catalysts weighed 77.5 mg/g.

7.7 WATER ADDITION EXPERIMENTS

The fact that the main part of the gas evolved by Raney nickels in a TPD experiment was desorbed exothermically at 200°C-220°C, when most of the water associated with the alumina trihydrate in the catalyst is lost, led naturally to the investigation of the effect of water vapor on Raney nickel catalysts. The TPD system was arranged to introduce into the carrier gas about 25 torr of water vapor for desired intervals of time by flowing argon through a water saturator. Water vapor was introduced to the catalyst at a constant furnace temperature, usually at a time when hydrogen evolution was not large. In each case introduction of water yielded an exothermic desorption peak (Fig. 7.9). The exothermic effect was evident at lower temperatures (84°C). When the temperature was increased (upper part of Fig. 7.9) a large exothermic effect accompanied the hydrogen evolution. In some experiments water was added from room temperature to 700°C, while in other experiments addition was done at 550°C-700°C. The reason for adding water at temperatures higher than 550°C was to make sure that, for ethanol-stored catalysts, methane and carbon monoxide evolution had ended. Of course, at higher temperatures, the chance of oxidizing nickel is greater too. However, even at lower temperatures, addition of water does not favor formation of CH_4 and CO as the equilibrium in the reaction

$$H_2 + 2C_2H_5OH \rightleftharpoons 3CH_4 + CO + H_2O \qquad (9)$$

is displaced to the left. The exothermic evolution of hydrogen

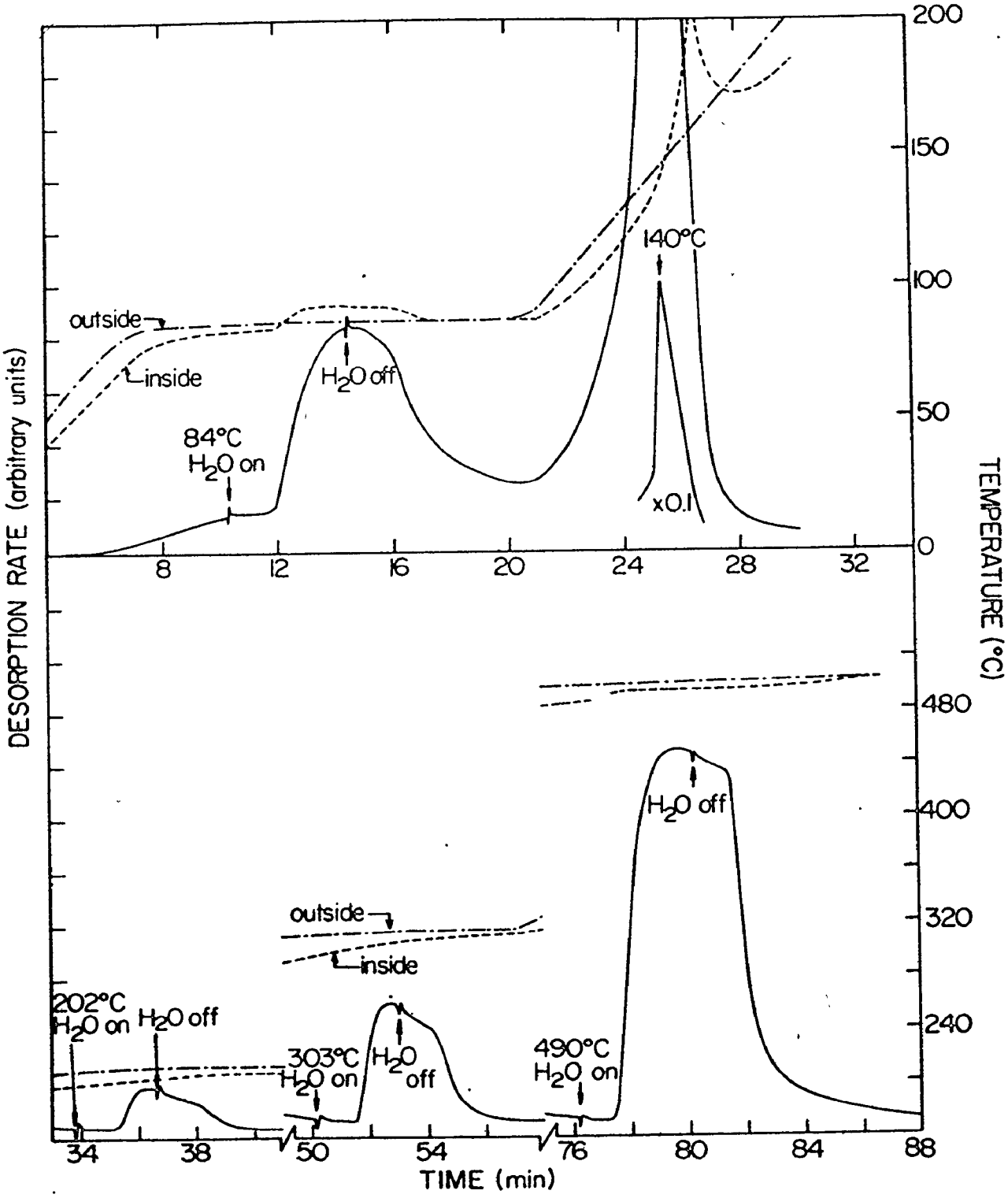

Figure 7.9 The effect of H_2O vapor on type II A-2 Raney nickel. Temperatures measured inside and outside the TPD cell are shown by broken lines.

at each addition of water was noticed for both water-stored (commercial) and ethanol-stored catalysts (II A-1, II A-2 and IV A). The amount of hydrogen evolved in a water addition test was up to 3.2 times larger than in a regular TPD for the COM catalyst (Table 7.7). The values for the ratios of the amount of gas evolved in a water addition TPD to the amount of gas desorbed in a regular TPD are approximate and are actually the ratios of the corresponding total peak areas. When water is added to Raney nickel, hydrogen can be formed in one of these reactions

$$2/3\ Al + H_2O_{(g)} = 1/3\ Al_2O_3 + H_2 \qquad \Delta H^\circ_{298} = -70.5\ Kcal/mole \qquad (10)$$
$$K^{298}_{eq} = 1.56\times10^{52}$$

$$Ni + H_2O_{(g)} = NiO + H_2 \qquad \Delta H^\circ_{298} = +0.5\ Kcal/mole \qquad (11)$$
$$K^{298}_{eq} = 1.05\times10^{-3}$$

$$Ni + 2H_2O_{(g)} = Ni(OH)_2 + H_2 \qquad \Delta H^\circ_{298} = -13.0\ Kcal/mole \qquad (12)$$
$$K^{298}_{eq} = 0.19$$

Reactions (11) and (12) are thermodynamically limited as the equilibrium constant of reaction (11) is of the order of magnitude 10^{-3} at room temperature and is still very small at 700°C (about 5.2×10^{-3}). Reaction (10) is the only one favored at room temperature as well as high temperature. ΔH° at 700°C is -68.6 Kcal/mole, i.e., it does not change much with temperature. However, due to the presence of active surface nickel on which surface processes can occur, it is possible that reactions (11) and (12) do not have thermodynamic limitations.

Table 7.7

Gas Evolution and Nickel Oxidation Data for Water Addition TPD Experiments

Type of Catalyst	$Al_2O_3.3H_2O$ wt %	Ratio of Gas Evolved in Water Addition TPD to Regular TPD	wt % of Total Nickel Oxidized	% of Surface Nickel Oxidized
COM	7.10	3.2	0.55	11.7
II A-2	17.83	2.5	0.61	9.9
II A-1	17.26	1.9	-	-
IV A	48.95	1.0	-	-

In water addition experiments, generally the ratio P_{H_2}/P_{H_2O} calculated from the TPD chromatogram by the method described in Appendix D was higher than the equilibrium constant, K_{eq} for nickel oxidation by water vapor (reaction 11), so we suggest that bulk nickel oxide was not formed (see Table 7.8). Similar experiments with hydrogen as carrier gas on samples used in regular TPD tests gave no indication of water evolution, as would be expected if bulk or surface NiO has been formed. In experiments made on samples from water addition tests, water was found corresponding to about 0.6% of total nickel or about 11% of surface nickel being oxidized (Table 7.7). The corresponding volume of hydrogen due to oxidation of nickel by water was less than 2 cc(STP)/g of catalyst. Depending on the amount of water added, a commercial Raney nickel evolved between 44 and 77 cc(STP)H_2/g compared with 23.8 cc evolved in a regular experiment. COM catalysts contain enough metallic aluminum (7.1 wt %) to produce 88.5 cc H_2/g by reacting with water.

Table 7.9

Mass Balance in Water Addition TPD with COM Catalyst

H_2 Evolved in regular TPD (cc/sample)	H_2 Evolved in water addition TPD (cc/sample)	ΔH_2 (cc/sample)	Aluminum Oxidized (mg/sample)	Al_2O_3 formed (mg/sample)	Δw (mg/sample)	Δw experimental (mg/sample)
25.1	45.3	20.2	14.7	29.3	14.6	13.0

Table 7.8

P_{H_2}/P_{H_2O} Ratios Calculated from TPD Spectra of COM Catalysts in Water Addition Experiments

Experiment	Temperature (°C)	Calculated P_{H_2}/P_{H_2O}	K_{eq}
TPD-35	179	259.4×10^{-3}	1.62×10^{-3}
	186	176.9×10^{-3}	1.65×10^{-3}
	249	394.1×10^{-3}	1.95×10^{-3}
	428	272.1×10^{-3}	2.93×10^{-3}
	701	26.6×10^{-3}	5.15×10^{-3}
TPD-66	233	839.6×10^{-3}	1.80×10^{-3}
	398	1312.9×10^{-3}	2.75×10^{-3}
	678	809.1×10^{-3}	4.93×10^{-3}

A mass balance calculation was done with a commercial catalyst in a water addition test. Table 7.9 shows the extra hydrogen due to the reaction of aluminum and nickel with water. The amount of nickel oxidized (5.2 mg/sample) was determined by measuring the corresponding amount of water formed in a TPD experiment in which hydrogen was used as carrier gas. ΔH_2 in Table 7.9 was corrected for the hydrogen evolved due to nickel oxidation (1.97 cc/sample). The calculated weight increase due to aluminum oxidation was 12.3% higher than the experimental weight increase, a discrepancy which could be explained by the experimental error.

A IV A Raney nickel, containing about 49 wt % alumina trihydrate, evolved the same amount of gas in a water addition TPD as in a regular TPD. The water addition to the catalyst did not result in producing more hydrogen because of the large amount of water already present as alumina trihydrate. In both experiments the weight loss was about 87 mg/sample. Another interesting feature of the water addition TPD tests was the fact that, generally, the amount of hydrogen evolved as a result of a dose of water, corresponded to the stoichiometric amount according to reaction (10) or (11), i.e. $1H_2$ was produced for each H_2O introduced. As the equilibrium constant of reaction (11) is about 10^{-3}, it follows that oxidation of aluminum occurred.

7.8 SUPPORTED NICKEL CATALYSTS

This section describes the desorption of hydrogen from nickel-on-silica catalysts during TPD and water addition tests, similar to those done with Raney nickel catalysts. The purpose of this study was to find the extent of nickel oxidation by water

in water addition tests and the amount of hydrogen adsorbed on the nickel surface during the reduction of nickel oxide.

The NiO/SiO_2 catalyst was evacuated overnight at 200°C to 10^{-5} torr to remove the water adsorbed on the catalyst surface (6.1 wt %). The nickel content was determined in two ways:

1) by dissolving the sample in nitric acid and determining nickel by the dimethylglyoxime method
2) by reducing the catalyst with hydrogen in a temperature-programmed reduction (TPR) experiment and determining the amount of water formed from the TPR spectrum.

The second method has the advantage of a continuous and quantitative monitoring of the H_2O production. During the TPR of NiO/SiO_2 there were two maxima in the H_2O production at about 234°C.

The treatment of the sample for a TPD experiment consisted of removing the adsorbed water by evacuation at 200°C, then reducing the sample in hydrogen for 3 hours at 420°C, cooling the Ni/SiO_2 catalyst in flowing hydrogen to room temperature followed by evacuation to 10^{-5} torr. The sample was then ready for the TPD experiment. Argon was used as carrier gas, and a heating rate of 12.5°C/min from room temperature to 700°C. The desorption spectrum consisted of three hydrogen peaks: 102-122°C, 180°C and 466°C. The total amount of hydrogen desorbed to 700°C was 12.2 cc(STP)/g Ni.

However, in one experiment 16.2 cc H_2/g Ni were desorbed (Table 7.10). This value seems too high but not unlikely if it is

compared to 15.8 cc reported by Mars et.al.[29] as the volume of a hydrogen monolayer on a Raney nickel catalyst. However, the nickel surface area, determined by hydrogen chemisorption at -196°C, can accommodate only 6.1 cc H_2/g Ni. It is possible that at room or higher temperature, more hydrogen can be chemisorbed. The experimental data about the nickel on silica catalyst are presented in Table 7.10. The water addition tests were done in two different ways: after the hydrogen was evolved during the TPD, water was added at 700°C. Each dose of water produced a hydrogen peak. Water was added until no more hydrogen was evolved. Despite the fact that nickel oxidation by water vapor is favored thermodynamically at high temperatures, only 1.1% of the total nickel was oxidized. This corresponds to 12.6-18% of surface nickel, depending on the value chosen for hydrogen chemisorption on nickel (11.3 or 16.2 cc H_2/G Ni) and assuming Ni area constant to 700°C. The fraction of oxidized nickel was determined from the amount of hydrogen evolved after water addition. In the second method, water was added during the TPD test at constant temperature between 100°C and 700°C when hydrogen evolution was small. By comparing the ratios P_{H_2}/P_{H_2O} calculated from the TPD spectrum with the equilibrium constant for the reaction of nickel oxidation by water vapor it was found that in many instances the ratios P_{H_2}/P_{H_2O} were at least one order of magnitude larger than the equilibrium constant. If it is assumed that the thermodynamics apply to both bulk and surface nickel oxidation,

Table 7.10

TPD and Water Addition Tests Data for Nickel on Silica Gel Catalyst

*Ni Content (wt %)	BET Area (m^2/g)	Nickel Area (m^2/g Ni)	H_2 Evolved in TPD (cc(STP)/g Ni	H_2 Peaks in TPD (°C)	Additional H_2 Evolved in Water Addition TPD to 700°C (cc(STP)/g Ni)	wt % of Total Nickel Oxidized	% of Surface Nickel Oxidized
8.65	329.3	22.1	12.2-16.2	102-122	4.1	1.1	12.6-18.0
				180			
				466			

*Nickel content based on the weight of NiO/SiO_2

this means that adsorbed hydrogen has been "chased" from the nickel surface by water molecules. Even if it is considered that all the hydrogen desorbed after one dose of water was formed in the nickel oxidation reaction, about 1 wt % of total nickel was oxidized.

The conclusion of this section is that the fraction of nickel oxidized in a water addition test is very small. These chances for oxidizing Ni are even smaller in the TPD experiments with Raney nickel due to the presence of aluminum.

7.9 NICKEL-ALUMINUM ALLOYS

Nickel-aluminum alloys with a composition similar to Raney nickel catalysts (4-8% aluminum) were prepared in the laboratories of the Department of Metallurgy and Materials Science to study their behaviour towards adsorption of hydrogen and oxidation by water vapor in temperature-programmed desorption experiments. The chemical composition of these alloys is given in Table 7.11.

Table 7.11

Chemical Composition of Nickel-Aluminum Alloys

Nominal Composition (wt % Al)	Nickel Analysis (volumetric) wt % Ni	Aluminum Analysis *(AAS) wt % Al	Iron Analysis (AAS) wt % Fe_2O_3
4	96.20	4.07	-
8	92.04	7.74	0.12

*AAS: Atomic Absorption Spectroscopy

The nickel used in TPD experiments was electrolytic nickel obtained from Falconbridge Copper Ltd. It contained 99.9% Ni, 54 ppm carbon and 12 ppm cobalt. Ni and Ni-Al alloys were received as 5 cm×1 cm×1 cm ingots which were cut to small chips in a milling machine and the chips were used in the TPD experiments. The metal and alloy samples were heated in the TPD reactor in flowing hydrogen from room temperature to 700°C at a heating rate of 12.6°C/min. Then they were cooled to room temperature overnight in flowing hydrogen (40 ml/min) and evacuated to 10^{-5} torr. The samples were reweighted before TPD, as small amounts of oxides could have been reduced during the hydrogen treatment. Argon was used as carrier gas in the TPD experiments. The heating rate was the same as in the hydrogen treatment, 12.6°C/min, and the highest temperature reached in the experiments was usually 700°C. After TPD the sample was allowed to cool to room temperature in argon, a new TPD was done, this time with water vapor added to the argon from 100°C to 700°C. The addition of water was accompanied, usually at higher temperatures, by hydrogen evolution. The data obtained in the TPD experiments with Ni and Ni-Al alloys are given in Table 7.12. The amount of hydrogen desorbed to 700°C was 0.12-0.15 cc(STP)/g for the pure nickel sample. As the surface area of nickel chips was virtually zero, no significant amounts of hydrogen could be chemisorbed on the sample. The solubility of hydrogen in nickel is about 0.07 cc/g at 721°C and increases with increasing temperature to 0.13 cc/g at 1123°C[113]. As the maximum temperature of the hydrogen treatment of the sample was 700°C, this means that some hydrogen was dissolved in the mass

Table 7.12

TPD Data for Nickel-Aluminum Alloys

Experiment #	Al Content of Alloy (wt %)	H_2 Evolution Began at (°C)	Temperature of Peak Maxima (°C)	H_2 Evolved to 700°C (cc(STP)/g) Without H_2O	With H_2O	P_{H_2}/P_{H_2O}	K_{eq}	Wt % of Ni Oxidized
TPD-56	7.74	210	428	1.49		at 676°C		
TPD-56'	7.74				0.53	22	$\times 10^{-3}$ 4.9×10^{-3}	0.15
TPD-59	7.74	133	376	1.95		at 625°C		
TPD-59'	7.74				0.79	5.08×10^{-3}	4.42×10^{-3}	0.23
TPD-57	4.07	106	172	0.038		at 711°C		
TPD-57'	4.07				1.16	82.3×10^{-3}	5.03×10^{-3}	0.32
TPD-58	4.07	96	138	0.029		at 712°C		
TPD-58'	4.07				1.50	76.3×10^{-3}	6.04×10^{-3}	0.41
TPD-60	0	107	150;276*	0.12		at 607°C		
TPD-60'	0				0.015	4.5×10^{-3}	4.30×10^{-3}	0.38×10
TPD-61	0	112	142;297*	0.15				
TPD-61'	0				0.038			1.00×10

*: denotes the largest peak

of nickel. Indeed, cathodically charged nickel can be supersaturated with hydrogen, 0.14-0.76 cc/g. Also, Ni wire can be charged with hydrogen, if it is heated for one minute at 800°C in 40 torr of hydrogen. At 10^{-3} torr and 720°C a complete desorption of hydrogen occurs[113]. The position of the hydrogen peak in the TPD spectrum of the nickel sample (276°-297°C) suggests a relatively strong bond between hydrogen and nickel. The 8% aluminum alloy evolved between 1.49 and 1.95 cc H_2/g, i.e., 13 times more hydrogen than pure nickel. The order of magnitude of the amount of hydrogen sorbed by the alloy indicates a possible Ni-Al-H solid solution. The larger aluminum atom (r^3_{Al}/r^3_{Ni} = 1.52, where r is the atomic radius) may disturb the normal nickel lattice creating new positions where hydrogen atoms can be placed. Emmett[25] reports a lattice constant of 3.546 Å for a 8 wt % aluminum-nickel alloy, compared to 3.532 Å, the lattice constant for pure nickel.

The hydrogen peak at 376°-428°C is almost perfectly symmetrical, suggesting a second order reaction

$$2H_{(ads)} \rightarrow H_{2\,(gas)} \qquad (13)$$

The heat of desorption of hydrogen from the mass of nickel is -3.5 Kcal/mol, i.e. the desorption is exothermic. No thermal effects were recorded during the desorption of hydrogen, probably because of the small amounts of hydrogen desorbed.

The 4% aluminum alloy desorbed only a very small amount of hydrogen, 0.029-0.038 cc(STP)/g, and the temperature of the

peak maximum was 138°-172°C, lower than in the case of 8% Al alloy. Also, the hydrogen evolution started at about 100°C, indicating a weaker hydrogen-nickel bond than for 8% Al alloy. Two forms of hydrogen were present on the pure nickel sample: one desorbing at 142°-150°C and the second at 276°-297°C.

Addition of water vapor during TPD to nickel and 8% aluminum alloys resulted in a hydrogen peak only after 490°C. Obviously, the low reactivity of these samples towards water can be explained by the small surface area of these materials. Raney nickel, a fine powder with a surface area of about 80 m^2/g, reacts quite easily with water vapor at 70-80°C, forming hydrogen. However, the 4% aluminum alloy is more reactive towards water than pure nickel and 8% Al-Ni alloy, producing hydrogen from 100°C to 700°C. Nickel-aluminum alloy forms more hydrogen in water addition tests than pure nickel, probably because of the presence of metallic Al. Indeed, the ratios P_{H_2}/P_{H_2O} calculated from the TPD spectrum of 4% aluminum alloy in water addition tests were about 16 times larger than the equilibrium constant for the reaction $Ni + H_2O \longrightarrow NiO + H_2$, suggesting that Ni was not oxidized. The case of the 8% Al alloy is not so clear, as in one experiment P_{H_2}/P_{H_2O} was about 4 times higher than K_{eq}. The calculated P_{H_2}/P_{H_2O} was equal to K_{eq}, within the experimental error, for the pure nickel sample, when only 0.38×10^{-2} - 1.00×10^{-2} wt % of total Ni was oxidized by water. Even if we assume that only nickel was oxidized in the Ni-Al alloys during water addition tests the fraction of nickel oxidized is still a very small one,

0.15-0.41 wt %. The largest fraction of oxidized nickel in Raney nickel catalysts in water addition tests was about 1 wt % of total nickel, contributing less than 2 cc H_2/g of catalyst to the total amount of hydrogen evolved by Raney nickels. It should be noted that no NiO was found in a Raney nickel catalyst after a regular TPD experiment, i.e., where no water vapor was added to the sample. Thus, only metallic aluminum in Raney nickel reacted with water, adherent or associated with alumina trihydrate, generating part of the total hydrogen evolved during TPD.

The conclusion of the experiments described in this section can be summarized in the following table.

Al content of alloy wt %	H_2 evolved to 700°C cc(STP)/g		
	0	4	8
1. Heated and cooled in H_2 and evacuated	0.13	0.033	1.7
2. Sample from 1 plus H_2O	0.004	1.35	0.53

The 8% Al alloy sorbed a sizeable amount of H_2 and both alloys reacted with H_2O to a limited extent, particularly at higher temperatures.

CHAPTER 8

DISCUSSION, CONCLUSIONS AND RECOMMENDATIONS

8.1 GENERAL

The purpose of this chapter is to consider the results of this research, to discuss them in comparison with other research, and to make conclusions about the nature of hydrogen in Raney nickel catalysts. Also, recommendations about further work on Raney nickel catalysts are made.

8.2 DISCUSSION

The polemic on the nature of hydrogen in Raney nickel was delineated at the Paris meeting of ICC in 1960 by P. H. Emmett[25] and Mars, Scholten and Zwietering[29]: is the hydrogen evolved on heating Raney nickel, in excess of the amount that may be attributed to chemisorption, held interstitially in the nickel, or is the hydrogen produced by the reaction of residual aluminum and water?

Results of present research indicate that when Raney nickel is heated, except for chemisorbed hydrogen, hydrogen comes from the two sources mentioned above: the interstitial hydrogen and the reaction of aluminum and water.

Evidence supporting the existence of nickel-hydrogen solid solution or nickel-aluminum-hydrogen solid solution comes mainly from the data obtained for commercial catalysts. Table 8.1

Table 8.1

Hydrogen Content of Raney Nickel Catalysts Determined by Different Methods

Catalyst Type	H_2 Content, cc(STP)/g			
	HCl Dissolution	Thermal Desorption	$H_2 - D_2$ Exchange	TPD
COM	21.3±5.1	22.0±1.2	25.8±0.2	22.5±1.0
II A-1		26.4	26.5	
II A-2		26.9		
II A-3		54.6		
IV A		41.2	11.9-13.6	

The hydrogen content for II A and IV A catalysts was obtained by correcting the amount of H_2 evolved in thermal desorption for the H_2 consumed in the reaction with ethanol and equivalent to one third of the CH_4 evolved.

shows the hydrogen content, determined by different methods, for several types of Raney nickels. The agreement of the hydrogen content of COM determined by hydrogen-deuterium exchange with H_2 content determined by other methods suggests that this amount of hydrogen preexisted in the sample and was not formed in any reaction, such as Al or Ni oxidation by water. The possibility that part of the hydrogen came from the exchange of deuterium with the water bound to alumina trihydrate in the catalyst is eliminated because the H_2-D_2 exchange in the IV A Raney nickel, containing 49 wt % alumina trihydrate, resulted in a relatively small hydrogen content, 11.9-13.6 cc/g. The maximum amounts of H_2 chemisorbed on Raney nickel were obtained at -196°C and were 8.0 and 13.9 cc(STP)/g for COM evacuated at room temperature and 106°C, respectively. If it is assumed that COM Raney nickel has an average hydrogen content of 22 cc(STP)/g and the reaction of Al and H_2O produces a negligible or small amount of H_2, then at least 8 cc H_2/g must form a solid solution with nickel.

Magnetic data obtained by Macnab and Anderson[36] support the hypothesis of hydrogen as Ni-H or Ni-Al-H solid solutions. As hydrogen was removed from Raney nickel by heating, the magnetization increased about 0.63 μ_B (Bohr-magneton) per hydrogen atom. According to the equation

$$\sigma_o^* = 57.5\ (1 - 1.82\ nX) \qquad (1)$$

where σ_o^* is the saturation magnetization at 0 K per gram of alloy, n = 1 for hydrogen and n = 3 for aluminum, X is the atom fraction of H or Al in the solid solution and 57.5 corresponds to 0.606 μ_B

proposed by the authors mentioned above, an atom fraction of 0.55 of H eliminates ferromagnetism. If the relative amounts of H and Al in the nickel solid solution are known, the atom fractions of H and Al can be calculated from magnetic data using Eq. (1). Taking the limiting case of the solute being only H, the amount of hydrogen evolved on heating the catalyst to 500°C can be calculated from the magnetic data for samples pretreated at 25° and 500°C, assuming that chemisorbed and interstitial hydrogen have the same effect on magnetism. If the hydrogen is removed by heating at 500°C a hydrogen evolution of 26 cc/g is calculated for a COM Raney nickel, compared with 25.8 cc found by H_2-D_2 exchange, 22.5 cc by TPD and 22.0 cc by thermal desorption.

These data support the postulate that hydrogen is present interstitially in a Ni-H or Ni-Al-H solid solution. However, the importance of this conclusion is decreased by the fact that Eq. (1) has not been established for Ni-H solid solutions and, according to eq. (1), the hydrogen remaining at 500°C seems unrealistically large, 34 cc(STP)/g Ni.

In a recent paper Martin and Fouilloux[115] studied Raney nickel, free of Al_2O_3 and NiO, by means of magnetic techniques and concluded that evolved hydrogen cannot be the result of reaction of H_2O with metallic Ni or Al. The experimental observations were interpreted assuming that H_2 is mainly present as chemisorbed gas, but no values for metallic surface area are given. Some of Raney nickels studied by Martin et al. evolved nearly 50 cc(STP)H_2/g which would correspond to a nickel surface area of 182 m^2/g, a highly unrealistic figure even for the total surface area of a Raney

nickel catalyst. In the author's opinion, most of this hydrogen must have come from the mass of Ni and probably less than half of it from the Ni surface.

Hydrogen dissolved interstitially in Raney nickel has been described by the "screened proton model"[116]. This model assumes that hydrogen is ionized to protons. The positive charge of the metal ions is smoothed out into a uniform positive charge neutralizing the electron gas. The effect of introducing a proton into this hypothetical metal is considered from the standpoint of the Debye-Hückel theory of electrolyte solutions. The electrons will tend to cluster around the proton creating an increase in electron density. The screened proton model leads to conclusions that are consistent with the experimental observations. For example, the heat of solution for the following process

$$1/2\ H_2 \xrightarrow{M} H^+_{(ads)} + e^-_{(ads)} \qquad (2)$$

where M is a transition metal, can be calculated using an expression predicted by the screened proton model theory:

$$\Delta H_{exp} = 15.9\ eV - \phi + \varepsilon_{rep} + \varepsilon_{pol}. \qquad (3)$$

Here ΔH_{exp} is the experimental heat of solution, ϕ is the work function of the metal, ε_{rep} is the interaction energy between the screened proton and the ion core (mainly a repulsive term) and ε_{pol} is the energy change on going from the initially uniform electron density to the final situation where there is an increase in electron density around the proton. Due to a difference in ε_{rep} for Ni and Pd it is found that $\Delta H°$ for Ni is +7.0 Kcal/mole

and -4.6 Kcal/mole for Pd, in agreement with the experimental data. It follows that the desorption of the interstitial hydrogen is a slightly exothermic process. During hydrogen desorption from COM a small exothermic effect was recorded only when large amounts of samples were used. No thermic effects accompanied H_2 desorption from lower weights of COM catalysts. Readsorption experiments with COM Raney nickel indicated too the possibility of the presence of interstitial hydrogen as the amount of hydrogen put back into the catalyst exceeded the hydrogen which could be accomodated by the nickel surface.

The case of ethanol-stored Raney nickels is more complicated as, in addition to hydrogen, methane and carbon monoxide were also evolved on heating the catalysts due to the presence of residual ethanol and acetaldehyde left on the Raney nickel surface. All the reactions indicated by Table 8.2 could occur on ethanol-stored Raney nickels. It was proved that reactions 4 and 5 occur only to a limited extent. Both exothermic and endothermic peaks were recorded in a TPD spectrum of II A and IV A samples, corresponding mainly to reaction 1 and 2 (Table 8.2), respectively. The exothermal effect could also be produced by reaction 3. The larger amounts of hydrogen evolved from samples II A-3 and IV A (Table 8.1) certainly cannot be attributed only to chemisorption. The large exothermic effect (ΔT = 130°C) accompanying a hydrogen peak at about 220°C, the temperature characteristic of bayerite losing most of its water, is a strong argument in favor of aluminum oxidation by water with formation of hydrogen.

Table 8.2

ΔH°_{298} for Reactions Occuring on Raney Nickel Catalysts During Thermal Desorption

	Reaction	ΔH°_{298}, Kcal/mole
1)	$2/3\ Al + H_2O(g) = 1/3\ Al_2O_3 + H_2$	-70.5
2)	$Al_2O_3.3H_2O = Al_2O_3 + 3H_2O(g)$	+70.4 (ref. 112)
3)	$H_2 + 2C_2H_5OH(g) = 3CH_4 + CO + H_2O$	-25.4
4)	$Ni + H_2O(g) = NiO + H_2$	+ 0.5
5)	$Ni + 2H_2O(g) = Ni(OH)_2 + H_2$	-13.0
6)	$(1/x)Ni.H_{2x(absorbed)} = Ni + H_2(g)$	- 7.0
7)	$(1/x)Ni.H_{2x(adsorbed)} = Ni + H_2(g)$	+10.0 → 30.0 (ref. 114)

Addition of water vapor to Raney nickel produced an exothermic hydrogen peak in the TPD spectrum confirming that Al oxidation is another source of hydrogen when heating Raney nickel catalysts. The amount of hydrogen evolved in water addition tests was more than 3 times that for regular TPD experiments, depending on the amount of water added. IV A Raney nickel evolved the same amount of hydrogen in water addition experiments as in a regular TPD due to the presence of a relatively large amount of water bound to $Al_2O_3 \cdot 3H_2O$ ($\sim$ 49 wt %) in the catalyst. The additional water did not have any effect on H_2 evolution.

8.3 CONCLUSIONS

The nature of hydrogen in Raney nickel catalysts was studied by the following methods: hydrochloric acid dissolution, amalgamation, thermal desorption in a volumetric apparatus, hydrogen-deuterium exchange and temperature-programmed-desorption.

The hydrochloric acid dissolution method determined the preexistent hydrogen, i.e., the chemisorbed hydrogen and the hydrogen in solid solution with nickel. The hydrogen-deuterium exchange method was used to measure the amount of exchangeable hydrogen, at least equal to the preexistent hydrogen, i.e., the hydrogen coming from the surface (chemisorbed) and the bulk (Ni lattice) of the Raney nickel. For reasons shown earlier (page 161) it is not likely that the hydrogen associated with $Al_2O_3 \cdot 3H_2O$ and from C_2H_5OH and CH_3CHO adsorbed on Raney nickel, exchanged with deuterium. The volume of hydrogen determined by amalgamation corresponded to the chemisorbed hydrogen and/or

the hydrogen in solid solution with nickel. COM Raney nickel reacted faster with Hg at room temperature than II A samples.

Thermal desorption determines the amount of preexistent hydrogen and the hydrogen formed in the reaction of Al oxidation by water bound to alumina trihydrate. The same holds true for temperature-programmed desorption with the difference that during the TPD run there is less chance of oxidizing Al, water vapor being carried away by argon. Most or all the hydrogen in COM catalysts is chemisorbed and in solid solution with nickel. On heating COM samples, hydrogen desorption was accompanied by a small exotherm only observed for large samples. Due to the low content of alumina trihydrate in COM catalysts, only small amounts of hydrogen are produced by the reaction of Al and water. Temperatures of peak maxima obtained for Raney nickels and gibbsite in TPD experiments are listed in Table 8.3. The peak at 206°C in the TPD spectrum of COM Raney nickel, accompanied by a very small exotherm, is attributed mostly to hydrogen from the nickel surface and lattice. After hydrogen was readsorbed (more than 50% of the hydrogen initially evolved) on COM (Section 7.5), a TPD experiment showed two new peaks, at 118°C and 254°C. These peaks were attributed to two different kinds of hydrogen, not present in the original TPD spectrum and adsorbed on sites characterised by different activation energies of desorption. Also, part of the readsorbed hydrogen is probably in solid solution with nickel, as the values for hydrogen readsorption were higher than hydrogen chemisorption on Raney nickel at room temperature.

The interpretation of the TPD spectra of the ethanol-stored catalysts (II A and IV A) is complicated by the presence of ethanol and species derived from it, adsorbed on the catalysts. The gas evolved in the temperature range 170°C-240°C was probably a mixture of H_2, CH_4 and CO (Section 7.6). Gas evolution in this temperature range was accompanied by large exotherms. Gibbsite loses most of its water at about 220°C and both Al oxidation by water vapor and C_2H_5OH hydrogenolysis on Raney nickel are exothermic reactions (Table 8.2). Depending on the amount of gibbsite and metallic Al present in the catalyst, hydrogen can still be produced by the oxidation of Al above 270°C. However, the gas evolution beyond 270°C was not accompanied by an exotherm, suggesting that Al oxidation did not occur. Instead, strongly chemisorbed hydrogen or hydrogen in solid solution with nickel was evolved. Most of the peaks below 150°C were not accompanied by thermal effects and were attributed to weakly chemisorbed hydrogen.

In the case of IV A Raney nickels, removal of constitutional water, i.e., water bound to gibbsite, produced an endothermic effect at about 220°C. Although exothermic reactions, producing H_2 and other gases including aluminum oxidation, also occur in this temperature range, the overall effect was endothermic, due to the large amount of constitutional water present in the IV A catalysts, and the peaks at 234°C and 267°C (Table 8.3) are endothermic. The overheating of large samples of II A during the exothermic desorption (ΔT = 130°C) of hydrogen

Table 8.3

Temperatures in the Maxima in the Desorption Rate for Different Types of Raney Nickel and $Al_2O_3 \cdot 3H_2O$

Catalyst	Start in Gas Evolution (°C)	Temperature of Peaks (°C) I	II	III	IV
COM	72		206		
[a]COM	50	118	202	254	
IIA-1	103	151	213*	234	440
IIA-2	63	170*	220		454
IIA-3	50	122	183*	242	288
IVA	78	153	234*	267*	542
$Al_2O_3 \cdot 3H_2O$	[b]165		[c]224		

* indicates the largest peak in the desorption spectrum

a: readsorption experiment

b: start in the evolution of H_2O vapor

c: maximum in the rate of desorption of H_2O vapor

and/or methane resulted in a distorted TPD pattern; most of the gas was evolved at the time of the exotherm, producing large, sharp peaks in the TPD spectrum. Complications by exo- and endothermic reactions, the broad peak maxima, and the limited range of heating rates employed prevented the estimation of activation energies by the methods described on p.108.

Water addition tests constituted a direct proof that hydrogen was produced in the reaction between metallic Al in Raney nickel and water evolved from alumina trihydrate. Oxidation of nickel did not occur in the regular TPD experiments, that is on heating the catalysts in argon, and only to a small extent in water-addition tests.

Previous magnetochemistry experiments do not lead to an unambiguous explanation of the nature of hydrogen in Raney nickel. The increase in the specific magnetization obtained by heating Raney nickel can be explained by either the removal of hydrogen from the Ni surface or lattice and by oxidizing Al in a solid solution of aluminum in nickel.

The nature of hydrogen in Raney nickel catalysts is a multiple one: chemisorbed hydrogen, hydrogen in solid solution with nickel or Ni-Al alloys,and in addition hydrogen is formed by the reaction of metallic aluminum with water associated with alumina trihydrate in thermodesorption and T.P.D. experiments.

8.4 RECOMMENDATIONS

It is suggested that in further work on Raney nickel, the following recommendations and research proposals be taken into account:

a continuous determination of CH_4, CO and H_2 could be done by using three sets of matched pairs of thermistors and absorption tubes[117]. Argon carrier gas is passed over three reference thermistors, the TPD cell, the first analysis thermistor, an ammoniacal cuprous chloride solution for CO absorption, a dry-ice trap to remove H_2O vapor, the second analysis thermistor, a CuO tube at 400°C to convert H_2 to H_2O, a dry-ice trap to remove H_2O, and finally the third analysis thermistor. The three thermistors detect the total gas (H_2 + CH_4 + CO), H_2 + CH_4, and CH_4 respectively. The signal can be recorded on a three pen recorder, and the individual gas contents of the mixture can be obtained by subtraction of appropriate signals. Also, this analysis can be done by using three thermal conductivity detectors in series.

2) Chemical analyses of Raney nickel should include the determination of metallic aluminum and separately, of the alumina.
3) If possible, preparation of Raney nickels free of metallic Al and/or Al_2O_3 (possibly at 150°C in an autoclave).
4) Removing completely the storage liquid from the catalysts without affecting the hydrogen content or the structure of Raney nickel.
5) Improving the hydrochloric acid dissolution method, as this is the only method which can determine the hydrogen preexisting in Raney nickel before thermal desorption, i.e., excludes the hydrogen formed between Al and H_2O when Raney nickels are heated. Then determine the hydrogen evolved in a thermal desorption experiment with a new sample and compare the results.

6) Thermal gravimetry and differential thermal analysis experiments in connection with TPD.

7) A comparative study of the properties of Raney nickel, other Raney catalysts (like Raney cobalt and zinc) and Urushibara catalysts.

8) Removal of nickel from Raney nickel by treatment with carbon monoxide at about room temperature, and examination of residues by electron microscopy, X-ray diffraction and physical adsorption. Determine the hydrogen content of Raney nickel with part of Ni removed by thermal desorption and/or TPD.

9) Treatment of Raney nickel with D_2O vapor in water addition TPD experiments and analyse the effluent. Follow Al oxidation by weight change.

10) Determine the hydrogen content of a Raney nickel prepared by activation of a Ni-Al alloy by water (possibly in a closed autoclave at about 200°C).

11) Study the properties and hydrogen content of nonpyrophoric Raney nickel (possible preparation by anodic oxidation of Raney nickel).

12) When unrealistic large amounts of hydrogen are considered as chemisorbed, metallic surface area determinations should be made.

APPENDIX A

A-1 REAGENTS USED IN THE ANALYSIS

1. 1 N Nitric acid solution
2. 6 N Nitric acid solution
3. 30% Ammonium hydroxide
4. 1 N Sodium hydroxide solution
5. 33% Triethanolamine aqueous solution
6. Murexide indicator powder (500±0.01 g indicator + 10±0.1 g sodium chloride powder)
7. 0.025 M EDTA (Ethylenediamine tetraacetic acid, disodium salt) solution
8. 0.05 M EDTA solution
9. 0.025 M Nickel chloride solution
10. 0.025 M Lead nitrate solution
11. 0.5% Xylenol orange solution
12. Hexamethyleneamine
13. 10% Ammonium fluoride solution
14. Tartaric acid
15. Dimethylglioxime alcoholic solution (10 g per liter)

A-2 DISSOLUTION OF RANEY NICKEL

Raney nickel was evacuated for 24 hours at 23°C and 10^{-5} torr to give a 0.5-1.0 g of dry sample. At the end of the period of evacuation and after weighing the sample, water was introduced

over the catalyst through a side funnel provided with a teflon vacuum stopcock. The wet sample was then transferred to a 250 ml beaker. The procedure used was taken from ref. (70), slightly modified by the author. 50-100 ml of 1N sodium hydroxide solution was slowly added to the catalyst and the beaker was covered with a watch glass. The beaker was put on a hot plate to make sure that aluminum has been completely dissolved, then enough time was allowed the suspension to cool and decant. If no Al was present in the sample, no reaction occured upon sodium hydroxide treatment. When samples containing large amounts of alumina trihydrate were dissolved, more concentrated alkali solution (20 wt %) was added and the sample was boiled on the hot plate to dissolve as much alumina as possible. The supernatant liquid was then decanted into a 500 ml volumetric flask and nitric acid was added, 1 ml at a time with mixing, to acidify the solution. Depending on the amount of aluminum present, a precipitate of aluminum hydroxide occurs which redissolves upon complete acidification. 50-100 ml of 1:3 nitric acid was added to the beaker containing the residue and heated to complete dissolution. This portion was combined quantitatively with that from the 500 ml volumetric flask filtering if necessary. The solution was allowed to cool to 20°C in an ice bath, diluted to volume with distilled water and shaken. Aliquots of this solution were used to determine Ni, Al and Fe.

A-3 DETERMINATION OF NICKEL BY THE DIMETHYLGLYOXIME METHOD

The method used was taken from ref. 69 and was slightly modified by the author. Dimethylglyoxime, $CH_3.CNOH.CNOH.CH_3$, was recommended by L. Tschugaeff[73] as a reagent for nickel. When a dilute, neutral solution of a nickel salt is treated with an alcoholic solution of dimethylglyoxime, a red, crystalline precipitate of nickel dimethylglyoxime is formed:

$$Ni(NO_3)_2 + 2(CH_3)_2C_2(NOH)_2 =$$

$$[(CH_3)_2C_2NOH.NO]_2Ni + 2HNO_3 \qquad (1)$$

nickel dimethylglyoxime

The salt is soluble in mineral acids so that precipitation is incomplete because of the acid set free in the reaction. The precipitation becomes quantitative if the mineral acid is neutralized by ammonia. The precipitate is soluble in absolute ethanol but practically insoluble in iced water. The sensitivity of the method is 4-5 ppm.

A 50 ml aliquot of Raney nickel solution is pipetted in a 250 ml beaker and 3 mg of tartaric acid added to complex both Al and Fe. Then aqueous 30% ammonia is added until the pH was 7 and one more ml of ammonia was added again. The beaker was placed on a hot plate and when the temperature reached 70°C, dimethylglyoxime (DMG) solution was poured directly into the nickel solution, while stirring vigorously with a glass rod. The amount of DMG solution added was 0.4 ml of 1% solution for

every mg of nickel and 5 ml in excess. The solution was then allowed to cool to room temperature with occasional stirring and filtered through a fritted-glass crucible of medium porosity, 30 ml capacity. The precipitate was washed well with cold water, dried at 150°C to constant weight, cooled in a dessicator and weighed as nickel dimethylglyoxime. The amount of nickel as weight percentage, was calculated as follows:

$$\text{Nickel, percent} = \frac{A \times 0.2032 \times 10}{B} \qquad (2)$$

where A: grams of nickel dimethylglyoxime

B: grams of Raney nickel sample used.

To check the method, a known nickel solution was prepared. 99.9% of nickel ball bearings were cleaned of oxide in 1N HNO_3, washed with distilled water, absolute ethanol and chloroform, dried in filter paper and finally weighed, 0.3665 g. By the DMG method it was found 0.3670±0.0008 g.

A-4 DETERMINATION OF NICKEL BY CHELATOMETRY[70]

In this method Al and Fe are masked by forming strong complexes with triethanolamine and nickel is titrated with EDTA in the presence of murexide as indicator. The procedure is divided into three parts:

1) Standardization of EDTA solution
2) Chelatometric nickel titration
3) Calculations.

EDTA (ethylendiamine tetracetic acid) is a multidentate ligand which forms coordination complexes with certain ions or molecules[74].

These complexes are called "chelates". The disodium salt of the EDTA is used in titrations because of its solubility in water:

$$Ni^{2+} + H_2Y^{-2} \rightarrow NiY^{2-} + 2H^+ \qquad (3)$$

where H_2Y^{-2} is the anion of the disodium EDTA.

To standardize the 0.025 M EDTA solution, 25 ml of 0.025 $NiCl_2$ solution are pipetted in a 500 ml Erlenmayer flask containing a magnetic stirring bar. 10 ml of 33% triethanolamine solution are added and the solution stirred on a magnetic stirring base. 30 ml of 30% NH_4OH are added and the solution is diluted to a volume of 250-300 ml. Then the indicator powder (murexide) is added and titration is done with 0.025 M EDTA to a deep violet color.

The normality of EDTA is:

$$\frac{25 \times 0.2500}{\text{ml titration, EDTA}} = \text{Normality EDTA} \qquad (4)$$

To a 50 ml aliquot in an Erlenmayer flask containing a magnetic stirring bar is added 10 ml of 33% trietanolamine solution, stirred, 35 ml of concentrated NH_4OH added and the solution diluted with distilled water to a volume of 250-300 ml. The solution is titrated with 0.025 M EDTA in the presence of murexide to the same deep violet color used for the EDTA standardization.

The percent Ni in the sample is given by:

$$\frac{(\text{ml EDTA titration})\ N_{EDTA} \cdot 0.05871}{\text{Sample weight, grams}} \times 100 = \text{wt \% Ni}$$

N_{EDTA} = normality of EDTA.

A-5 DETERMINATION OF ALUMINUM BY CHELATOMETRY[70]

The principle of the method is to treat the solution with an excess of EDTA and complex both Al and Ni. The solution is boiled to complete complexation. Excess EDTA is eliminated with a lead salt. Ammonium fluoride is added to liberate all EDTA complexed with Al. EDTA is then titrated with lead nitrate to a xylenol orange end point. A 50 ml aliquot of Raney nickel solution was pipetted in a 250 ml beaker and, with the aid of a pH-meter, the pH is adjusted to 4±0.1 by adding 1N NaOH. A slight excess of 0.05 M EDTA is added to complex both Al and Ni. An approximate composition of the solution should be known. 1 ml of 0.05 M EDTA corresponds to 2.9345 mg Ni and 1.3485 mg Al. Excess EDTA must be less than 5 ml of 0.05 M EDTA. The solution is then boiled for 2 minutes and allowed to cool. Using a pH-meter solid hexamethylenamine is added, while stirring, to bring the pH to 5±0.1. 2-3 drops of xylenol orange is added and the excess EDTA is titrated with 0.025 M lead nitrate solution from yellow-green to a violet end point. 10 ml of 10% aluminum fluoride is then added to complex Al^{3+} and likewise the corresponding amount of EDTA. The solution is boiled 3-4 minutes and cooled to 15°C±1°. If the solution turned violet on boiling, 1N HNO_3 is added to get a green color and is titrated with 0.025 M lead nitrate to a violet end point.

The percent Al in the sample is

$$\frac{(\text{ml } Pb(NO_3)_2 \text{ titration})(0.02500)(0.02698).10}{\text{Sample weight, grams}} = \text{wt \% Al} \quad (5)$$

To check the accuracy of the method, 0.2008 g of Al wire (Fisher catalog No. A-557) was dissolved in 1N NaOH by boiling for 1 hour.

Chelatometric determination of Al gave a value of 0.1999 g ± 0.0012.

Whenever only two experimental determinations were made and two identical values were obtained, both of them were given in the Tables A-1 and A-2.

Table A-1.1

Chemical Composition of Raney Nickels

ney ckel pe	Sample Weight (g)	Sample Disso- lution	Nickel Content gravi- metric (mg)	Nickel Content volu- metric (mg)	Nickel Content wt %	Total Aluminum Content volu- metric (mg)	Total Aluminum Content aas (mg)	Total Aluminum Content wt %	Metallic Al mg	Metallic Al wt %	Fe_2O_3(aas) mg	Fe_2O_3(aas) wt %	$Al_2O_3 \cdot 3H_2O$ mg	$Al_2O_3 \cdot 3H_2O$ wt %
COM I	0.2892	HNO_3+ NaOH	260.8 ± 1.3	-	90.2 ± 0.5	17.6 ± 0.1	-	6.08 ± 0.03	12.3 ± 0.7	4.3 ± 0.2	0.80 ±0.02	0.29 ±0.01	15.3 ± 2.0	5.3 ±0.7
COM I	0.3667	HNO_3+ NaOH	331.7 ± 1.1	334.5 ± 0.3	90.5 ± 0.2	22.8	-	6.2 ± 0.1	16.9 ± 0.6	4.6 ± 0.2	1.10 ±0.02	0.29 ±0.01	17.0 ± 1.7	4.6 ±0.5
M	0.4944	HCl+ NaOH	441.9 ± 0.8	446.1 ± 0.2	89.4 27.7	27.7	27.5	5.58 ± 0.02	15.2 ± 0.4	3.1 ± 0.1	1.40 ±0.03	0.28 ±0.01	35.8 ± 1.1	7.2 ±0.2
COM	0.3785	HNO_3+ NaOH	337.9 ± 1.4	337.4 337.4 ± 0.2	89.2 ± 0.1	22.3	-	5.89 ± 0.03	13.1 ± 0.5	3.5 ± 0.1	1.10 ±0.02	0.29 ±0.01	26.6 ± 1.4	7.0 ±0.4
IIA-1	0.6778	HNO_3+ NaOH	520.5 ± 1.3	493.4 ± 5.6	76.8 ± 0.2	71.1 ± 0.4	-	10.49 ± 0.06	30.6 ± 0.8	4.5 ± 0.1	9.70 ±0.19	1.43 ±0.03	117.0 ± 2.0	17.3 ±0.3
IIA-2	0.4643	HNO_3+ NaOH	326.3 ± 1.4	331.3 ± 0.4	70.3 ± 0.3	54.7 54.7	53.5	11.7 ± 0.2	12.3 ± 1.1	2.7 ± 0.2	4.29 ±0.02	0.92 ±0.02	121.3 ± 2.3	26.1 ±0.5
IIA-2	0.8388	HNO_3+ NaOH	596.0 ± 1.2	593.4 ± 1.2	71.1 ± 0.2	98.6 ± 0.6	-	11.75 ± 0.07	26.3 ± 1.0	3.1 ± 0.1	7.72 ±0.02	0.92 ±0.02	208.9 ± 2.3	24.9 ±0.3

aas: atomic absorption spectroscopy
: average total Al content 27.6±0.1 mg
: average Ni content 337.7±0.9 mg
: sample evacuated at 120°C
: average total Al content 54.3±0.7 mg

Table A-2.1

Chemical Composition of Raney Nickels

Raney Nickel Type	Sample Weight (g)	Sample Dissolution	Nickel Content: gravimetric (mg)	Nickel Content: volumetric (mg)	Nickel Content: aas (mg)	Nickel Content: wt %	Total Aluminum Content: volumetric (mg)	Total Aluminum Content: aas (mg)	Total Aluminum Content: wt %	Metallic Al: mg	Metallic Al: wt %	Fe_2O_3 (aas): mg	Fe_2O_3 (aas): wt %	$Al_2O_3 \cdot 3H_2O$: mg	$Al_2O_3 \cdot 3H_2O$: wt %
II A-3	0.4025	HNO_3 + NaOH	281.2 ± 1.3	270.3	280.0	69.9 ±0.3	-	60.0 ±1.4	14.9 ±0.3	28.4 ±1.7	7.1 ±0.4	0.90 ±0.02	0.22 ±0.01	92.4 ± 2.8	23.0 ±0.7
II A-3	0.6161	HNO_3 + NaOH	391.9 ± 1.6	400.6	432.0 ± 5.1	70.1 ±0.8	-	95.0 ±1.9	15.4 ±0.3	48.5 ±0.9	7.9 ±0.6	1.10 ±0.02	0.18 ±0.01	134.6 ± 8.1	21.8 ±1.3
I A	0.5781	HNO_3 + NaOH	275.3 275.3	279.5 ± 0.7	-	48.0 ±0.4	-	110.0 ±1.4	19.0 ±0.2	12.4 ±2.0	2.2 ±0.3	6.40 ±0.10	1.11 ±0.02	282.0 ± 4.3	48.8 ±0.7
IV A	0.5899	HNO_3 + NaOH	281.2 ± 1.5	285.2 285.2	-	48.1 ±0.4	-	115.0 ±2.1	19.5 ±0.3	15.9 ±2.7	2.7 ±0.4	4.70 ±0.09	0.80 ±0.02	286.3 ± 4.9	48.5 ±0.8
I A	0.8362	HNO_3 + NaOH	414.3 ± 0.3	413.5 ± 0.1	-	49.5 ±0.1	149.4 ± 0.6	-	17.9 ±0.1	8.5 ±0.7	1.0 ±0.1	6.70 ±0.13	0.80 ±0.02	407.0 ± 0.9	48.7 ±0.1
Alloy	1.4160	HNO_3	706.9 ± 1.1	711.3 ± 1.5	-	50.1 ±0.1	689.2 689.2	690.0	48.7 ±0.1	-	-	13.70 ±0.30	0.97 ±0.02	-	-
Nickel on Silicagel	3.0529	HNO_3	263.4 ± 1.2	265.6 ± 3.4	-	8.63 ±0.04	-	-	-	-	-	-	-	-	-

aas: atomic absorption spectroscopy
: sample evacuated at 107°C

b : average Ni content 277.4 ± 2.5 mg
c : average Ni content 283.1 ± 2.5 mg
d : sample evacuated at 117°C; average Ni content 413.9 ± 0.2 mg

APPENDIX B

B-1 DETERMINATION OF VOID VOLUME IN THE ADSORPTION APPARATUS

Referring to Fig. 5.1 we wish to determine the total void volume which includes the volume of the capillary tubing to the right of S_2 not accounted for by the glass bulbs and the burette, the volume between S_2 and S_3 and below S_3. The trap was immersed in liquid nitrogen. The glass bulbs and the burette are maintained at 25°C by thermostatted circulating water. Keeping S_2 and S_3 open, He is admitted via S_1 which is then closed. At pressure P, the number of moles of He admitted is

$$n = P(V_B + V_v)/RT \qquad (1)$$

where V_B is the total volume of gas in the calibrated bulbs and burette, T is 298.16 K and V_v is the void volume we wish to calculate. Rearranging equation (1), we obtain

$$PV_B = - PV_v + nRT \ .$$

A series of P and V_B readings are taken, and PV_B is plotted atainst P. Since nRT is constant, we expect a linear graph of slope $-V_v$, the desired void volume. Such a plot is shown in Fig. B-1.1. The value V_v = 108.66 cc.

B-2 GAS CHROMATOGRAPHIC ANALYSIS OF GASES EVOLVED IN THERMODESORPTION

The gas chromatograph used in the analysis of gases evolved in thermodesorption was a Varian Aeregraph, model A 90-P3 equipped

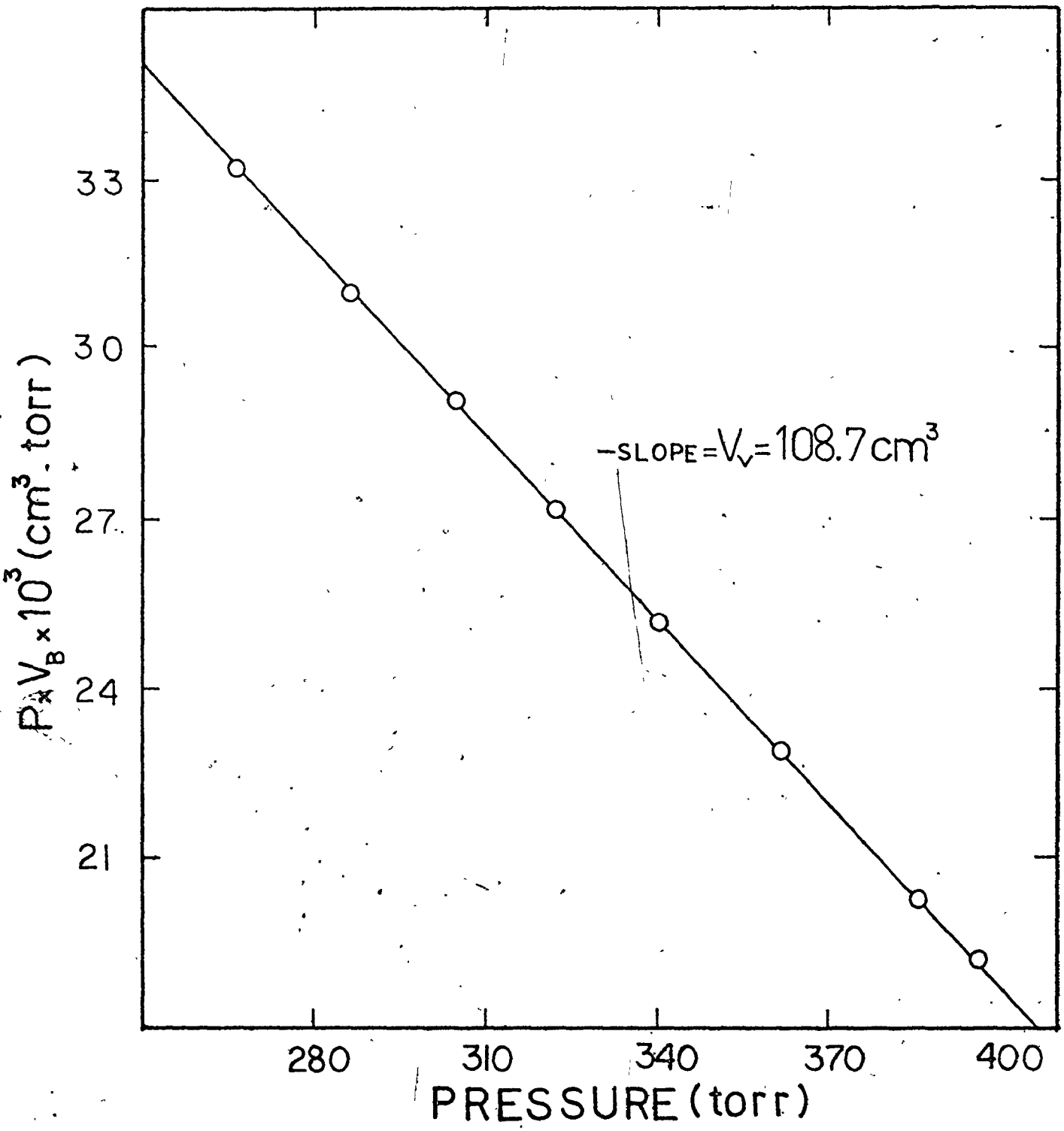

Figure B-1.1 Helium void space plot.

with a thermal conductivity detector.

The conditions of the G.C. analysis were the following:

- 6 ft of copper tubing column, 1/4 inch o.d. filled with 80-100 mesh Fisher activated coconut charcoal, kept at room temperture
- thermal conductivity cell, intensity of the current 110 mA
- argon (Matheson high purity) carrier gas with a flow rate of 60 cc/min.

The gas sample tube was made from two 3-way high vacuum stopcocks with two glass tubings between them; one line was a capillary glass tubing and used to flush out the air and the second was the sample tube itself with a volume of 4.5 cm^3. The sample tube could be attached to the adsorption system by means of a male joint and evacuated to 10^{-5} torr before a gas sample was taken. Before the gas sample was introduced into the argon flow in the chromatograph, the air was flushed out from the lines of the sample tube and chromatograph with the two 3-way stopcock system. The following gases could be separated on the coconut charcoal column: hydrogen (retention time 1.41 minutes), air (r.t. = 3.23 min), carbon monoxide (r.t. = 4.35 min) and methane (r.t. = 11.61 min). All gases used for calibration of the thermal conductivity cell were supplied by Matheson of Canada, Ltd., and Canadian Liquid Air Co. Ltd. at better than 99.8% purity. The calibration procedure consisted of using a gas sample valve with different sample loops of known volumes to introduce gas samples in the argon stream. The area of the peaks measured by a Hewlett-Packard HP 3373B digital integrator plotted

against the volume of gas, yielded straight lines of the form $y = mx + b$. The parameters m and b for different gases and attenuation 8 of the chromatograph are given below:

Gas	m ($\mu V\text{-sec}/cm^3$)	b μV-sec
Hydrogen	620,000.0	0
Carbon monoxide	38,235.3	1300
Methane	116,666.7	6200

Here y is the area of the peak in microvolts-seconds (μV-sec), m is the area per unit volume of gas in $\mu V\text{-sec}/cm^3$ and b is the intercept in μV-sec. The sample tube was filled with gas at pressures large enough to avoid working in extreme concentration ranges.

APPENDIX C

C-1 CALIBRATION OF THE GAS CHROMATOGRAPH DETECTOR IN H_2-D_2 EXCHANGE EXPERIMENTS

The detector of the gas chromatograph used (A 90 P-3 Varian Aerograph) for the chemical analysis of mixtures of hydrogen, deuterium and hydrogen deuteride was a thermal conductivity cell. The calibration of the response of the detector to H_2, HD and D_2 species was made by injecting known amounts of a 50:50 H_2-D_2 mixture into the G.C. before and after equilibration. The equilibration of the 50:50 hydrogen-deuterium mixture was done in a 400 ml equilibration bulb over a tungsten wire heated to approximately 1000 K (red hot) for several hours. The volume measurements were made in a BET adsorption system to which the equilibration bulb was connected. The equilibrium constant for the reaction

$$H_2 + D_2 \rightleftharpoons 2HD \qquad (1)$$

is 3.895 at 1000 K[83]. An error of 100°C in the temperature of the wire makes such a small change in the equilibrium constant that variation in the calculated percentages of hydrogen, deuterium and hydrogen deuteride in a mixture are within experimental error[84]. Gas samples from the BET system were taken by means of a U sample tube (number 4 in Fig. 6.1) which could be connected to the GC system through standard tapered joints.

From the chromatographic data of the initial H_2-D_2 mixture and of the equilibrated H_2, HD and D_2 mixture, the ratio between the sensitivities of these isotopic species was calculated.

The area of a peak A measured on the recorder is given by the equation

$$A = m \cdot S \tag{2}$$

where m is the number of moles of a certain species, S is the sensitivity for that species in area units per mole. The equilibrium constant for the reaction (1) is

$$K_{eq} = x^2 (m_{H_2} - x)^{-1} (m_{D_2} - x)^{-1} \tag{3}$$

where x is the equilibrium concentration of HD in moles/l $(m_{H_2} - x)$ and $(m_{D_2} - x)$ are the equilibrium concentrations of H_2 and D_2 respectively, expressed in moles/l, and m_{H_2} and m_{D_2} are the initial concentrations. Substituting m from equation (2) into equation (3), we obtain

$$K_{eq} = A_{HD}^2 . A_{H_2}^{-1} . A_{D_2}^{-1} . S_{H_2} . S_{D_2} . S_{HD}^{-2} \tag{4}$$

If the quantity $A_{HD}^2 . A_{H_2}^{-1} . A_{H_2}^{-1} . A_{D_2}^{-1}$ is termed A, then we have for K_{eq}

$$K_{eq} = A . S_{H_2} . S_{D_2} . S_{HD}^{-2} \tag{5}$$

Multiplying equation (5) by $\frac{S_{H_2}}{S_{H_2}}$ we obtain

$$K_{eq} = A . \left(\frac{S_{H_2}}{S_{HD}}\right)^2 . \left(\frac{S_{D_2}}{S_{H_2}}\right) \tag{6}$$

The expression $\frac{S_{D_2}}{S_{H_2}}$ is calculated from hydrogen-deuterium ratio equal to 1.014 and from the ratio of hydrogen peak area to deuterium peak area equal to 0.9895±0.0054 (see Table C-1.1):

$$\frac{S_{D_2}}{S_{H_2}} = \left(\frac{A_{D_2}}{A_{H_2}}\right)\left(\frac{m_{H_2}}{m_{D_2}}\right) = 0.932 \qquad (7)$$

The value of A from equation (6) was determined experimentally from the GC analysis of the equilibrated hydrogen-deuterium mixture. A difference of about 9% between the two values obtained for A (4.4 and 4.8) did not have a significant effect on the gas composition (Table C-1.2). As the equilibrium constant at 1000 K, K_{eq}, is known, the ratio S_{H_2}/S_{HD} is then determined from equation (6). From S_{H_2}/S_{HD} and S_{D_2}/S_{H_2} the last ratio, S_{D_2}/S_{HD} is obtained. The values of the last three expressions are given in the Table C-1.3. We now wish to find the gas composition in mole percent and we know the area of the H_2, HD and D_2 peaks:

$$A_{H_2} = m_{H_2} \cdot S_{H_2} \; ; \; A_{D_2} = m_{D_2} \cdot S_{D_2} = m_{D_2} \cdot (1.025\ S_{H_2})$$

$$A_{HD} = m_{HD} \cdot S_{HD} = m_{HD} \cdot \left(\frac{1}{0.909} \cdot S_{H_2}\right)$$

$$\therefore \quad A_{H_2} = m_{H_2} \cdot S_{H_2}$$

$$\frac{A_{D_2}}{1.025} = m_{D_2} \cdot S_{H_2} \qquad (8)$$

$$A_{HD}(0.909) = m_{HD} \cdot S_{H_2}$$

We find mole percent hydrogen as follows:

$$\frac{A_{H_2}}{A_{D_2}/1.025+A_{H_2}+A_{HD}\cdot(0.909)} = \frac{m_{H_2}\cdot S_{H_2}}{m_{D_2}\cdot S_{H_2}+m_{H_2}\cdot S_{H_2}+m_{HD}\cdot S_{H_2}} \qquad (9)$$

S_{H_2} is cancelled from the numerator and denominator of expression (9) and if we multiply the left side of equation (9) by 100, we obtain mole percent hydrogen:

$$100\times\frac{A_{H_2}}{A_{D_2}/1.025+A_{H_2}+A_{HD}\cdot(0.909)} = \frac{m_{H_2}}{m_{H_2}+m_{HD}+m_{D_2}}\times 100 = \text{mole \% } H_2 \qquad (10)$$

In a similar way it is calculated the percentage of the other isotopic species.

C-2 GAS CHROMATOGRAPHIC SEPARATION OF H_2, HD and D_2

C-2.1 General

The advantage of the gas chromatographic technique of separation of the hydrogen isotopes over mass spectrometry is convenience and the simple instrumentation required in gas chromatography. An alumina column at low temperatures with helium as carrier gas leads to the separation of the nuclear spin isomers of hydrogen and deuterium. Since the HD/ortho-H_2 separation factor is nearly unity at 64-77.5 K, these species are not separated. However, the presence on the surface of the alumina of a catalyst which makes ortho-para interconversion rapid relative to motion along the column, causes ortho and para-H_2 isomers to appear as a single peak with a retention time intermediate between the retention times expected for the individual isomers in the

Table C-1.1

Gas Chromatographic Data for a Hydrogen-Deuterium Mixture Before Equilibration (H_2/D_2 = 1.014)

Sample Size cc(STP)	Hydrogen Peak Area (μV-sec)	Deuterium Peak Area (μV-sec)	Hydrogen Area / Deuterium Area
1.600	28,030	28,430	0.9859
1.536	27,090	27,140	0.9982
0.044	20,010	20,220	0.9896
0.041	18,790	19,090	0.9843
-	15,200	15,360	0.9896

Hydrogen Inlet = 109.397 cc(STP)

Deuterium Inlet = 107.883 cc(STP)

$$\text{Average } \frac{\text{Hydrogen Peak Area}}{\text{Deuterium Peak Area}} = 0.9895 \pm 0.0054$$

Table C-1.2

The Chromatographic Data for the Equilibration of a Hydrogen-Deuterium Mixture ($\frac{H_2}{D_2}$ = 1.014) Over a Tungsten Wire at 1000 K

Sample Size cc(STP)	H_2 Peak Area μV-sec	D_2 Peak Area μV-sec	HD Peak Area μV-sec	A*
First Run				
1.052	8470	8677	18520	4.667
1.200	9757	10180	21660	4.723
1.161	9329	9652	20870	4.837
1.070	8340	8730	18990	4.953
Second Run				
-	13030	13390	28030	4.503
-	12680	12840	27140	4.524
-	12550	12750	26170	4.280
-	11970	11710	24580	4.310
-	11790	11680	24340	4.302
-	11320	10930	23500	4.463
-	10800	10490	22330	4.401

*$A = A_{HD}^2/(A_{H_2})(A_{D_2})$; The average value of A for the first 4 determinations is 4.795±0.123 and for the last 7 determinations is 4.398±0.102

Table C-1.3

The Ratio Between the Sensitivities of H_2, H_D and D_2 Calculated from the Chromatographic Data in Tables C-1.1 and C-1.2 and using A* = 4.596 and $K^{**}_{eq_{1000K}}$ = 3.895

S_{H_2}/S_{HD}	S_{D_2}/S_{H_2}	S_{D_2}/S_{HD}
0.909	1.025	0.932

* A = (Area of HD Peak)^2/Area of Hydrogen Peak)·(Area of Deuterium Peak)

** $K_{eq}^{1000\ K} = [HD]^2/[H_2].[D_2] = 3.895$ (ref. 83)

absence of equilibration. Since HD is unaffected, separation of H_2, HD and D_2 into three peaks results. The first complete separation of the H_2, HD and D_2 by GC was accomplished by Smith and Hunt[84,85] on chromia-alumina columns and Moore and Ward[86] on alumina packings coated with ferric oxide. Both Fe^{3+} and Cr^{3+} are paramagnetic substances and cause rapid para-ortho H_2 interconversion. Peak tailing is eliminated by adsorbing small amounts of carbon dioxide on the alumina. Larger molecular species are less efficient in reducing peak tailing, presumably due to their inability to penetrate fine pores. Ammonia and water vapor can also be used in reducing tailing. Oxygen adsorbed on alumina is also quite effective in producing rapid ortho-para equilibration. Columns of strongly activated (480°C, 8 hours) iron-free alumina also lead to ortho-para equilibration, probably due to the presence of free radicals formed by heating on the alumina surface. Partial deactivation with CO_2 restores ortho-para separation, i.e., the conversion of ortho-H_2 to para-H_2 does not take place. Removing the CO_2 produces the rapid ortho-para equilibration. When helium is used as carrier, the effluent gases are converted to their corresponding oxides with copper oxide to increase their sensitivity at the thermal conductivity detector. In addition to alumina, the following packings were used to separate the hydrogen isotopes and spin isomers: 5 Å molecular sieve, 13x molecular sieve, charcoal, and silica gel[87-97].

C.2.2 Preparation of the Chromatographic Column

Choosing the best column for the separation of the H_2, HD and D_2 proved to be difficult because of the tailing, poor separation and instability of the different columns tried. In this work several column preparations were used:

1. 5 ft of 1/4" o.d. copper tubing column filled with 80 mesh, 5A molecular sieve.
2. 13 ft of 3/16" o.d. copper tubing column filled with 80-100 mesh Alcoa Al_2O_3 + Fe_2O_3 (Bastick recipe[95])
3. 6 ft of 1/4" o.d. copper tubing column filled with 80-100 mesh Alcoa Al_2O_3 (Venugoplan recipe[94])
4. 2 ft of 1/4" o.d. copper tubing column filled with 80-100 mesh Fisher coconut charcoal
5. 17 ft of 1/4" o.d. copper tubing column filled with 80-100 mesh Alcoa Al_2O_3 + Fe_2O_3 (Shipman recipe[93])
6. 11.5 ft of 1/4" o.d. copper tubing column filled with 35-65 mesh Kaiser Al_2O_3 + $MnCl_2$ (Yasumori recipe[96])
7. 17 ft of 1/4" o.d. copper tubing column filled with Al_2O_3 + $MnCl_2$ (Yasumori recipe[96])
8. 7.2 ft of 3/16" o.d. copper tubing column filled with 80-100 mesh Baker basic Al_2O_3 + $MnCl_2$ (Yasumori recipe[96]).

From all these columns only the 6th column gave proper results with a good separation and stability and no tailing. When the column was too "active" a small amount of CO_2, ammonia or water vapor was adsorbed on it, to reduce the number and/or the strength of the adsorption centers on the surface of the alumina.

The column packing was prepared according to Yasumori and Ohno[96] with slight modifications. The gamma-alumina support supplied by Kaiser Chemicals and was spherical with an average particle diameter of 5.5 mm. It was crushed, mixed and 35-65 mesh fraction was selected. 85.5 g of alumina was dried at 450°C for 23 hours. 73.3 g of dried alumina was immersed in 550 ml of 0.075 M $MnCl_2$ aqueous solution for 22 hours. The alumina was quickly washed with distilled water and dried at 200°C for 12 hours, packed into a copper column (11.5 ft × 1/4" o.d.) and then treated in a current of helium at 200°C for 23 hours.

C-2.3 Gas Chromatographic Analysis

The isotopic mixture of H_2, HD and D_2 was analyzed by a modified Aerograph A 90-P3 gas chromatograph equipped with a thermal conductivity detector. The modifications rerouted the carrier gas and enabled the use of a liquid nitrogen bath for the chromatographic column. After the separation on the GC column, the hydrogen isotopes were passed through a U tube filled with copper oxide at 600°C and converted to H_2O, HDO and D_2O which had higher signal response in the presence of helium. The conditions of the GC analysis were the following:

Filament current, 212 mA

Temperature of the thermal conductivity cell, 112 mA

Column temperature: - 190°C

Temperature of the CuO furnace: 600°C

Helium flow rate: 85.7 cc/min

Isotopes retention time: H_2, 15.5 min; HD, 17 min; D_2, 21.3 min.

A typical chromatogram of a H_2-HD-D_2 mixture is shown in Fig. C-2.1.

C-3 DEAD SPACE FACTOR

The dead space factor F is defined as the number of cc at S.T.P. of gas per unit pressure which are present to the left of the stopcock S_2 (S_2 being open) but not adsorbed on the sample (Fig. 5.1). The dead space factor was determined in adsorption experiments (Chapter 3) and hydrogen-deuterium exchange experiments performed in a BET adsorption apparatus. The difference between the BET apparatus and the adsorption apparatus described in Chapter 5 is that the graduated burette is replaced in the BET system by five calibrated gas bulbs surrounded by a thermostatted water jacket and there is no manostat to keep the pressure constant during adsorption and desorption. Also the liquid nitrogen trap in Fig. 5.1 was not present in the BET apparatus. Keeping in mind the difference between the two adsorption systems we will refer to Fig. 5.1 in describing the procedure of determining the dead space factor for the BET apparatus. The volume of the two 5 gas bulb systems is known and this includes the volume of the capillary tubing between S_2, S_1 and the zero mark of the manometer (void volume).

F is a function of the temperature of the sample tube because the gas density changes and the sample tube volume changes slightly due to glass expansion/contraction. Helium is used to determine F because it is not usually adsorbed on most solids at -196°C. With water circulating through the gas

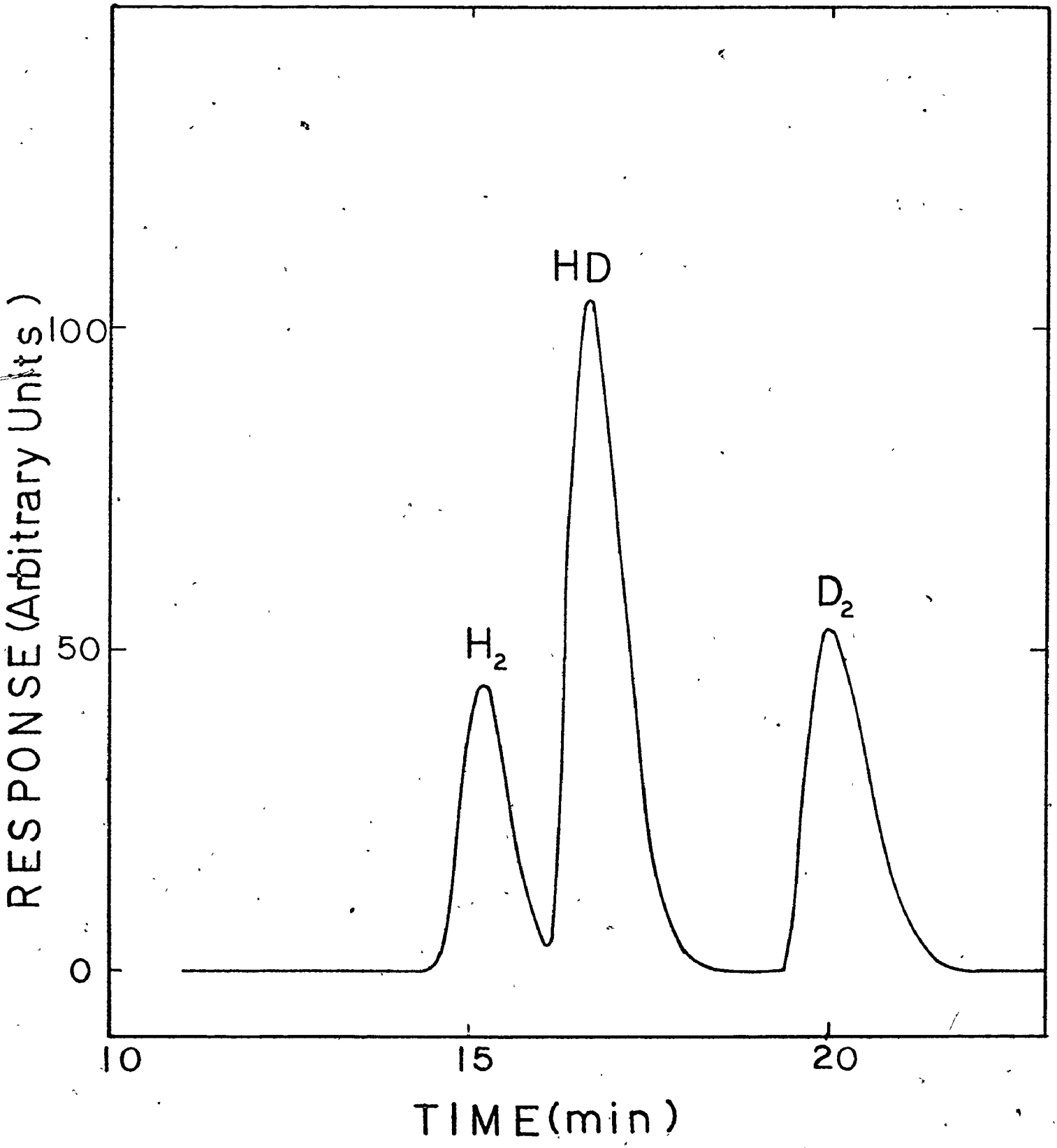

Figure C-2.1 Chromatogram of 0.69 cc sample of H_2,HD,D_2 mixture on a 11.5 ft. x 1/4 inch o.d. column of $MnCl_2$ on Al_2O_3 at -196°C with 85.7 cc/min He flow rate.

bulb jackets He is allowed to enter via S_1 to the right of S_2, with S_2 closed. The inlet volume V_I (cc(STP)) can be calculated with knowledge of gas bulb volume V_B, pressure P and temperature T. Four different readings of V_B and P are taken and an average value for V_I is obtained. Now S_2 is open (S_3 being open too) and a series of P and V_B readings are taken to determine the residual bulb volume V_R (cc(STP)) to the right of S_2, at the pressure P. The dead space factor is given by

$$F = (V_I - V_R)/P \qquad (11)$$

F is determined in this way at different sample tube bath temperatures, where

$$V_I - V_R = Q + \frac{VP}{T}\frac{273}{760} + \frac{vP}{300}\frac{273}{760} \qquad (12)$$

P = pressure, mm Hg

V = Volume in thermostatted bath, to the left of S_2

v = volume at room temperature (300°K), to the left of S_2

T = temperature in °K of volume in thermostatted bath

Q = amount adsorbed cc(STP)/g.

Therefore:

$$F = \frac{Q}{P} + \left(\frac{V}{T} + \frac{v}{300}\right)\frac{273}{760} \qquad (13)$$

On most solids the amount of He adsorbed in zero, i.e. Q = 0. Equation (13) becomes

$$FT = \frac{273}{760}\left(V + \frac{vT}{300}\right) \qquad (14)$$

The values on a FT versus T plot fall on a straight line. Data in this form are plotted in Fig. C-3.1 between -196°C and +25°C.

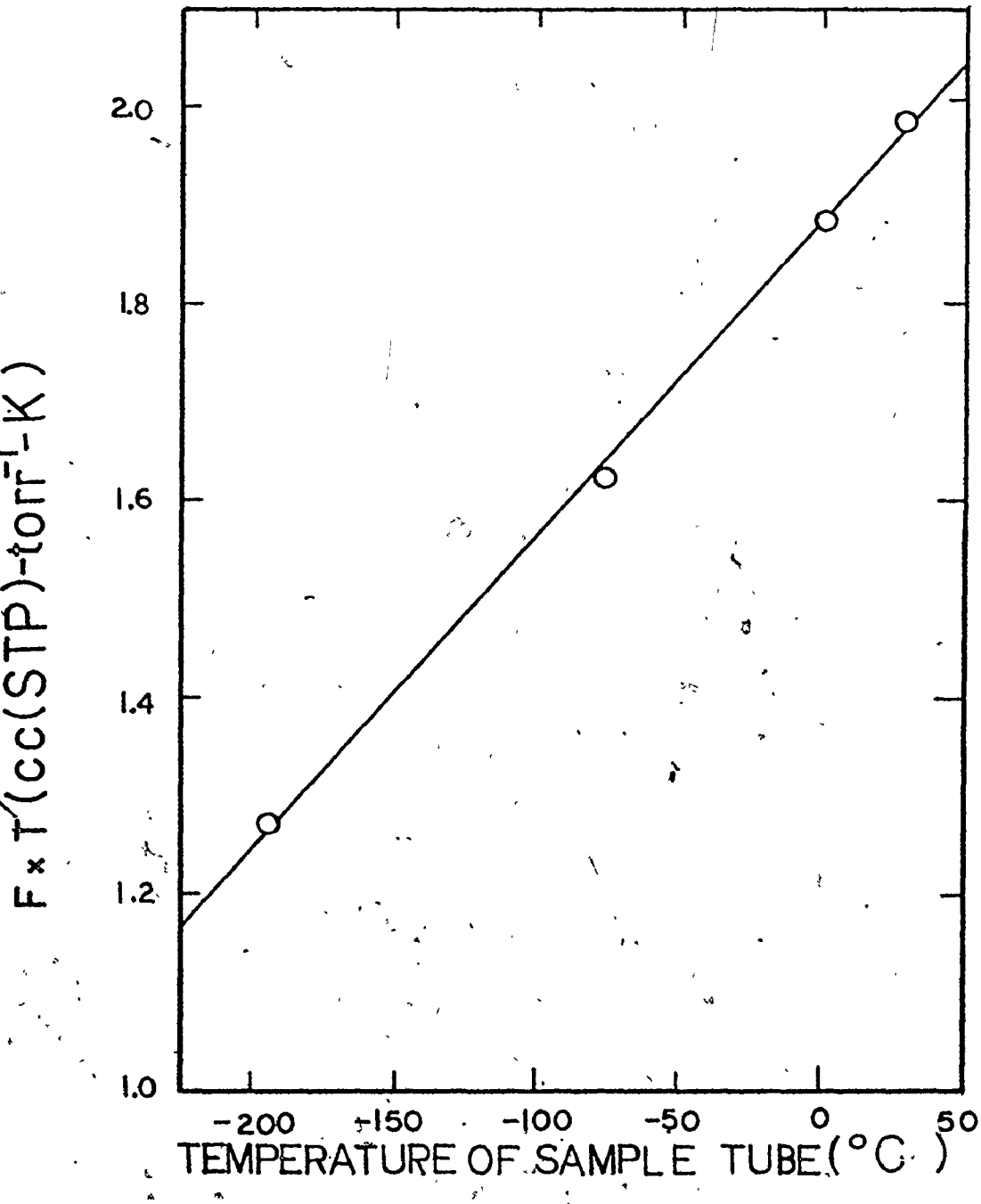

Figure C-3.1 Temperature dependance of dead space factor.

APPENDIX D

D-1 CALIBRATION OF THE THERMAL CONDUCTIVITY DETECTOR

The interpretation of a temperature programmed desorption (TPD) spectrum, similar to a chromatogram, required a correlation between concentration and signal response for hydrogen. The calibration procedure consisted of injecting different known volumes of hydrogen and recording the corresponding areas. A Varian Aerograph 6-port linear gas sampling valve was used with several sample loops of known volume. The amount of hydrogen injected was corrected to STP conditions. Occasionally, the hydrogen calibration curve was checked by injecting known amounts of gas measured in a volumetric apparatus (see procedure in Appendix B). The conditions of the TPD analysis are given in Table D-1.1. The recorded areas were measured by both digital and disc integrators, and two calibration curves were obtained. About 2 calibrations per month were made and over the experimental period the calibration factor for hydrogen was 62,726 μV-sec/cc H_2 ± 4.3% for the digital integrator and 8046 counts/cc H_2 ± 6.6% for the disc integrator. The digital integrator was not used for some experiments involving long flat peaks because of its low sensitivity for detecting changes of slope. The maximum slope sensitivity of the digital integrator was 0.03 millivolts/minute for the up slope and 0.01 mV/min for the down slope. When the slope of the input signal

Table D-1.1

TPD Operating Conditions

Carrier gas	:	argon
Carriger gas flow rate (for both measuring and reference cell)	:	40 ml/min
Detector temperature	:	Room temperature
Filament current	:	100 mA
Chart speed	:	1/2 inch per minute
Attenuation	:	Variable between 1 and 512
Integrator sensitivity	:	Maximum
Integrator attenuation	:	1, occasionally 10
Integrator mode of analysis	:	Manual operation

reached the value selected for the up slope, integration started. Area was printed and stop analysis occured when the input signal decreased to 50% of the value selected for down slope. Whenever a TPD pattern was such that the sensitivity of the digital integrator was not sufficient to measure the area accurately, disc integrator readings were used. The hydrogen calibration curve is shown in Fig. D-1.1. Up to about 0.7 cc of hydrogen sample there is a linear relationship between the signal response and the volume of gas sample. The hydrogen concentration corresponding to 0.7 cc hydrogen sample was about 0.5 cc/min. When the argon flow rate was 40 ml/min TPD experiments were performed in the linear range of hydrogen concentrations.

Fig. D-1.2 shows a straight line with a small intercept for the hydrogen calibration up to about 0.6 cc of gas sample. The slope of the line represents the calibration factor and was calculated by the least squares method. The signal response of methane, carbon monoxide and ethane was also linear and the calibration factors when argon and hydrogen were used as carrier gases, are given in Table D-1.2.

Another method used for hydrogen calibration was to plot V/A versus the peak height, h (Fig. D-1.3):

$$V/A = mh + b \qquad (1)$$

Here V is the volume of hydrogen sample, A is the corresponding area and h is the peak height. The slope m and the intercept b are determined from the graph or by the least square method.

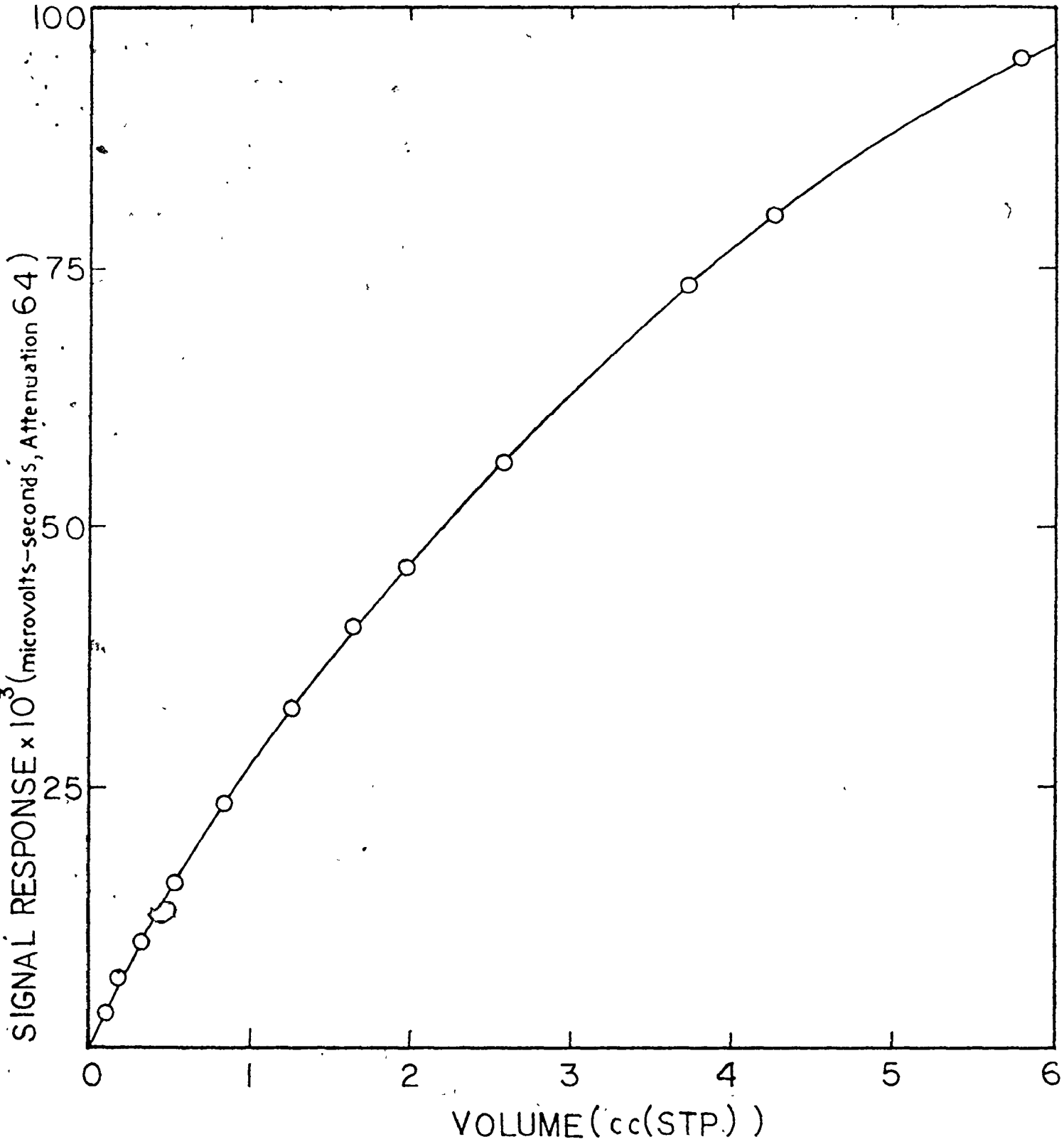

Figure D-1.1 Detector calibration for hydrogen.

It can be seen from Fig. D-1.3 that V/A is a linear function of h and gives a line almost parallel to the abscissa. If the plot A versus V (Fig. D-1.2) did not have a small intercept, then V/A versus h would have given a line parallel to the abscissa. The values for m and b in eq. (1) are 0.0644 and 149.1×10^{-7} respectively when digital integrator readings are used; for the disc integrator $m = 6.2\times10^{-4}$ and $b = 1.183\times10^{-4}$. The units for m are $cm^3\cdot(\mu V\text{-sec})^{-1}\cdot(mm)^{-1}$ and b is measured in $cm^3\cdot(\mu V\text{-sec})^{-1}$ when the digital integrator units for area are used. To obtain the volume of hydrogen evolved in a TPD experiment the total area of the peak is divided into small parts, the corresponding A's and h's are measured and their values substituted in formula (1). The total volume of hydrogen evolved is the sum of the volumes corresponding to each area. The agreement between this method and the method which uses the slope of the line in Fig. D-1.2 as a calibration factor is good. As an example we take a TPD experiment made with 0.2790 g of commercial catalyst. The total response signal obtained was 377,647 μV-sec (digital integrator) and 49,700 counts (disc integrator). The calibration factors were: 60,671.5 μV-sec/cc H_2 and 7496 counts/cc H_2. The volume of hydrogen found by this method was 22.3 cc(STP)H_2/g (digital integrator) and 23.6 cc H_2/g using the disc integrator. The peak height method gave the following results: 21.8 cc H_2/g (digital integrator) and 22.7 (disc integrator).

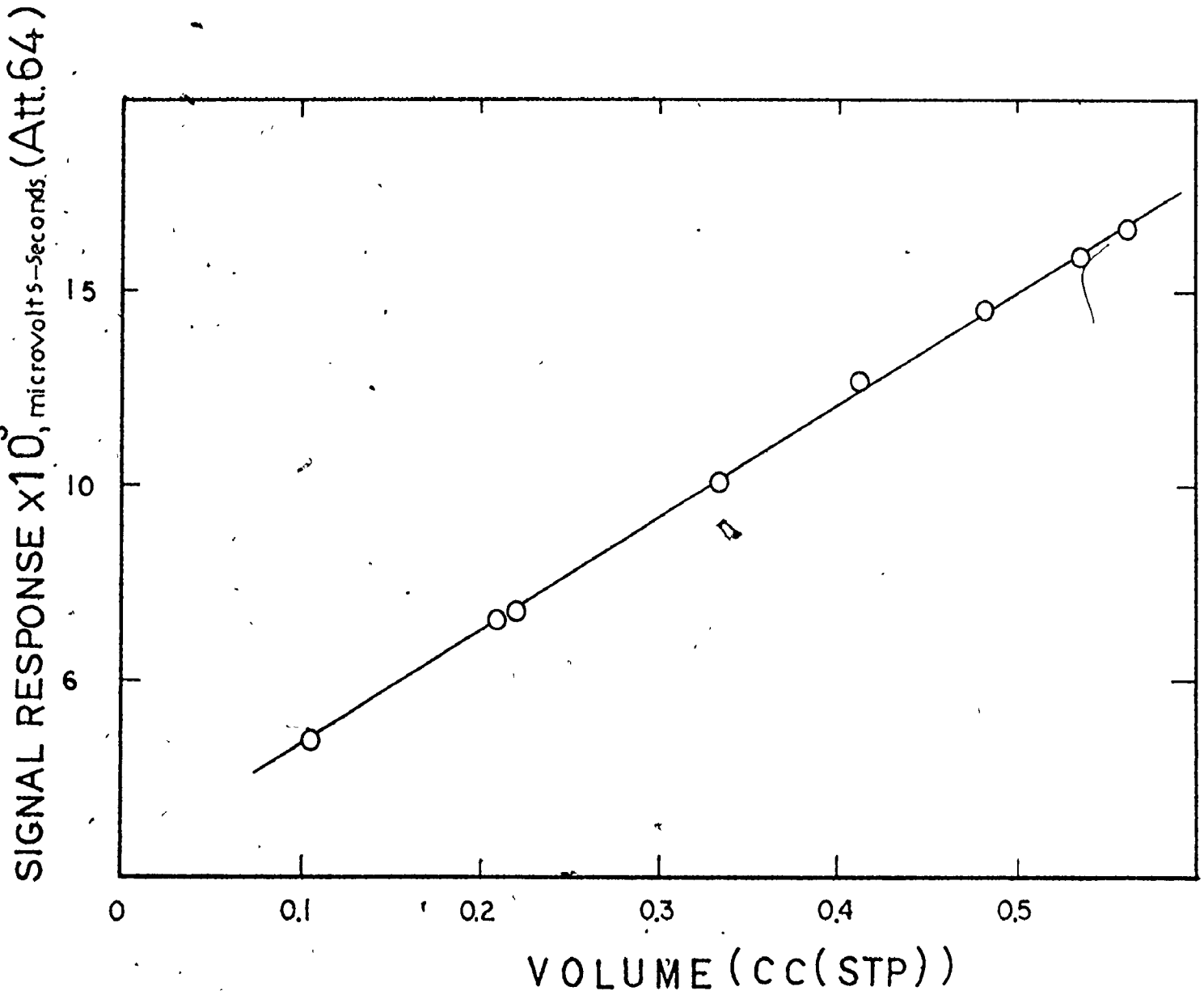

Figure D-1.2 Detector calibration for hydrogen (linear range).

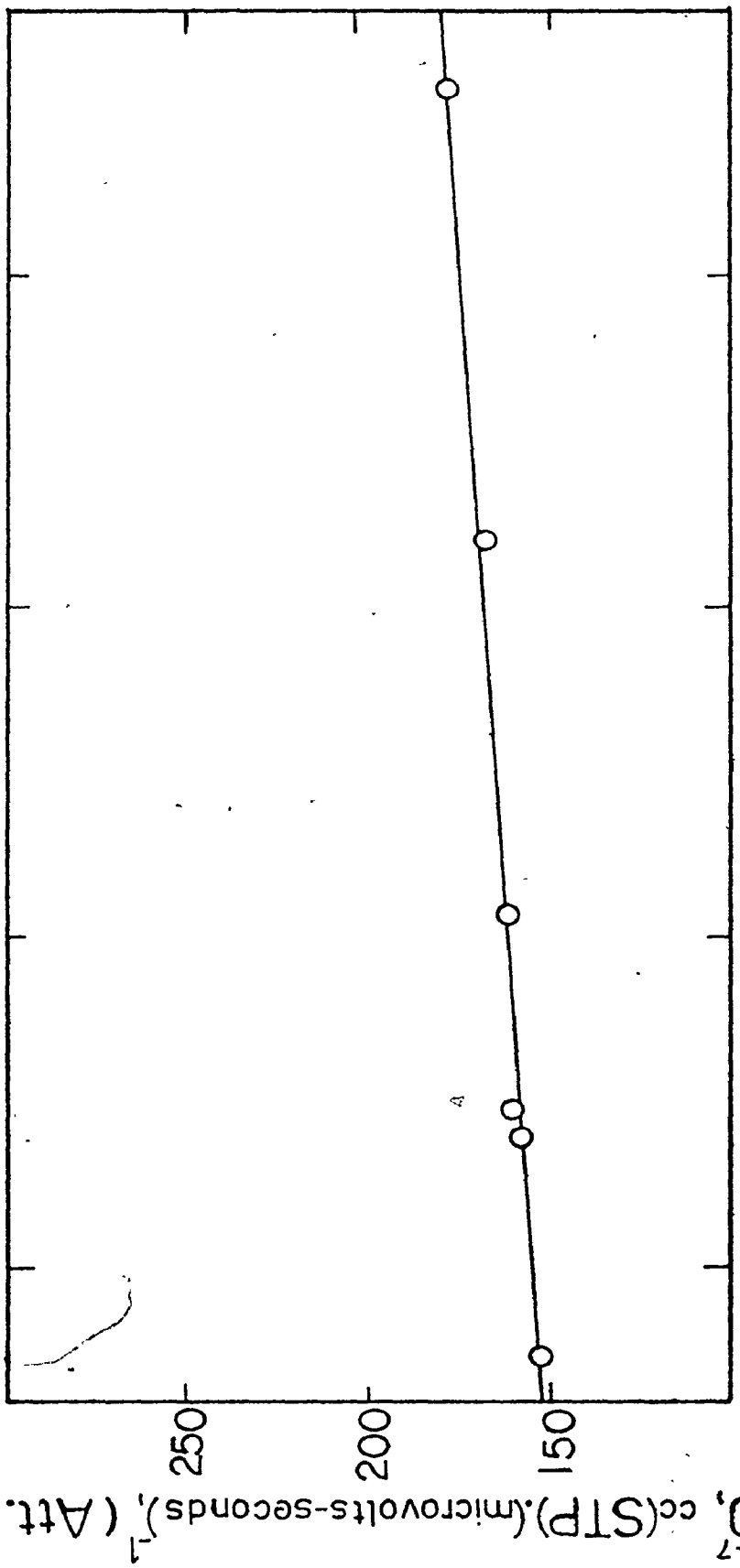

Figure D-1.3 V/A versus peak height plot for hydrogen chromatographic calibration.

Table D-1.2

Calibration Factors for CH_4, CO, C_2H_6, H_2 and H_2O

Component	Carrier Gas	Calibration Factor (Attenuation 32)	
		Digital Integrator (μV-sec/cc)	Disc Integrator (counts/cc)
Methane	Ar	12,802.0	1656.8
Methane	H_2	2724.0	350.4
Carbon Monoxide	Ar	6462.7	837.3
Carbon Monoxide	H_2	2911.0	367.3
Ethane	H_2	3968.2	526.5
Hydrogen	Ar	62,726.0	8046.0
H_2O	H_2	1938.1	255.6

D.2 CALCULATION OF HYDROGEN CONCENTRATION FROM THE TPD SPECTRUM

We want to calculate the concentration of hydrogen in the argon stream from the response of the thermal conductivity cell. The hydrogen calibration peaks have the shape of a gaussian curve, the ordinate is Y and the abscissa is t = time - retention time. (Fig. D-2.1)

The area of the peak A is:

$$A = \int_{-\infty}^{+\infty} Y\, dt = \int_{-\infty}^{+\infty} Be^{-a^2t^2}_{dt} = \frac{B\sqrt{\pi}}{a} \qquad (2)$$

where B is the peak height and a is a constant. The area of the peak is also given by

$$A = \beta\gamma V \qquad (3)$$

where β is a calibration factor and represents the area produced by 1 cc(STP) assuming that there is a linear relationship of the form y = mx between the area A and the volume of gas V.

γ in equation (3) relates the peak height with the corresponding peak area and is determined experimentally from the area of rectangular peaks obtained when the recorder pen traces a line parallel to the base line at different peak heights over different periods of time. γ is then obtained by plotting A/t versus B and taking the reciprocal of the slope of the line obtained in this way. A/t versus B gives also a straight line of the form y = mx. If $T_{1/2}$ represents the width of the peak at half height (B/2), then

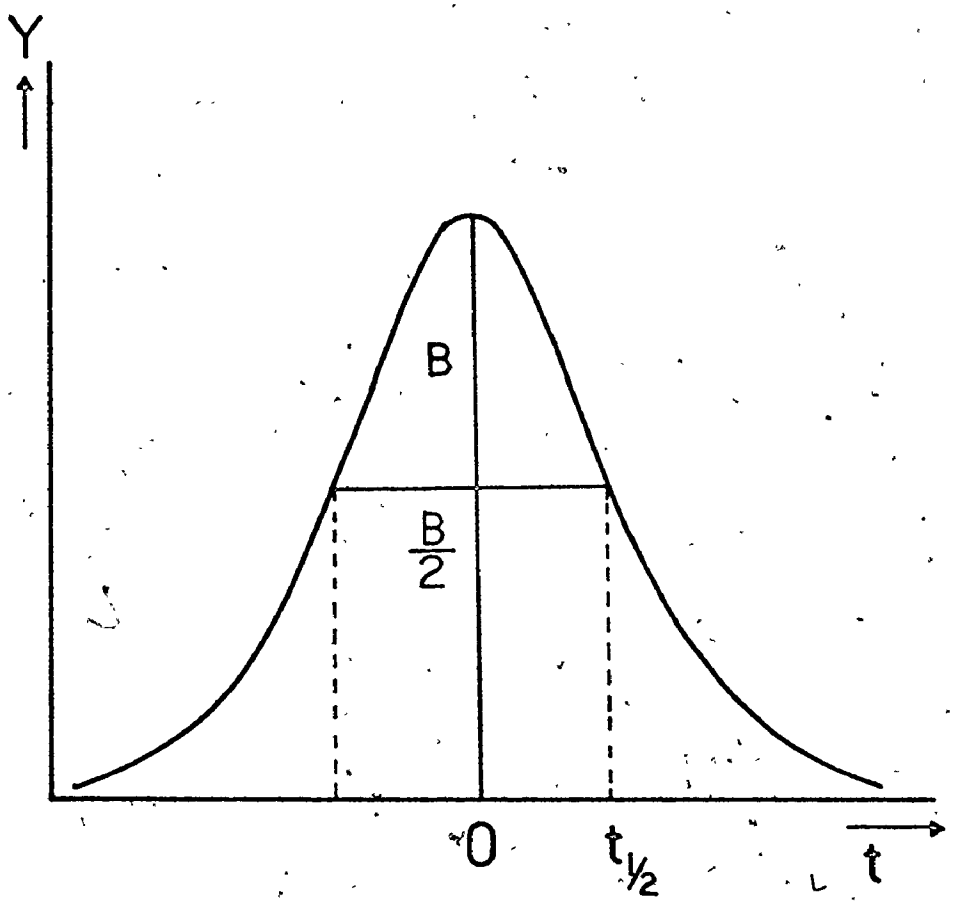

Figure D-2.1 Gaussian curve used in the calculation of the hydrogen concentration from the TPD spectrum.

$$1/2 = e^{-a^2 t_{1/2}^2} \qquad (4)$$

where $t_{1/2} = T_{1/2}/2$

$$\therefore \quad a = \frac{2\sqrt{\ell n 2}}{T_{1/2}} \qquad (5)$$

From eq. (2), in which we substituted the value of a, and eq. (3) we finally obtain:

$$V/T_{1/2} = \frac{1.0645}{\gamma\beta} B \qquad (6)$$

$V/T_{1/2}$ is the concentration of hydrogen in units of volume per unit time, let's say cc/min and is calculated by measuring only the peak height from the TPD spectrum. γ and β are determined in calibration experiments.

For hydrogen in argon $\gamma_{DIG} = 4.136\times10^{-3} \frac{(\text{millimeters})(\text{minutes})}{(\text{microvolts-seconds})}$ using digital integrator units for peak area and $\gamma_{DISC} = 32.110\times10^{-3} \frac{(\text{millimeters})(\text{minutes})}{(\text{counts})}$ when using disc integrator units for peak area. The calibration factor β for hydrogen is given in Table D-1.2.

D-3 CALCULATION OF H_2/H_2O IN WATER ADDITION TPD EXPERIMENTS

We wish to calculate the ratio H_2/H_2O from a TPD spectrum when water vapor is added to the Raney nickel sample at different temperatures. The hydrogen concentration $V/T_{1/2}$ expressed in cc(STP)/min was calculated as shown in Section D-2. To calculate the fraction of hydrogen in the argon stream we take the ratio

$$(V/T_{1/2})/((V/T_{1/2}) + 40) \qquad (7)$$

where 40 is the argon flow rate in ml/min. The ratio H_2/H_2O is given by

$$\frac{P_{H_2}}{P_{H_2O}} = \frac{\left[\frac{\frac{V}{T_{1/2}}}{\frac{V}{T_{1/2}} + 40}\right](P_{H_2} + P_{Ar})}{P_{H_2O}} \qquad (8)$$

Here $P_{H_2} + P_{Ar} = P_{atm} - P_{H_2O}$

where P_{atm} is the atmospheric pressure and P_{H_2O} is the vapor pressure of water at room temperature.

D-4 CALCULATION OF EQUILIBRIUM CONSTANTS FROM FREE ENERGY FUNCTIONS

The free energy function is

$$-\frac{F°-H°_{298}}{T} \qquad -\frac{F°-H°_{o}}{T} \qquad (9)$$

where F° is the standard Gibbs free energy, $H°_{298}$ is the standard enthalpy at 298 K and $H°_{o}$ is the standard enthalpy at 0 K. Because the free energy function is not very sensitive to changes in temperature its value can be tabulated at fairly large temperature intervals and its value at intermediate temperatures obtained by graphical interpolation without undue loss of accuracy. We wish to calculate the equilibrium constant of the reaction

$$Ni + H_2O \rightleftharpoons NiO + H_2 \qquad (10)$$

using free energy functions (FEF). If the FEF is based on $H°_{298}$ then the equilibrium constant is obtained by subtracting the value of the enthalpy of formation $\Delta H°_{298}$ divided by the absolute

temperature T from Δ(FEF) for the reaction (10):

$$\Delta\left(-\frac{F^\circ - H^\circ_{298}}{T}\right) - \frac{\Delta H^\circ_{298}}{T} = -\frac{\Delta F^\circ}{T} = R \ln K_{eq} \qquad (11)$$

$$\ln K_{eq} = \frac{\Delta\left(-\frac{F^\circ - H^\circ_{298}}{T}\right) - \frac{\Delta H^\circ_{298}}{T}}{R} \qquad (12)$$

ΔH°_{298} is the enthalpy change of formation of the indicated substance from the elements in their standard reference states. Both enthalpy change and free energy function change during a reaction can be obtained as follows:

$$\Delta(\text{function})_{\text{reaction}} = \sum_i \nu_i (\text{function}) \qquad (13)$$

where ν_i are the stoichiometric coefficients in the chemical equation. The stoichiometric coefficients are positive for the products and negative for the reactants. The thermodynamic functions of the substances involved in the reaction (10) and used in the calculation of K_{eq} are given in Table D-4.1. The calculated values for the equilibrium constant are given in Table D-4.1 and plotted in Fig. D-4.1. The experimental data of Pease and Cook[100] for nickel oxidation by water vapor are compared with the calculated values: at 600°C both calculated and experimental values are 4.2×10^{-3} and at 485°C the calculated value is 3.27×10^{-3} compared to 3.03×10^{-3}, the experimental value.

Table D-4.1

Thermodynamic Functions for H_2O, H_2, Ni and NiO (ref. 118)

Substance	$-(F^\circ - H^\circ_{298})/T$, cal/deg			ΔH°_{298}, Kcal
	298.15 K	500 K	1000 K	
H_2O	45.12	46.03	49.38	-57.798
H_2	31.21	32.00	34.76	0
Ni	7.14	7.90	10.77	0
NiO	9.08	10.40	15.53	-57.3
*$\sum_i \nu_i \Delta f_i$ for the reaction	-11.97	-11.53	-9.86	0.498

Table D-4.2

Equilibrium Constant $K_{eq} = \frac{P_{H_2}}{P_{H_2O}}$ for the Reaction

$Ni + H_2O \rightleftharpoons NiO + H_2$ at Various Temperatures

Temperature, K	298.15	500	1000
Equilibrium constant K_{eq} ($\times 10^{-3}$)	1.045	1.830	5.448

*f_i is the free energy function or ΔH°_{298}

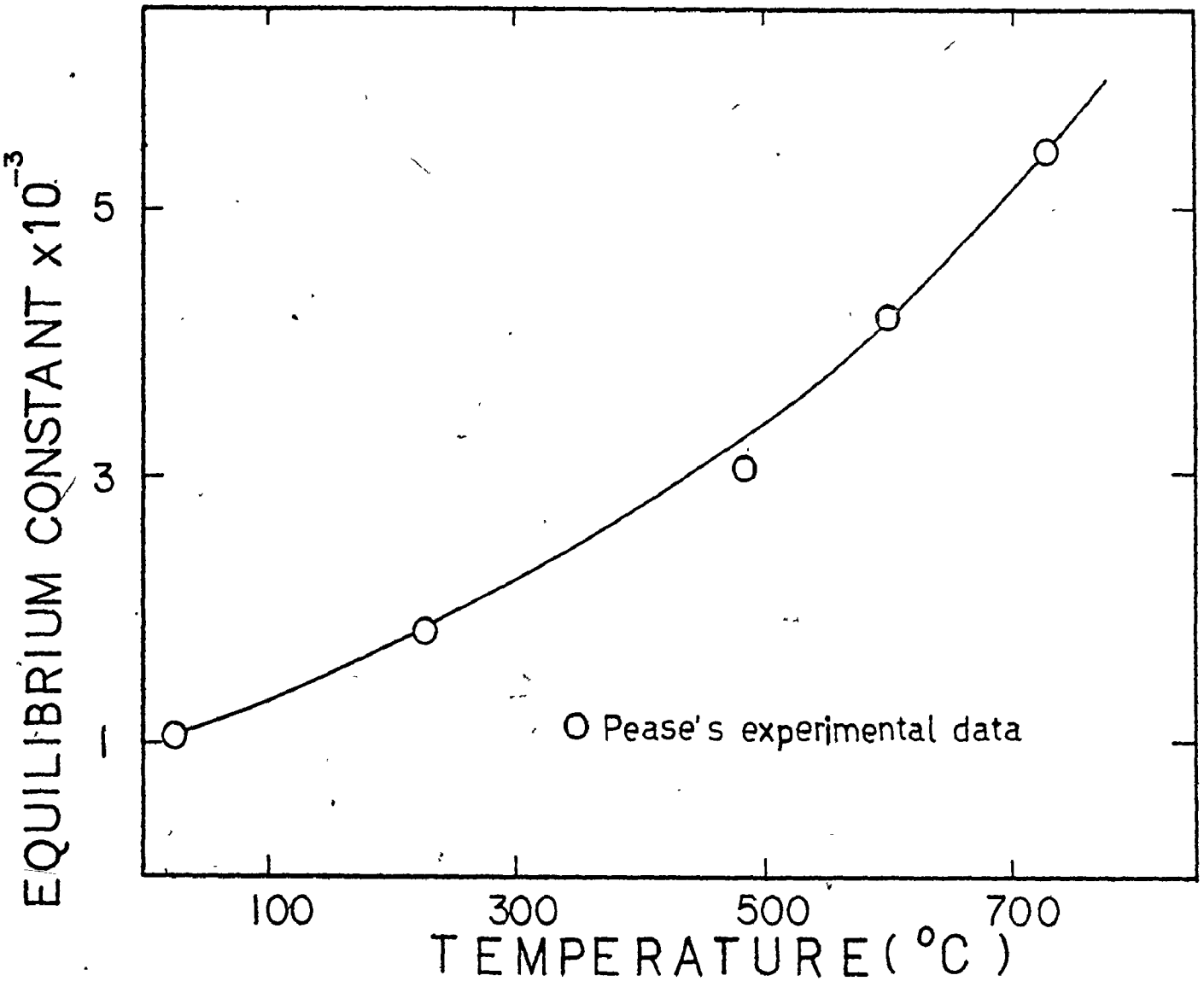

Figure D-4.1 Equilibrium constant for the reaction $Ni + H_2O \rightleftharpoons NiO + H_2$ as function of temperature calculated from free energy functions.

BIBLIOGRAPHY

1. Raney, M., U.S. Patent 1,563,787 (Dec. 1925).
2. Raney, M., U.S. Patent 1,628,191 (May 1927).
3. German Patent 408,811 (April 1923).
4. Russian Patent 38,127 (1933).
5. British Patent 282,112 (Dec. 1927).
6. French Patent 729,357 (Jan. 1932).
7. Raney, M., U.S. Patent 1,915,473 (June 1933).
8. Lieber, E. and Morritz, F.E., Advances in Catalysis 5, 417 (1953).
9. Sassoulas, R., and Trambouze, Y., Bull. Soc. Chim. France 5, 985 (1964).
10. Freel, F., Pieters, W.J.M., and Anderson, R.B., J. Catalysis, 16, 281 (1970).

10a. Alexander, W.O., and Vaughan, W.B., J. Inst. Metals 61, 247 (1937).

11. Mason, D. McA., Dirksen, H.A., and Linden, H.R., Inst. Gas Technol. Res. Bull. 31, 137 (1963).
12. Adkins, H. and Billica, H.R., J. Amer. Chem. Soc. 70, 695 (1948).
13. Sassoulas, R., Thesis, Lyon (1963).
14. Freel, J., Pieters, W.J.M. and Anderson, R.B., J. Catalysis 14, 247 (1968).
15. Robertson, S.D., and Anderson, R.B., J. Catalysis, 23, 286 (1971).
16. Terminazov and Beletskii, Dokl. Akad. Nauk. S.S.S.R., 55, 735 (1947).

17. Fouilloux, P., Martin, G.A., Renouprez, A.J., Moraweck, B., Imelik, B., and Prettre, M., J. Catalysis, 25, 212 (1972).

18. Raney, M., Ind. Eng. Chem., 32, 1199 (1940).

19. Bougault, I.J., Cattelain, E., and Chabrier, P.C., Bull. Soc. Chim. France, 5, 1699 (1938).

20. Freidlin, L. Rh., and Ziminova, N.I., Doklady Akad. Nauk., 74. 955 (1950).

21. Sokolskii, D.V., and Bezverkhova, S.T., Doklady Akad. Nauk. 94, 493 (1954).

22. Csuros, Z., Dusza, Zs., and Petro, J., Acta Chim. Acad. Sci. Hungar., 30, 461 (1962).

23. Mozingo, R., J. Amer. Chem. Soc., 65, 1013 (1943).

24. Smith, H.A., Chadwell, A.J., and Kirslis, S.S., J. Phys. Chem., 59, 820 (1955).

25. Kokes, R.J., and Emmett, P.H., J. Amer. Chem. Soc., 81, 5032 (1959).

26. Vandael, C., Ind. Chim. Belge, 17, 581 (1952).

27. Moreau, A., Thesis, Nancy (1959).

28. Kagan, H., Thesis, Paris (1962).

29. Mars, P., Scholten, J.J.F., and Zwietering, P., 2nd Inter. Congr. Catalysis, Paris, 1245 (1960).

30. Tarama, K., Kubomatsu, T., and Kishida, K., J. Chem. Soc. Japan, Pure Chem. Sect., 82, 1633 (1961).

31. Vidal, J., Lefebvre, G., and Coussemant, F., Bull. Soc. Chim. France, 257, 3909 (1963).

32. Menard, J.M., Trambouze, Y., and Prettre, M., Bull. Soc. Chim. France, 30, 401 (1963); Menard, J.M., Thesis, Lyon, (1962).

33. Bezaudun, J., Dalmai, G., Imelik, B., and Prettre, M., C.R. Acad. Sc. Paris, 258, 1779 (1964); Bezaudun, J., Thesis, Lyon (1964).

34. Lenfant, P., Thesis, Lyon (1965).

35. Jamey, J. P., Thesis, Lyon (1966).

36. Macnab, J.I., and Anderson, R.B., J. Catalysis, 29, 338 (1973).

37. Zapletal, V., Soukup, J., Ruzicka, V., and Kolomaznik, K., Scientific Papers of the Inst. Chem. Technol., Prague C17, 73 (1972) Organic Chemistry and Technology.

38. Coenen, J.W.E., 2nd Inter. Congr. Catalysis, Paris, Discussions, 1265 (1960).

39. Selwood, P.W., "Adsorption and Collective Paramagnetism", 189 pp. Academic Press, New York (1962).

40. Dietz, R.E., and Selwood, P.W., J. Chem. Phys. 35, 270 (1961).

41. Hume-Rothery, W., "Atomic Structure for Students of Metallurgy", Institute of Metals, London, England, (1946).

42. Sokolskaya, A.M., and Sokolskii, D.V., Kinet. i. Kataliz, 6, 658 (1965).

43. Csuros, Z., and Petro, J., Acta Chim. Acad. Sci. Hungar., 29, 321 (1961).

44. Hata, K., "New Hydrogenating Catalysts" - Urushibara Catalysts. 247 pp., Halsted Press Division, John Wiley and Sons, New York, (1971).

45. Anderson, R.B., "Experimental Methods in Catalytic Research", Academic Press, New York, (1968)

46. Brunauer, S., Emmett, P.H., and Teller, E., J. Am. Chem. Soc., 60, 309 (1938).

47. Mars, P., Mond. v.d., Th., and Scholten, J.J.F., Ind. and Eng. Chem. Product Res. and Devel., 1, No. 3, 161 (1962).

48. Kokes, R.J., and Emmett, P.H., J. Amer. Chem. Soc. 83, 29 (1961).

49. Huff, J.R., Jasinski, R.J., and Parthasarathy, R., Ind. Eng. Chem., Process Res. Rev., 3(2), 159 (1964).

50. Freel, J., Robertson, S.D., and Anderson, R.B., J. Catalysis, 18, 243 (1970).

51. Sinfelt, J.H., and Yates, D.J.C., J. Catalysis 8, 82 (1967).

52. Yates, D.J.C., and Sinflet, J.H., J. Catalysis 8, 348 (1967).

53. Brooks, C.S., and Christopher, G.L.M., J. Catalysis 10, 211 (1968).

54. Boudart, M., Adv. in Catalysis 20, 153 (1969).

55. Benton, A.F., and White, T.A., J. Amer. Chem. Soc., 52, 2325 (1930).

56. Sadek, H., and Taylor, H.S., J. Amer. Chem. Soc., 72, 1168 (1950).

57. Taylor, H.S., J. Amer. Chem. Soc., 53, 578 (1937).

58. Bond, G.C., "Catalysis by Metals", Academic Press, New York (1962).

59. Beeck, O., Smith, A.E., and Wheeler, A., Proc. Roy. Soc. (London) 177A, 62 (1940); Beeck, O.,Rev. Mod. Phys., 17, 61 (1945).

60. Eucken, A., and Hunsmann, W., Z.physik. Chem.,B44, 163 (1939).

61. Taylor, H.S., and Liang, S.C., J. Amer. Chem. Soc., 69, 1306 (1947).

62. Beeck, O., Ritchie, A.W., and Wheeler, A., J.Colloid. Sci. 3, 505 (1948).

63. Taylor, A., and Floyd, R.W., J. Inst. Met. 81, 25 (1952).

64. Paul, R., Bull. Soc. Chim. France, 8, 507 (1941).

65. "Selected Powder Diffraction Data for Minerals", 1st Edition, published by JCPDS, Swarthmore, U.S.A., (1974).

66. Boniszewski, T., and Smith, G.S., Phys. Chem. Solids 21, 115 (1961).

67. Janke, A., and Michel, P., Comptes Rendus Ac. Sc., T251 nr. 8, 1001 (1960).

68. Lippens, B.C., Ph.D. Thesis, Delft (1961).

69. Welcher, F.J., Editor, "Standard Methods of Chemical Analysis", 6th Edition, Vol. II, part A, p. 826. D. Van Nostrand Co., Inc., New York (1963).

70. Cavallaro, F., and Jordan, R.L., "WRC Analytical Procedure No. 542 and 543" (W. R. Grace Co.).

71. Welcher, F.J., "The Analytical Uses of Ethylenediamine-Tetraacetic Acid", pages 72 and 40. D.Van Nostrand Co., Inc., Princeton, N.J. (1958).

72. Kolthoff, I.M., Elving, P.J. and Sandell, E.B., "Treatise on Analytical Chemistry", Vol. II, Part II, page 404, Interscience Publ. Inc., New York, (1962).

73. Tchugaeff, L., Z. Anorg. Chem., 46, 144 (1905); Ber. 38 2520 (1905)

74. Fritz, J.S. and Schenk, G.H. Jr., "Quantitative Analytical Chemistry", 2nd Ed., Allyn and Bacon Inc., Boston (1972).

75. Dirksen, H.A., and Linden, H.R., Research Bulletin No. 31, Institute of Gas Technology, Chicago (1963).

76. Aubry, J., Thesis, Grenoble, (1941).

77. Hackspill, L., and Rohmer, R., Bull. Soc. Chem. France, 9, 541 (1942).

78. Robertson, S.D. and Anderson, R.B., To be published in J. Catalysis.

79. Eagan, J.D., Ph.D. Thesis, McMaster University, Hamilton (1972).

80. Stifel, G.R., Master's Thesis, McMaster University (1966).

81. Emmett, P.H., Editor, "Catalysis", Vol. IV, p. 12, Reinhold Publishing Co., New York (1956).

82. Pines, H., and Steingaszner, P., J. Catalysis, 10, 60 (1968)' Kobilinski,T.P., and Pines, H., J. Catalysis, 17, 384; also 375 and 394 (1970); Licht, E., Schächter, Y.; and Pines, M., J. of Catalysis, 31, 110 (1973); Licht, E., Schächter, Y., and Pines, H., J. Cat. 38, 423 (1975).

83. Wooley, H.W., Scott, R.B. and Brickwedde, F.G., J. Research Natl. Bur. Standards, 41, 379 (1948).

84. Hunt, P.P., and Smith, H.A., J. Phys. Chem., 65, 87 (1961).

85. Smith, H.A., and Hunt, P.P., J. Phys. Chem. 64, 383 (1960).

86. Moore, W.R., and Ward, H.R., J. Phys. Chem., 64, 832 (1960).

87. King, J. Jr., J. Phys. Chem. 67, 1397 (1963).

88. Conti, M.L. and Lesimple, M., J. Chromatography, 29, 32 (1967).

89. Kwan, T., J. Res. Inst. Catalysis, 8, 18 (1960).

90. Van Hook, W.A., and Emmett, P.H., J. Phys. Chem. 64, 673 (1960).

91. Furuyama, S. and Kwan, T., J. Phys. Chem., 65, 190 (1961).

92. Schultz, W.R., and LeRoy, D.J., Can. J. Chem. 42, 2480 (1964).

93. Shipman, G.F., Anal. Chem. 34, 877 (1962).

94. Venugoplan, M. and Kutschke, K.O., Can.J. Chem. 41, 548 (1963).

95. Bastick, J., Baverez, M., and Castagne M., Bull. Soc. Chim. Fr., 1292 (1965).

96. Yasumori, I. and Ohno, S., Bull. Chem. Soc. Japan 39, 1302 (1966).

97. Carter, E.H. Jr., PhD. Thesis, University of Tennessee (1962).

98. Schuit, G.C.A. and Van Reijen, L.L., Adv. Catalysis 10, 242 (1958).

99. Taylor, H.S., and Pace, J., 2, 578 (1934).

100. Pease, R.N., and Cook, R.S., J. Am. Chem. Soc., 48, 1199 (1926).

101. Zapletal, V., Soukup, J., Ruzicka, V., and Kolomaznik, K., Coll. Czech. Chem. Comm., 33, 2436 (1968); 34, 1444 (1969); 35, 598 (1970); also in Chem.listy 62, 210 (1968).

102. Zapletal, V., Soukup, J., Ruzicka, V., Koppova, A., and Kolomaznik, K., "Scientific Papers of the Institute of Chemical Technology", Prague, C17,37 (1972).

103. Amenomiya, Y., and Cvetanovic, R.J., J. Phys. Chem., 67, 144 (1963).

104. Amenomiya, Y., and Cvetanovic, R.J., J. Phys. Chem., 67, 2705 (1963).

105. Amenomiya, Y., and Cvetonovic, R.J., J. Phys. Chem., 67, 2046 (1963).

106. Redhead, P.A., Vacuum, 12, 202 (1962).

107. Carter, G., Vacuum, 12, 245 (1962).

108. Cvetanovic, R.J., and Amenomiya, Y., Advan. Catal., 17, 103 (1967).

109. Cvetanovic, R.J., and Amenomiya, Y., Catal. Rev., 6, 21 (1972).

110. Smutek, M., Cerny, S., and Buzek, F., Advan. Catal., 24, 343 (1975).

111. Littman, H.L., and Dew-Hughes, B., Paper presented at the 132nd meeting of the ACS at New York, Sept. 1957 and at the Boston Meeting of the ACS, April 1959.

112. Tran-Huu-Thé, Thèse, Lyon (1955).

113. Smith, D.P., "Hydrogen in Metals", The University of Chicago Press, Chicago (1948).

114. Emmett, P.H., "Catalysis", vol. I, p. 80, Reinhold Publishing Co., New York (1954).

115. Martin, G.A., and Fouilloux, P., J. Cat., 38, 231 (1975).

116. Ebisuzaki, Y., and O'Keefe, M., Prog. Solid State Chem., 4, 187 (1967).

117. Feates, F.S., and Keep, C.W., Trans. Far. Soc., 66, 3156 (1970).

118. Lewis, G.N., Randall, M., Pitzer, K.S., and Brewer, L. "Thermodynamics", 2nd Ed., McGraw-Hill Co., New York (1961).